INFORMATION TO USERS

This manuscript has been reproduced from the microfilm master. UMI films the text directly from the original or copy submitted. Thus, some thesis and dissertation copies are in typewriter face, while others may be from any type of computer printer.

The quality of this reproduction is dependent upon the quality of the copy submitted. Broken or indistinct print, colored or poor quality illustrations and photographs, print bleedthrough, substandard margins, and improper alignment can adversely affect reproduction.

In the unlikely event that the author did not send UMI a complete manuscript and there are missing pages, these will be noted. Also, if unauthorized copyright material had to be removed, a note will indicate the deletion.

Oversize materials (e.g., maps, drawings, charts) are reproduced by sectioning the original, beginning at the upper left-hand corner and continuing from left to right in equal sections with small overlaps.

Photographs included in the original manuscript have been reproduced xerographically in this copy. Higher quality 6" x 9" black and white photographic prints are available for any photographs or illustrations appearing in this copy for an additional charge. Contact UMI directly to order.

ProQuest Information and Learning
300 North Zeeb Road, Ann Arbor, MI 48106-1346 USA
800-521-0600

UMI®

Université d'Ottawa · University of Ottawa

NEURONAL PROGENITOR ENRICHMENT IN THE ADULT CX32 KNOCKOUT (KO) MOUSE

Sandy Beyko

A Thesis Submitted to the Faculty of Graduate and Postdoctoral Studies in Partial Fulfillment of the requirement for the degree of Master of Science
University of Ottawa

Department of Biochemistry, Microbiology and Immunology
Faculty of Medicine

© Sandy Beyko, Ottawa, Canada, 2001

National Library of Canada
Acquisitions and Bibliographic Services
395 Wellington Street
Ottawa ON K1A 0N4
Canada

Bibliothèque nationale du Canada
Acquisitions et services bibliographiques
395, rue Wellington
Ottawa ON K1A 0N4
Canada

Your file Votre référence

Our file Notre référence

0-612-66012-5

The author has granted a non-exclusive licence allowing the National Library of Canada to reproduce, loan, distribute or sell copies of this thesis in microform, paper or electronic formats.

The author retains ownership of the copyright in this thesis. Neither the thesis nor substantial extracts from it may be printed or otherwise reproduced without the author's permission.

L'auteur a accordé une licence non exclusive permettant à la Bibliothèque nationale du Canada de reproduire, prêter, distribuer ou vendre des copies de cette thèse sous la forme de microfiche/film, de reproduction sur papier ou sur format électronique.

L'auteur conserve la propriété du droit d'auteur qui protège cette thèse. Ni la thèse ni des extraits substantiels de celle-ci ne doivent être imprimés ou autrement reproduits sans son autorisation.

Canada

THESIS ABSTRACT

The connexin (Cx) family of channel-forming proteins is comprised of 15 or more members that form intercellular channels directly connecting the cytoplasm of adjacent cells (gap junctions). Cx proteins are found in both oligodendrocytes and neurons in the central nervous system (CNS) and myelinating Schwann cells in the peripheral nervous system (PNS). In humans, mutations in the gap junction Cx32 gene are associated with a inherited demyelinating disorder of the PNS, Charcot-Tooth-Marie disease (CMTX). In the CNS, Cx32 is one of the predominant Cxs expressed during the later stages of differentiation, neurogenesis, cell migration, and neural circuit formation. Thus, it is hypothesized that intracellular communication via Cx32-mediated channels plays a role in regional specification and arrangement of structures within the CNS. However, the impact of endogenous Cx32 expression and/or null mutation on neuronal differentiation have yet to be determined. To test the hypothesis that Cx32 expression influences CNS development, the cerebral development of Cx32 knockout (KO) mice was compared to that of wild-type (WT) littermate controls. We demonstrate that the hippocampal formation of KO mice exhibit morphological abnormalities including the enrichment of a hyperchromatic cell type identified by Nissl staining and biochemical abnormalities including an increase in immunogenic markers of neural progenitor cells and a reduction in immunogenic markers of terminally differentiated neurons. *In vitro* analysis of hippocampal cultures demonstrated that KO cultures express more cells with a neural stem cell phenotype than WT cultures. It is not known whether these abnormalities are the result of the loss of Cx32 or the result of Cx compensation in that levels of Cx26, Cx30, Cx36, Cx37, and Cx47 were found to be elevated in the KO hippocampal

formation relative to WT. Based on these data, we speculate that the Cx32 KO mouse may represent an *in vivo* model of neural progenitor enrichment.

ACKNOWLEDGMENTS

I wish to thank my supervisor, Dr. Steffany A.L. Bennett, who gave me the opportunity to work on this project. I appreciate all of her time, patience, support, and assistance in the past two years. I would further like to thank the members of my thesis advisory committee Dr. J. Phipps, Dr. D. Franks, Dr. L. Klein, Dr. A. Mackenzie, and Dr. R. Slack for all their helpful suggestions and comments. I wish to extend further gratitude to Dr. D. Franks for the use of the microscopy equipment and his expert advice. I would like to thank Dr. J. Chen for all of his expert advice and technical support. I would like to make special acknowledgement to Lysanne Melanson-Drapeau for her much appreciated Western analysis data.

Finally, I wish to thank all my lab members, friends, and family for their guidance, support, and encouragement. Thank you all very much.

This work was supported by grants from NSERC to SALB and the Aventis/Harvard Initiative in Apoptosis to SALB and DP.

TABLE OF CONTENTS

Title Page..... i
Abstract..... ii
Acknowledgements..... iv
Table of Contents..... v
List of Tables..... vii
List of Figures..... viii
List of Abbreviations..... x

CHAPTER I: GENERAL INTRODUCTION

1.1 Intracellular communication..... 1
1.1.1 What are gap junctions..... 2
1.1.2 Connexins → Connexons → Gap Junctions..... 2
1.1.3 Connexin32..... 4
1.1.4 Human peripheral neuropathy and Cx32 mutations..... 5
1.1.5 Animal model of CMTX..... 7
1.1.6 Cxs in the CNS..... 8
1.1.7 Why study Cx32?..... 10
1.2 Neurogenesis..... 14
1.2.1 What is a neural stem cell?..... 16
1.2.2 Neural progenitors in the hippocampal formation..... 18
1.3 Objectives and summary..... 20

CHAPTER II: MATERIALS AND METHODS

2.1 Generation of KO and WT mice..... 21
2.2 Morphological analyses..... 22
2.3 Quantitative analysis..... 22
2.3.1 Quantitation of the hyperchromatic cells in KO animals..... 22
2.3.2 Immunodensitometry of the KO and WT DG of the various antibodies..... 24
2.4 Immunohistochemistal Characterization..... 24
2.4.1 Tissue Preparation..... 24
2.4.2 Antibodies..... 24
2.5 Colony assay of neural precursor cultures..... 26
2.6 Reverse Transcriptase and PCR of KO and WT mice RNA..... 27
2.6.1 Isolation of total RNA..... 27
2.6.2 Reverse Transcriptase..... 27
2.6.3 Polymerase chain reaction(PCR) amplification of RT products..... 28

CHAPTER III: RESULTS

3.1) Anatomical abnormalities detected in the midbrain of KO mice.....31
3.2) Quantitation of the enriched hyperchromatic cell population in the KO mice.....38
3.3) Characterization of lineage markers in the KO and WT hippocampal formation by immunohistochemistry and Western analysis.....42
3.4) *In vitro* characterization of primary hippocampal cultures from KO and WT mice.....61
3.5) Expression of connexin-family members in the KO and WT brain.....65

CHAPTER IV: GENERAL DISCUSSION AND CONCLUSION

Discussion.....74
Conclusion.....81

REFERENCES

References.....83

LIST OF TABLES

Table 1 Cx gene expression and related genetic disorders. 13

Table 2: Primer pairs used to amplify Cx and GAPDH mRNA from KO and WT brain areas.....30

Table 3: Comparison of Cx gene expression in the KO and WT hippocampal formation. 68

Table 4: Comparison of Cx gene expression in KO and WT brain regions.....73

LIST OF FIGURES

Figure 1: Schematic diagram of the molecular steps leading to the formation of intercellular channels.....3

Figure 2: Schematic diagram of prototypical connexin.....4

Figure 3: Strategy used to generate and analyze the KO mouse.....8

Figure 4: Cx32 protein levels increase following NGF-induced neuronal differentiation when PC12-AC cells.....12

Figure 5: Anatomy of the hippocampus and the different steps that constitute neurogenesis.....19

Figure 6: The midbrain of the 129/C57Bl KO mouse is cytoarchitecturally different from a WT C57Bl mouse.....35

Figure 7: Genotype and expression analysis of the KO mouse backbred into a C57Bl background.....36

Figure 8: Identity of our backbred KO and WT.....37

Figure 9: Location of the hippocampal formation and anatomical levels chosen for further analysis in the murine brain.....40

Figure 10: Quantitation of the hyperchromatic cells in KO and WT mouse hippocampal formations.....41

Figure 11: Nestin protein levels are increased in the DG of KO animals.....50

Figure 12: Nestin-positive cells in the DG of KO and WT mice.....51

Figure 13. PCNA protein levels are comparable in KO and WT hippocamapal formation.....52

Figure 14. Expression of anti-A2B5 and anti-O4 oligodendrocyte lineage markers are not detected in KO or WT hippocampal formation.....53

Figure 15. GAP43 protein levels are reduced in the DG and hippocampus of KO animals.....54

Figure 16. MAP1 protein levels are moderately reduced in the hippocampal formation of KO animals.....55

Figure 17. TUJ1 immunoreactive protein is dramatically reduced in the KO DG.....56

Figure 18. NeuN immunoreactivity is reduced in KO hippocampal neurons.....57

Figure 19. NF160 proteins levels are reduced in the hilar region of the DG.....58

Figure 20. GFAP protein levels are comparable in KO and WT hippocampal formation, but there is a change in protein localization in the DG of KO mice. 59

Figure 21. GalC protein levels are comparable in KO and WT hippocampal formation 60

Figure 22: Hippocampal KO neurons cultured in the presence of basic fibroblast growth factor (bFGF) express neural stem cell markers..... 63

Figure 23: bFGF-treated KO colonies can be terminally differentiated to neurons by exposure to brain derived neurotrophic factor (BDNF)..... 64

Figure 24: Location of primers used to detect Cx32 transcript.....68

Figure 25: Cx mRNA expression in the hippocampal formation of KO and WT mice determined by RT-PCR.....69

Figure 26: Cx mRNA expression of subventricular zone, entorhinal cortex, parietal/temporal cortex, and hypothalamus from KO and WT mice determined by RT-PCR.....70

Figure 27: Cx mRNA expression of thalamus, frontal cortex, striatum, and brainstem from KO and WT mice determined by RT-PCR..... 71

Figure 28: Cx mRNA expression of cerebellum and occipital cortex from KO and WT mice determined by RT-PCR.....72

Figure 29: Neuronal progenitor enrichment in the adult KO mouse hippocampal formation.....73

LIST OF ABBREVIATIONS

ANOVA	analysis of variance
BDNF	brain derived neurotrophic factor
bFGF	basic fibroblast growth factor
BrdU	5-bromo-2'-deoxyuridine
°C	degrees Celsius
Ca^{2+}	Calcium
CA1	CA1 field, hippocampus
CA3	CA3 field, hippocampus
cAMP	cyclic adenylate cyclase
cDNA	complementary DNA
CL	cytoplasmic loop
CMTX	charcot-marie-tooth disease
CNS	central nervous system
Cx	connexin
DAB	3,3'-diaminobenzidine
DG	dentate gyrus
dNTP	deoxynucleotide triphosphate
DNA	deoxyribonucleic acid
DTT	dithiothreitol
E11	embryonic day 11
EDTA	ethylenediamenetetraacetic acid disodium salt
ES	embryonic stem cells
GAP43	growth associated protein-43
GalC	galactocerebroside
GAPDH	glyceraldhyde-phosphate-dehydrogenase
gc	granule cell
gcl	granule cell layer
GrDG	granular layer, dentate gyrus
GFAP	glial fibrillary acidic protein
ICM	inner cell mass
IP3	1,4,5-triphosphate
K^+	Potassium
kd	kilobase
kDa	kilo daltons
KO	knockout
LiCl	lithium chloride
LMol	lacunosum moleculare layer, hippocampus
MAP1	microtubule-associated protein 1
MAP2	microtubule-associated protein 2
$MgCl_2$	magnesium chloride
min	minute
mf	mossy fibers
ml	milliliter
mM	millimolar

mRNA	messenger RNA
Na^{2+}	sodium
neo	neomycin
NeuN	nuclear protein
NF160	neurofilament 160
NGF	nerve growth factor
Or	oriens layer, hippocampus
ORF	open reading frame
P6	postnatal day 6
P21	postnatal day 21
PBS	phosphate buffered saline
PC12	pheochromocytoma cell line
pc	pyramidal cell
pcl	pyramidal cell layer
PCNA	proliferating cell nuclear antigen
PCR	polymerase chain reaction
PNS	peripheral nervous system
PoDG	polymorphic layer, dentate gyrus
Py	pyramidal cell layer
Rad	stratum radiatum, hippocampus
RNA	ribonucleic acid
RT-PCR	reverse-transcriptase chain reaction
SDS	sodium dodecyl sulfate
SLu	stratum lucidem, hippocampus
TUJ1	class III beta-tubulin isotype
µl	microliter
µg	microgram
µm	micrometer
UTR	untranslated region
UV	ultraviolet
WT	wildtype

I. GENERAL INTRODUCTION

1.1 INTRACELLULAR COMMUNICATION

Organisms have developed multiple strategies to co-ordinate cellular activity during development. In the central nervous system (CNS), communication between cells can occur either at chemical synapses, in which a neurotransmitter is released into the synaptic cleft to interact with receptors on neighbouring cells, or through direct exchange of second messengers through intercellular channels that physically link adjacent cells. These channels are known as gap junction intercellular channels or simply gap junctions.

The adult CNS is derived from a single layer of neuroepithelial cells within the neurotube. During neurogenesis, pluripotent stem cells within the ventricular zone undergo asymmetric division to (a) self-renew and (b) produce a partially committed daughter cell capable of migrating and differentiating into one of many cell types within the CNS. Clearly, the complexity of the adult CNS cytoarchtecture and function depend upon a delicate balance between cell growth, cell differentiation, and cell death, both to regulate cell number and to ensure regional differentiation. This balance is modulated, in part, by metabolic cooperation between cell groups. Cells in close apposition coordinate a synchronized response by the direct exchange of ions, metabolites, and other messengers through gap junctions. It is important to note that (1) gap junctional communication is maximal in the developing nervous system and (2) neurogenesis occurs prior to the formation of chemical synapses (for a review see Rozental et al, 2000). Thus, it is predicted that genetic mutations or deletions in any of the genes encoding structural subunits of gap junction channels (connexins) likely have dramatic consequences on CNS development.

1.1.1 What are gap junctions?

Communication through gap junctions mediates intercellular signalling in non-excitable cells during cell growth and proliferation, cellular homeostasis, tissue differentiation, and embryonic development (Moennikes et al, 1999; Bruzzone et al, 1996; Lo, 1999; Dermietzel & Spray, 1993). Gap junctions are unique in that they couple cells both electrically and metabolically (Rozental et al, 1998). In vertebrates, these channels are enclosed proteinaceous cylinders that permit bidirectional exchange of small molecules and secondary metabolites between cells, including ions (i.e. Na^{2+}, K^{+}, Ca^{2+}), amino acids, cyclic nucleotides (i.e. cAMP, cGMP), 1,4,5-trisphosphate (IP3), and vitamins (for a review see Bruzzone et al, 1996). Gap junctions have pore diameters that enable intercellular passage of small molecules with molecular weights up to 1 kDa (Bennett & Goodenough, 1978; Loewenstein, 1981; Dermietzel & Spray, 1993).

1.1.2 Connexins→ Connexons→ Gap Junctions

Six connexin (Cx) protein subunits oligimerize at the level of the phospholipid bilayers to form a symmetric hexameric single-membrane channel (hemichannel) called a connexon (Dermietzel et al, 1990; Pfahnl et al, 1997). A connexon must dock to its counterpart elaborated by a neighbouring cell to form a complete intercellular channel and initiate intercellular communication. Thus, a gap junction results from the alignment of two connexons that span the plasma membrane of adjacent cells forming an axial, hydrophilic pore directly connecting cell-cell cytoplasm (Figure 1). Up to several hundreds of these channels are commonly found in clustered assemblies designated gap junction plaques (Husler et al, 1998; Spray, 1998). The type of channel generated by

different cell types is dictated by the diversity in Cx expression (Dermietzel et al, 1989; Dermietzel & Spray, 1993; Bennett et al, 1991). Intercellular channels can be heterogeneous or homogeneous in Cx content in that adjacent cells can elaborate homomeric or heteromeric connexons giving rise to homotypic or heterotypic channels (White & Bruzzone, 1996; Nicholson et al, 1999; Vaney & Weiler, 2000; Ahmad et al, 1999). Assembly of different Cx proteins into homogeneous or heterogeneous channels likely confers signaling specificity by defining electrical conductance and metabolic permeability (Niessen et al, 2000; Quist et al, 2000; for a review see White & Bruzzone, 1996).

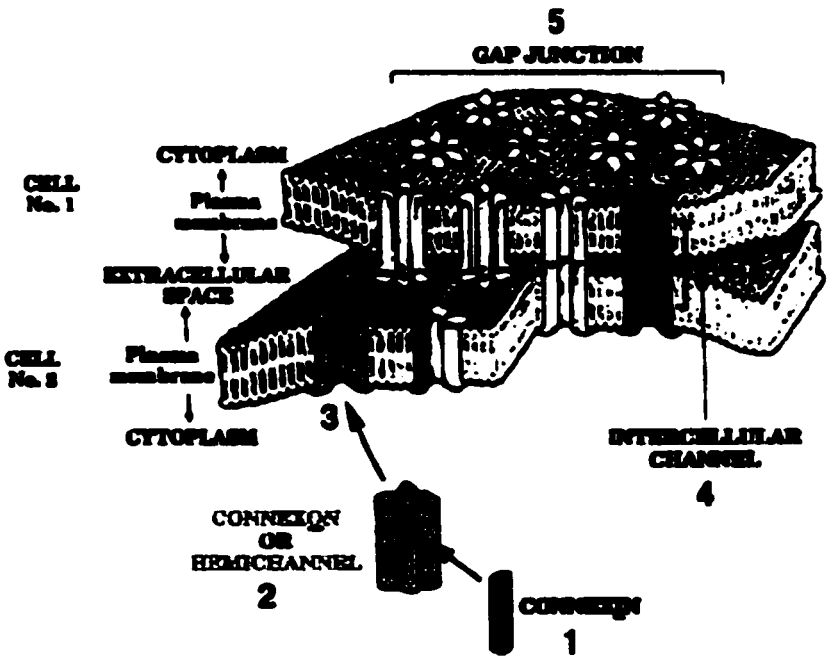

Figure 1. Schematic diagram of the molecular steps leading to the formation of intercellular channels. The protein subunits (connexins, Cxs) oligermize in a hexameric structure (connexon) that is transported to the plasma membrane. Connexons from adjacent cells interact to form complete intercellular channels. Clusters of these channels define a gap junction (adapted from VanSlyke & Musil, 2000).

Cx proteins are part of a multi-gene family encoded by over 15 different Cx genes. Cx proteins share the same basic structure, including two extracellular loops, four transmembrane domains, and three cytoplasmic domains (Figure 2; Spray, 1998; White & Bruzzone, 1996; Willecke & Haubrich, 1996). The amino acid sequence is highly conserved among species. Cx diversity is restricted to the cytoplasmic loop and carboxyl terminal regions that can vary in sequence and length (Davies et al, 1996; Willecke & Haubrich, 1996). These variations are assumed to account for the distinct biophysical, permeability, and regulatory properties of different Cxs (Bennett et al, 1991; White & Bruzzone, 1999). Cx regulation is achieved primarily through phosphorylation, and proteolytic cleavage at the carboxyl terminus (Laird, 1996; Spray, 1998).

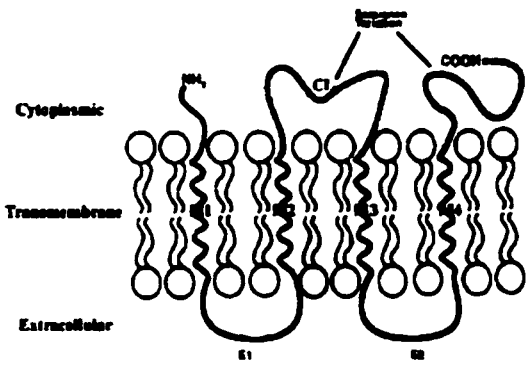

Figure 2. Schematic diagram of prototypical connexin. A Cx is composed of four membrane spanning regions (M1-M4), two extracellular loops (E1 and E2) and three cytoplasmic portions; (the amino (NT) and carboxyl (CT) terminal domains and the central cytoplasmic loop (CL)). Variations in Cx molecular weight are due to variable lengths of the CL and CT sequences (adapted from White & Bruzzone, 1996; Hulser et al, 1998)

1.1.3 Connexin32

Cx32 was the first Cx gene to be cloned (Paul, 1986). The primary sequence predicts an integral membrane protein of 283 amino acids (Nicholson et al, 1999), and a molecular weight of 32 kDa (Paul, 1986). Note that, although other nomenclatures exist,

gap junction proteins are currently named according to their predicted molecular weight (Bennett et al, 1991). Cx32 is predominantly expressed in non-neuronal cells such as hepatocytes, epithelial cells, pancreatic acinar cells, and epithelia of the lactating mammary gland (Nicholson et al, 1999; Dermietzel & Spray, 1993). In peripheral nervous system (PNS) and CNS, protein primarily localizes to the myelinating Schwann cells and oligodendrocytes (Scherer et al, 1995; Nicholson et al, 1999; Dermietzel et al, 1997). There is considerable controversy as whether or not Cx32 is expressed in neurons (Bennett et al, 1999; Bergoffen et al, 1993; Rash et al, 2000; Dermietzel et al, 1989). However, the appearance of Cx32 mRNA and protein in CNS coordinates with postnatal development events such as glial and neuronal maturation, synaptogenesis, myelination, and vascularization (Belliveau et al, 1991).

1.1.4 Human peripheral neuropathy and Cx32 mutations

In humans, mutations in the Cx32 gene are the genetic determinant responsible for demyelinating neuropathy in X-linked Charcot-Tooth-Marie disease (CMTX) (Bergoffen et al, 1993; Yoshimura et al, 1998); a genetic disorder with a population frequency of 1 in 3000 (White & Paul, 1999; Abram et al, 2000). CMTX was the first disease to link Cx mutations to a genetic disorder (Bergoffen et al, 1993; Ressot et al, 1998). Mutations of Cx genes are now known to underlie a variety of human diseases. For example, Cx26 mutations cause hereditary non-syndromic deafness (White et al, 1998; White & Paul, 1999), while Cx50 mutations lead to visual impairments or blindness (White & Paul, 1999). In CMTX, patients suffer with distal muscle weakness, axonal atrophy, reduction in nerve conductance, degeneration of sensory and motor nerves, and sensory impairment

(Garcia, 1999; Bahr et al, 1999; Sahenk & Chen, 1998; Spray & Dermietzel, 1995). Mice lacking Cx32 also develop a late-onset peripheral neuropathy with features similar those of CMTX (Scherer et al, 1998). Salient to this thesis, Bahr et al (1999) recently reported neuronal dysfunction in the CNS of CMTX patients, resulting in cerebral motor, visual, and acoustic pathway impairment. Approximately 165 CMTX-associated mutations have been identified in the Cx32 gene (Bergoffen et al, 1993). At least 12 of the 165 mutations affecting the Cx32 gene result in a null phenotype (Castro et al, 1999; Nicholson et al, 1999; Ainsworth et al, 1998). Cx32 mutations interfere with channel-forming abilities in Schwann cells via failure to translate protein, loss-of-protein function, or altered gating properties (Sahenk & Mendell, 1999; Bergoffen et al, 1993; Abrams et al, 2000; Ressot et al, 1998; Barrio et al, 1999; Nicholson et al, 1999). Cx32 channels provide a direct pathway for diffusion of nutrients, small molecules and ions between the perinuclear and periaxonal Schwann cell cytoplasm (Scherer et al, 1995). It is hypothesized that a series of radially arrayed gap junctions could form a pathway for the diffusion of small molecules and ions directly across the myelin sheath. This pathway would effectively decrease nutrient diffusion distance by 1,000-fold (Scherer et al, 1998). In support of this hypothesis, immunohistochemical distribution of Cx32 protein concentrate in the paranodal regions of the nodes of Ranvier and the Schmidt-Lanterman incisures (Bergoffen et al, 1993; Scherer et al, 1995; Spray & Dermietzel, 1995; Zhao et al, 1999).

1.5. Animal model of CMTX

Dr. Klaus Willecke (Institute of Genetik, Universitat Bonn) generated a Cx32-null mouse by disrupting the Cx32 coding region in the mouse genome through insertion of the neomycin resistance gene via homologous recombination. The methodology underlying targeted disruption of the Cx32 gene and generation of the KO mice is described in (Nelles et al, 1996) and a short description is depicted in Figure 3. Interestingly, the pathological changes seen in Cx32 knockout (KO) mice are similar to, but less pronounced than, those seen in CMTX patients. Young KO mice do not exhibit a demyelinating neuropathy (Nelles et al, 1996). Older mice develop a progressive demyelinating peripheral neuropathy beginning 4 months of age. Motor fibers are more affected than sensory fibers (Scherer et al, 1998; Martini & Carenini, 1998; Neuberg et al, 1998). Demyelination in mice is characterized by thin myelin sheaths, cellular onion bulb formation, and enlarged periaxonal collars (Willecke et al, 1999; Scherer et al, 1998; Martini & Carenini, 1998). Nerve conductance properties are only slightly altered and there is no apparent muscle weakening, suggesting that the phenotype in mice does not completely match the phenotype in CMTX patients. Thus, KO mice exhibit subtle defects in the PNS, as compared to humans (White & Paul, 1999). This may be due to the fact that murine Schwann cells express Cx46 and oligodendrocytes express Cx45 in addition to Cx32. These Cxs are not present in human cells (Nicholson et al, 1999).

Mice deficient in Cx32 are viable, fertile, normal in appearance and have no overt behavioral abnormalities. They do exhibit abnormalities in the liver, an organ where Cx32 is abundantly expressed. There is a decreased ability to mobilize glucose from

hepatic glycogen stores by 78% (Nelles et al, 1996; White & Paul, 1999) and a high incidence of spontaneous hepatocarcinogenesis (Moennikes et al, 1999).

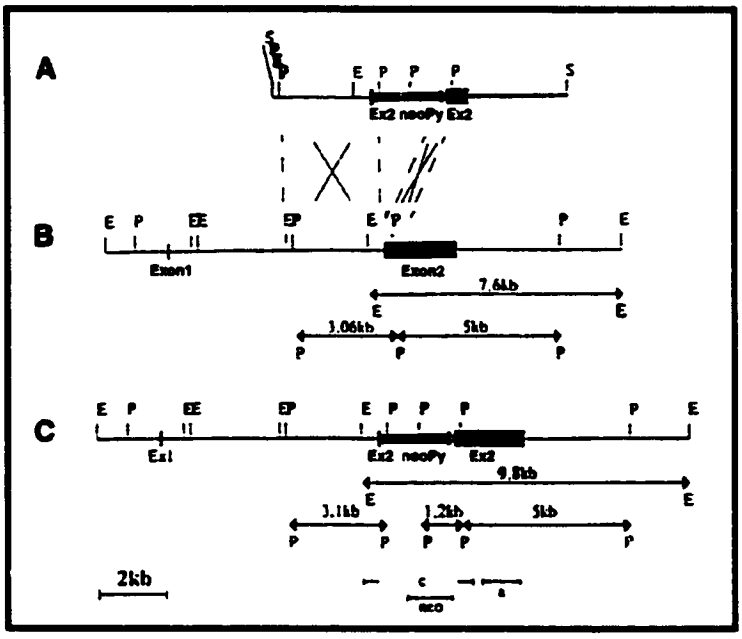

Figure 3. Strategy used to generate and analyze the Cx32 KO mouse. **(A)** The targeting vector with neomycin insertion into Exon 2 of the mouse Cx32 gene. The restriction sites are labeled in red. The DNA shown downstream of Exon 2 (orange) was derived from pBluescript SK+. **(B)** Mouse Cx32 gene with the noncoding Exon 1 and Exon 2 containing the complete open reading frame. **(C)** Disruption of the Cx32 coding region via homologous recombination by insertion of neomycin resistance gene. KO animals were generated by Dr. Klaus Willecke (Institute for Genetik, Universitat Bonn). Animals were backbred into C57Bl background by Caterina Sellitto and Steffany Bennett in the laboratory of Dr. David Paul (Neurobiolgy, Harvard University) as described in the results (adapted from Nelles et al, 1996).

1.6. Cxs in the CNS

Cx expression in the brain is diverse. Intercellular communication is hypothesized to mediate regional specification and the formation of developmental subcompartments in the brain (Dermietzel & Spray, 1993; Nadarajah & Paravelas, 1999; Bennett et al, 1991). Gap junctions represent an electrical and metabolic communication system regulating functions in a number of vertebrate CNS structures. It is tempting to speculate that Cx channel formation during embryogenesis provides intercellular passage of morphogens and other developmentally relevant factors between neural progenitors that initiate neural precursor proliferation, terminal differentiation and/or neuronal

migration. Electronic coupling in cortical progenitor cells has been shown to influence circuit formation and cell migration (Naderajah et al, 1997).

Out of the 15 Cx proteins identified, at least eight (Cx26, Cx30, Cx32, Cx36, Cx37, Cx43, Cx45, and Cx47) are found in the adult rat brain (Rash et al, 2000; Dermietzel & Spray, 1993). Table 1 summaries the localization of several Cx genes expressed in rodents. In early brain development, neuroepithelial cells of the ventricular zone are coupled into clusters by gap junctions. These clusters contain radial glia and neuronal precursors, but no differentiating or migrating neurons (Nadarajah & Parnalvelas, 1999). In the rodent CNS, different patterns of Cx26, Cx30, Cx32, and Cx43 mRNA expression correlate with important developmental events (Nadarajah et al, 1997; Nagy et al, 1999). Cx43 is expressed throughout neurogenesis by astrocytes, neurons, and radial glia. It is hypothesized that during migration neurons establish contact and communicate through Cx43-containing channels with the structural support that they use to migrate to their final position in the brain (Nadarajah & Parnalvelas, 1999; Nagy et al, 1999). Cx26 is expressed during neurogenesis in cortical progenitor cells and by the second week postnatal Cx26 exhibits an inverted relationship with Cx32. Thus, Cx26 mRNA levels decline as Cx32 mRNA expression increases. Cx32 is predominantly expressed during the later stages of neurogenesis, differentiation, cell migration, and neural circuit formation into adult brain (Nadarajah & Parnalvelas, 1999; Dermietzel et al, 1989). Cx32 is expressed by oligodendrocytes and some neurons in the CNS (Scherer et al, 1995; Bergoffen et al, 1993; Dermietzel et al, 1989; see review for Bruzzone & Ressot, 1997). Cx30 mRNA appears in the second postnatal week when myelination has been initiated or has progressed substantially, but does not appear to be

expressed by oligodendrocytes (Nagy et al, 1999). In adult rodent brain, Cx30 is found in astrocytes, ependymal, and leptomenigeal cells (Kunzelmann et al, 1999; Nagy et al, 1999).

In the adult CNS, gap junctions couple a variety of neuronal groups in the CA1 and CA3 pyramidal cell fields of the hippocampus and the dentate gyrus (DG). Rash et al (2000) has recently provided evidence that Cx36-mediated neuronal gap junctions facilitate widespread electrical and metabolic coupling in the adult brain. Cx36 expression is predominant in neuronal cells of the mammalian CNS (Circirata et al, 2000), highly abundant in areas such as the hilar border, the polymorphonuclear layer of the DG, the CA1 pyramidal cell field, the stratum radiatum, the stratum oriens, and the lacunosum moleculare hippocampal subfields (Belluardo et al, 1999; Srinivas et al, 1999; Rozental et al, 2000). This expression pattern is similar to that of Cx47. Teubner et al (2001) demonstrate mRNA expression in pyramidal neurons of the cortex and hippocampus and in the granular and molecular cell layers of the DG. Kunzelmann et al (1999) has reported the presence of Cx45 in hippocampal and cortical oligodendrocytes. Granule cells of the DG are also known to express Cx26, Cx32, and Cx43 (Nagy et al, 1999; Dermietzel & Spray, 1993; Rozental et al, 2000).

1.7. Why Study Cx32?

Intercellular communication has been demonstrated by many to control the fate of cells (Lacanda et al, 2000; Rozental et al, 2000; Gramsch et al, 2001; Princen et al, 2001). Salient to my research, Cx32 has been implicated in oligodendrocyte differentiation in the CNS and in Schwann cell differentiation in the PNS. Cx32 is also expressed by some

neurons in adult CNS (Dermietzel et al, 1989; Bergoffen et al, 1993), but there is considerable controversy to whether neurons express functional Cx32-containing gap junctions (Rash et al, 2000). It may be that Cx32-containing connexons are functioning as hemichannels and not as gap junctions. Functional Cx32-mediated hemichannels have been demonstrated *in vitro* (Castro et al, 1999) and CMTX-associated mutations have been shown to impede hemichannel activity (Castro et al, 1999). More recently, neuronal dysfunction in the CNS has been demonstrated in CMTX patients with apparent defects in cerebral motor, visual, and acoustic pathways (Bahr et al, 1999; Nicholson et al, 1999). The molecular mechanisms responsible for these pathologies have yet to be identified.

What role (if any) does Cx32 play in neuronal differentiation? In my honours thesis research project, I examined Cx32 expression in an *in vitro* model of neuronal differentiation. The expression of Cx32 protein was studied in partially committed neural precursors that express low levels of endogenous Cx32. I choose PC12 cells, a rat pheochromocytoma cell line that can be differentiated to a neuronal-like phenotype by exposure to nerve growth factor (NGF) in the presence of low serum media. PC12 cells are communication deficient, but through careful cloning we were able to isolate a clonal line that expresses low endogenous level of Cx32. The western blot in Figure 4 demonstrates that Cx32 protein levels progressively increase during NGF-induced neuronal differentiation. The band detected is just below the 32 kDa marker at 27 kDa, this is consistent with previous published results (Dermietzel et al, 1990). These data provided preliminary evidence to suggest that Cx32 can be expressed in partially committed neural precursors *in vitro*. Given that Cx32 plays a role in the differentiation of CNS cells as indicated by the literature and, may be involved in neuronal

differentiation in the PNS, as suggested by my honours thesis research, are alterations in CNS development associated with a loss of Cx32?

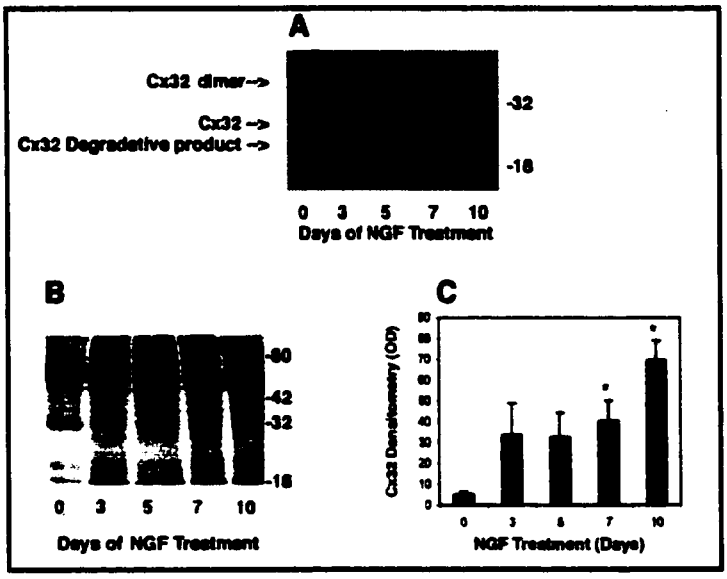

Figure 4. Cx32 protein levels increase following NGF-induced neuronal differentiation when PC12-AC cells. (A) A representative Western immunoblot following NGF treatment (Day 0-10). Low levels of Cx32 are detectable at Day 0. Expression of Cx32 protein increases between Day 3 and Day 10 of NGF treatment. Protein was extracted from cells plated at different densities such that the final cell count would be $1x10^5$/cells per dish on the day of extraction. **(B)** Commassie blue stained gel of the same proteins in A representing the loading control for the immunoblot in Panel A. **(C)** Densitometry on 5 separate immunoblots. The asterisks indicate that there is a statistically significant increase in Cx32 protein levels compared to Day 0. Data represents Mean ± SEM. [ANOVA, F-4.8; df=4, 20; $p<0.01$; Dunnett's post-hoc t-test, $p<0.05$]

The impact of endogenous Cx32 over expression and/or null mutation on neuronal differentiation have yet to be determined. Cx32 appears relatively late in certain regions of the developing brain, including the cerebral cortex (Dermietzel et al, 1989) and is implicated in differentiation, late neurogenesis, and neural circuit formation (Nadarajah & Parnalvelas, 1999). Despite the fact that, in mice, there are at least two gap junction proteins expressed by oligodendrocytes, their molecular diversity may not be functionally redundant. Therefore, studying the cerebral architecture of Cx32 deficient mice will provide further insight into the role of Cx32 in CNS development and differentiation.

Table 1. Cx Gene Expression and Related Genetic Disorders.

Table 1: Connexin (CX) Gene Expression and Related Genetic Disorders

Connexins	Group	Disease in Humans	Knockout mice	Reported Localization in Literature (Dermietzel &Spray, 1993; Willecke &Haubrick, 1996; Nicholson et al, 1999)
Cx26	β	Non-syndromic deafness	Embryonic lethality	Liver, Endometrium, Myometrium, Pancreas, Kidney, Testis, Neuroepithelium, Ependyma Pinealocytes, and Leptomeninges
Cx30	β	?	?	Brain, Skin
Cx31.1	β	Erythrokeratodermia or deafness	?	Skin
Cx36	β	?	?	Brain
Cx32	α	Charcot-Marie Tooth Disease (peripheral neuropathy)	Demyelinating peripheral neuropathy, hepatic tumours	Liver, Schwann Cells, Oligodendrocytes, (Neurons?), Kidney, Pancreas, Testis, and Endometrium
Cx37	α	?	Leads to infertility in female mice	Lungs, Endothelium, and Smooth Muscle
Cx43	α	Not viable	Die of cardiopulmonary anomalies shortly after birth	Heart, Myometrium, Lens Epithelial Cells, Pancreas, Skin, Kidney, Lung, Testes, and Astrocytes, Fibroblast, Ependyma, Neuroepithelium of Embryonic Brain
Cx45	α	?	?	Kidney, Skin and Myelinating Oligodendrocytes
Cx46	α	Hereditary Cataracts	Nuclear cataracts later in life	Lens Fiber Cells, and Schwann Cells
Cx47	α	?	?	Brain, Spinal Cord

1.2 NEUROGENESIS

In the CNS, complex patterns of gap-junctional communication are observed throughout neural development and are maximal during neurogenesis (the birth of new neurons) as reviewed above. Expression of distinct Cx family members during cerebral development may play a role in regional specification through the restriction and differential passage of molecules between glial and neuronal groups. It is interesting to note that electrotonic coupling between neurons decreases following the formation of synapses (Goodman & Spitzer, 1979), leading to the suggestion that there is a reciprocal relationship between the degree of coupling via gap junctions and the development of a neuronal phenotype (Rozental et al, 1993).

In early embryogenesis, local cellular interactions determine regionalization along the major axes of the embryo. The early framework of the primordial nervous system in vertebrate embryos is the result of gastrulation. The hollow blastula transforms into a multilayered embryo called the gastrula that produces the three embryonic germ layers at defined stages during development: endoderm, ectoderm, and mesoderm. Neural induction begins when the process of gastrulation forms the notochord (along the primitive pit) that sends inductive signals to the overlying ectoderm that cause a subset of ectodermal cells to differentiate into neural precursors or dividing stem cells. The neural tube eventually is formed and this gives rise to the CNS – the brain and spinal cord (Purves et al, 1997). Embryonic stem (ES) cells (or pluripotent stem cells) are electrically coupled during the blastocyte stage and are involved in neurogenesis, morphogenesis, and organogenesis. ES cells are a homogeneous proliferative precursor cell population derived from the inner cell mass (ICM) during the blastocyte stage. ES

cells become uncoupled as differentiating cell types diverge in function (Cameron & Rakic, 1991; Weissman, 2000; Watt & Hogan, 2000). These stem cells form the primitive neural tube and have unique properties such as the ability to migrate interstitially and the ability to differentiate into both neuronal and glial progeny (also known as multipotentiality) (for a review see Gage, 2000). Thus, it is hypothesized that environmental signals transferred via connexons (or hemichannels) and/or gap junctions may play an important role in stem cell fate.

Previously, the normal adult brain was considered to be in a state of post-mitotic quiescence. Certainly, most neurons in the adult CNS are terminally differentiated, exist through the life of the organism, and are not replaced when they die (Gage et al, 1995). Studies performed over the last ten years have identified neural progenitors/neural stem cell 'pools' in the adult brain not just at early stages of brain development (for a review see Gage, 2000). Thus, rare populations of neural stem cells are retained throughout life and are thought to participate in regeneration and repair. It is known that pluripotent cells in the developing CNS depend upon gap junctional communication for cell-cell communication in the absence of functional synapses (Rozental et al, 1998; Rozental et al, 2000; Belliveau & Naus, 1995). However, it still remains to be determined whether the rare adult neural stem cell relies on Cx-mediated communication. Furthermore, the Cx type(s) that are expressed in the stem cells, the possible changes that occur in Cx expression patterns during early development, and the functional implications of these changes on cellular differentiation have yet to be determined.

1.2.1 What is a neural stem cell?

The term "neural stem cell" describes precursor cells that are derived from the nervous system, have the capacity for unlimited self-renewal, and exhibit the potential for multi-lineage differentiation through asymmetric cell division. Asymmetric division produces one daughter cell that enters the pathway leading to differentiation and a second daughter cell that remains a proliferative self-renewing stem cell thereby sustaining the pool of proliferative cells. Stem cell potential is either toti- (capable of becoming any tissue or structure of the organism) or pluri- (open to diverse development). During development, progenitors become progressively more restricted in the cell types to which they can give rise (for a review see Gage, 2000).

The adult CNS retains immature progenitor cells that can give rise to progeny that divide, migrate, and differentiate into neurons, astroglia, and oligodendroglia (Gage et al, 1998; Kukekov et al, 1999; Luskin et al, 1997; Gage et al, 1995; Roy et al, 2000). Adult neural progenitors were first detected in the avian brain localized to distinct anatomical regions (Barnea & Nottebohm, 1989; Kirn & Nottebohm, 1993). Recent studies have identified an analogous population in adult human and rodent brains localizing to particular microenvironments: the subependymal zone (Kukekov et al, 1999; Luskin et al, 1997; Craig et al, 1999; Kirschenbaum et al, 1999; Chiasson et al, 1999), the DG of the hippocampal formation (Bayer et al, 1982; Fricker et al, 1999), and the olfactory epithelium (Lois & Allvarez-Bulla, 1994). The identification of adult mammalian neural stem cells is ground-breaking. Activation of these cells holds out the promise of new treatments for many types of neurodegenerative disease, such as stroke, Parkinson's and Alzheimer's diseases, epilepsy, spinal cord injuries, cancer, and multiple sclerosis. When

adult neural stem cells from mice are grown with embryonic cells *in vitro* or within an embryo *in vivo*, the adult stem cells revert to an unspecialized state and give rise to different cell lineages (Luskin et al, 1997; Roy et al, 2000; Kondo & Raff, 2000). Stem cells have the potential to repair missing cells and migrate to areas of damage, where they replace the depleted cells (Fricker et al, 1999). The limited capacity for structural repair in the mammalian brain is in part due to the inability of the mature CNS to generate new cellular elements in response to damage. Mammalian experiments show that neuroblasts and young postmitotic neurons obtained from defined parts of the neuraxis during development can survive, mature, and grow extensive functional axonal connections after transplantation to brain-damaged recipients, and both structurally and functionally replace lost neurons in the mature brain (Fricker et al, 1999). Because of the limited migratory capacity of differentiated cells, these types of implants have restrictions when integrating into the cellular architecture of the host. However, less differentiated precursors (premigratory stages of neuronal development) can make use of available endogenous or implanted substrates for activation of endogenous cells to promote "self-repair".

The pathways and lineages that neural precursors take in neurogenesis during development and adult life still need to be understood. It is possible that altering gap junctional communication during development might have an impact upon the number of neural stem cells retained into adulthood. Perhaps intercellular signals that pass through Cx32 or other Cx-mediated gap junction channels are essential for stem cell viability, proliferation, and/or differentiation.

1.2.2 Neural progenitors in the hippocampal formation

During the embryonic period, the postnatal period, and in adult brain, a high proportion of cells in the subgranular zone, the region between the hilus and the granule cell layer, and along the external limbs of the DG display signs of ongoing proliferation (as determined by BrdU labelling), migration, differentiation, and establishment of functional neuritic connections (Altman & Bayer, 1990). The rate of neurogenesis in the mouse subgranular zone of the DG greatly decreases with age (Gage et al, 1998; Kuhn et al, 1996; Kemperman et al, 1998). The estimated production of granule cells is approximately 85% of the total population being produced postnatally (Altman & Bayer, 1990). This finding suggests that neurogenesis in the DG is continuous into midlife, thus maintaining an equilibrium between production of new cells and neuronal loss (Gage et al, 1998; Kuhn et al, 1996).

It is likely that the adult mammalian DG of the hippocampal formation retains the capacity for self-renewal in order to maintain normal functions, like learning and memory (Gage et al, 1998; Roy et al, 2000). Recently, Gould et al (1999) reported that the proliferation of neural progenitors is elicited by hippocampus-dependent learning tasks in adult rats. Other studies have shown that behavioural enrichment improves the survival of new neurons generated in the DG (Kempermann et al, 1998; Gage et al, 1998). Thus, progenitor proliferation and differentiation may be associated with improved cognitive processes such as learning and memory (Peibner et al, 1999).

The granule cell population of the rat DG forms over an extended period that begins during gestation and continues into adulthood. New granule cells extend neurites along existing granule cell axons, called the mossy fiber pathway. These neurites project

through the hilus, into the CA3 cell field where they establish new functional connections with pyramidal cells (Figure 5; Parent et al, 1997; Gage et al, 1998; Gould & Cameron, 1996). The perforant path associated with memory originates in the entorhinal cortex (layer II) and terminates in the outer molecular layer of the DG; this pathway interconnects the hippocampus and neocortex (Morrison et al, 1997). With increasing age, the pyramidal cells in the entorhinal cortex and the CA1 and subiculum regions of the hippocampus become vulnerable to degeneration, whereas the CA3 region and the granule cells in the DG are resistant to age-related degeneration (Morrison et al, 1997). It is likely that the DG and CA3 resistance results from continued neurogenesis and replacement of damaged neurons by progenitors localized in the DG.

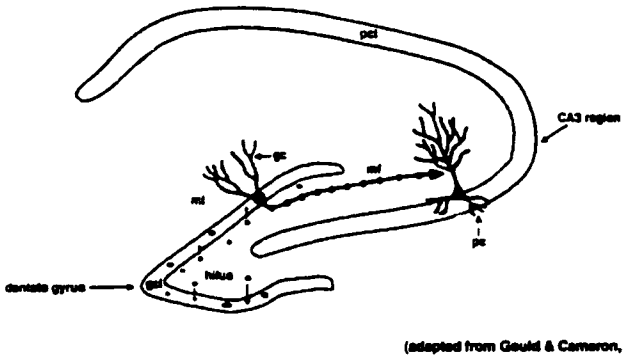

Figure 5. Diagrammatic representation of the anatomy of the hippocampal formation The granule cell (gc) somata are located in the granule cell layer (gcl), and their dendrites extend into the molecular layer (ml). The newborn granule cell axons extend neurites along the mossy fiber (mf) pathway, project through the hilus and synapse on the proximal dendrites of the pyramidal cells (pc) in the CA3 region. Radial glial cells guide the migrating dividing gc in the hilus to the gcl, their final destination, where neuronal differentiation is completed. (adapted by Gould & Cameron, 1996; Gage et al, 1998; Altman & Bayer, 1990; Parent et al, 1997)

1.3 OBJECTIVES and SUMMARY

The objective of this thesis is to test the hypothesis that Cx32 expression influences CNS development. To achieve this objective, the cerebral cytoarchitecture of adult KO mice was compared to that of WT mice to identify anatomical changes that arose as a result of cerebral development in mice lacking Cx32 protein. To date, we have demonstrated that KO mice exhibit morphological abnormalities, notably the appearance of an enriched population of hyperchromatic cells in the DG. We have characterized this population and present immunological and phenotypic data to indicate that these cells are likely an enriched population of neural progenitors. Finally, we demonstrate that the expression of several Cx family members is altered in the KO relative to the WT.

II. Materials & Methods

2.1 Generation of KO and WT mice

The generation and initial characterization of KO mice was performed in the laboratory of Dr. Klaus Willecke, (Universitat Bonn) as described in (Nelles et al, 1996). The genetic background of these mice is an undefined mix of 129sv and C57/BL6. To place the KO in a pure C57/BL6 genetic background, an extensive backcrossing program was performed in the laboratory of our collaborator Dr. David Paul (Harvard Medical School) by Drs. Caterino Sellitto and Steffany Bennett. In the short term, a reasonably accurate assessment of changes in cerebral morphology resulting from loss of Cx32 could be obtained from animals of mixed backgrounds as long as appropriate controls with a similar background were available. Heterozygote females were backbred into a C57Bl/6J (Harvard) background to the F2 generation. Time-matched matings of WT (x^+/x^-) and KO (x^-/y) breeding pairs were generated and littermates with identical genetic background analyzed in the studies described in this thesis. Genotypes were established by PCR analysis of genomic DNA isolated from tail clips.

KO (n=12) and WT (n=12) mice (3 months of age) were anesthetized with sodium pentobarbital and trans-cardially perfused with phosphate buffered saline (PBS: 10 mM phosphate buffer (PB), 154 mM NaCl, pH 7.2) followed by 4% paraformaldehyde in PBS. The brains were removed and post-fixed for 48-168 h in 4% paraformaldehyde and placed in 10mM PB pH 7.2 at 4°C. Tissue was embedded in paraffin according to standard histological procedure and serial coronal sections of 4 μm were cut on a rotary microtome. Alternatively, brains were post-fixed for 4 h in 4% paraformaldehyde in PBS.

2.2 Morphological Analyses

Serial 4 μm sections were cut through the midbrain (between bregma –1.26 to –3.76) of n=5 KO and n=5 WT 3 month old mice, Nissl-stained with cresyl violet or nuclei stained with Hoechst 33258, and examined by light or fluorescent microscopy (Olympus BH2 microscope). In preliminary studies, pyramidal layer in the hippocampal formation thickness was measured in digital photomicrographs of Hoescht-stained sections digitized at 100x magnification using ImagePro software.

2.3 Quantitative Analysis

2.3.1 Quantitation of the hyperchromatic cells in KO animals

To quantify the hyperchromatic cell population detected in KO mice, serial sections were assigned to one of six anatomically distinct levels. The six hippocampal levels quantified fall within the following ranges: level 1:bregma –1.26 to –1.66, level 2: bregma –1.68 to –2.08, level 3: bregma –2.10 to –2.50, level 4: bregma –2.52 to –2.92, level 5: bregma –2.94 to –3.34, level 6: bregma –3.36 to –3.76. Levels were defined by position from bregma according to the coordinates established by Franklin and Paxinos (1997). The hippocampal formation in each section was digitally captured at 200x magnification on a Olympus BH-2 microscope using a Sony DCC 3-chip digital colour camera on a Media Cybernetics running Image Pro Software version 3.01 (Carson, ON). In posterior sections, multiple images were captured and montaged to be able to visualize the entire hippocampal formation at the required magnification in a single image. Captured images were coded prior to analysis to ensure that the KO or WT identity of the

section was not known by the investigators performing cell counts. Two areas of interest (AOIs) were defined per image prior to counting: (1) the DG (including the polymorphonuclear layer) and (2) the CA pyramidal cell fields of the hippocampal formation. The area in μm^2 was determined for each AOI per image. The stratum oriens, stratum radiatum, laconosum moleculare, and molecular layer of the DG were excluded from further analyses. Cell profiles exhibiting hyperchromatic Nissl-stained bodies and oblong or oval shape often with discernable darkly stained neuritic extensions were identified and counted in the DG and pyramidal cell field AOIs of n=5 WT and n=5 KO animals by four different experimenters blind as to the KO or WT identity of the image. To accurately quantify these cell profiles, colour AOI images were converted to grayscale and a threshold was set by each experimenter that excluded cells falling below the normative staining intensity of the entire AOI. Cell profiles whose staining intensity exceeded this threshold were automatically quantitated using Image-Pro measurement module. Counts were then manually confirmed by each experimenter to establish that cell profiles scored as positives met the preset staining intensity criteria and the morphological criteria defining this population. The values obtained by the four independent assessors were averaged to yield a single measure per AOI per animal for use in further analyses. Data are expressed as the mean number of morphologically distinct, hyperchromatic cell profiles observed per 100 μm2 in the DG and pyramidal cell fields of WT and KO animals at each of six anatomical sections through the hippocampal formation.

2.3.2 Quantitation of immunoreactivity in the KO and WT DG

To quantify and compare the immunoreactivity of neural lineage markers observed in the DG of KO compared to WT mice, serial (4 μm) sections were cut between bregma –1.94 to –2.30. Sections were immmunoreacted with various lineage markers as described in 2.4. AOIs defining the DG (including the polymorphonuclear layer) was established prior to densitometric analysis. The DG in each section was digitally captured at 200x magnification on a Olympus BH-2 microscope using a Sony DDC 3-chip digital colour camera using Image Pro Software version 3.01 (Carson, ON). The area in μm^2 was determined for each AOI per image. Data are expressed as the percent area of the DG that exhibited immunoreactivity. To analyise the immunodensitometry of the KO and WT DG sections, colour AOI were converted to grayscale and a threshold was set by each experimentor. Staining intensity that exceeded the background threshold was quantified. Immunodensitometry was performed using ImagePro software by 3 independent assessors and then averaged to yield a single measurement per animal.

2.4 Immunohistochemistal Characterization.

2.4.1 Tissue Preparation

Paraffin-embedded sections were deparafinized in clearing solution (Stephens Scientific) and rehydrated through a series of graded alcohols followed by PBS. Sections were then incubated in 1% H_2O_2 for 30 minutes to inactivate endogenous peroxidases and epitope-unmasked by treatment with 1 mg/ml trypsin in 10mM PBS.

2.4.2 Antibodies

Sections were reacted overnight with the following primary antibodies at the indicated dilutions: Monoclonal anti-connexin32 M12.13; (Cx32; hybridoma supernatant kindly provided by Dr. David Paul, Harvard Medical School), 1:2; Monoclonal anti-neurofilament 160 (NF160) Sigma, 1:40; Monoclonal anti-nestin, Chemicon, 1:25; Polyclonal anti-galactocerebroside (GalC), Sigma, 1:50; Monoclonal anti-A2B5, ATCC, hybridoma supernatant, 1:10; Polyclonal anti-growth associated protein 43 (GAP-43), Chemicon, 1:100; Monoclonal anti-beta-tubulin isotype III (TuJ1), Research Diagnostics Inc., 1:125; Monoclonal anti-microtubule associated protein 2 (MAP2), Sigma, 1:125; Monoclonal anti-proliferating cell nuclear antigen (PCNA), Sigma, 1:1500; Polyclonal anti-glial fibrillary acidic protein (GFAP), Sigma, 1:50; Monoclonal anti-Nuclear protein (NeuN), Chemicon,1:50. Primary antibodies were incubated overnight at 4°C. The sections were washed in 10mM PBS (pH 7.2) and incubated for 1 hour at room temperature (RT) with secondary antibody conjugated with either anti-mouse IgG biotin conjugate (1:300, Sigma), or anti-rabbit IgG biotin conjugate (1:800, Sigma). Sections processed with biotin-conjugated secondary antibodies were incubated with ExtraAvidin-Peroxidase (1:50, Sigma) for 1 hour at RT. Primary, secondary, and tertiary antibodies were diluted in Ab buffer (10mM PBS, 0.3% Triton-X, 3% BSA, pH 7.5). Peroxidase-processed sections were incubated with 0.5 mg/ml 3,3-diaminobenzidine tetrahydrochloride (DAB) with or without 0.2 mg/ml metal enhancer (cobalt chloride) to visualize immunoreactivity. The reaction products of peroxidase yielded a blue/black and brown colour respectively. Sections were coverslipped with Permount (Fisher). The sections were

examined and photographed using an Olympus BH2 microscope at 20X and 40X objective.

2.5 Colony assay of neural precursor cultures

Primary neural precursor cultures were prepared from adult WT and KO mice at 3 months of age. Mice (n=3 animals/experiment) were anesthetized with pentobarbital. Hippocampi were dissected in Dissection Media (10 mM phosphate buffer, 154 mM NaCl, 2 mM glucose, 200 U/ml penicillin streptomycin) and rocked on a clinical orbitor until all samples could be collected. Tissue was transferred to a sterile 15 ml polystyrene tubes containing 3 ml 0.05% Trypsin/0.53 mM EDTA (1x, Invitrogen) and passed repeatedly through a 5 ml pipette. Additional 10x Trypsin/EDTA (2.5 ml) was added to each suspension. Tubes were rotated at 37°C for 10 min and incubated at room temperature for up to additional 20 min. Nine ml of Plating Media consisting of Neurobasal medium with B27 supplement (100 U/ml), 10% heat-inactivated fetal calf serum, 10% heat-inactivated horse serum, and 100 U/ml penicillin/streptomycin was added to each tube. Suspensions were transferred to sterile 50 ml polypropylene tubes and passed repeatedly through a 10, 5, and 1 ml pipette followed by trituration through a glass bore pasteur pipette. Cells were centrifuged and resuspended in 20 ml Plating Media. Trypan blue hemocytometer counts were performed. Cultures were not plated unless >95% of cells excluded the dye after the dissociation procedure. Primary cultures were plated at a density of $5x10^5$/cells ml in 4 well Lab-Tek culture slides (1 ml/well) coated with poly-D-lysine (50 µg/ml in double distilled H_20). On the following day, the media was changed to Maintenance Media consisting of Neurobasal medium with B27

supplement (100 U/ml), 100 U/ml penicillin/streptomycin, and basic fibroblast growth factor (bFGF; 20 ng/ml). After 7 days of cultures, cells were fixed in 4% paraformaldehyde in 10 mM PBS for 10 min and immunoreacted as described above with polyclonal anti-enolase (1:10, Calbiochem), monoclonal anti-NeuN (1:50, Chemicon), and monoclonal anti-nestin (1:50, Chemicon). Cultures were doublelabelled with anti-enolase and anti-nestin using FITC and Cy3 conjugated secondaries (1:600 and 1:800, Jackson) respectively. Colonies > 7 cells were analyzed. In some cases, colonies treated for 7 days with bFGF were differentiated for an additional 5 days in Neurobasal M edia supplemented with B27 supplement (100 U/ml), 100 U/ml penicillin/streptomycin, and brain derived neurotrophic factor (BDNF)

2.6 Reverse Transcriptase and PCR of KO and WT mice RNA

2.6.1. Isolation of total RNA

Hippocampi, subventricular zone, thalamus, hypothalamus, occipital lobe, entorhinal cortex, frontal cortex, parietal/temporal cortex, cerebellum, striatum, and brainstem were dissected and pooled from KO (n=2-4) and WT (n=2-4) animals per experiment. Samples were processed immediately or stored at –80°C. Total RNA was isolated in Trizol (Invitrogen) according to the manufacturer's protocol. Analyses were conducted in replicate or triplicate using different RNA samples

2.6.2. Reverse Transcription

Total RNA was reverse transcribed and PCR amplified to ascertain the presence of the mRNA of interest. 5 ug RNA was treated with RQI RNase-free DNase (0.15 U/ul; Promega) for 30 min at 37°C according to manufacturer's protocol. First-strand cDNA

synthesis was performed using random nucleotide primers (20 pmol pdN6, Promega) in the presence or absence of Superscript II reverse transcriptase (Invitrogen) to confirm lack of genomic DNA contamination according to the manufacturer's protocol.

2.6.3 Polymerase chain reaction(PCR) amplification of RT products.

Primers were designed to amplify Cx26, Cx30, Cx31.1, Cx32, Cx36, Cx37, Cx43, Cx45, Cx46, Cx47, nestin and GAPDH (Table 2). Optimal PCR conditions were established for each Cx primer pair using mouse genomic DNA template. Following primer optimization, detection of transcript in KO and WT samples was established by RT-PCR. PCR amplification of Cx26 and Cx43 was performed in reactions containing forward and reverse primers Cx26 (25 pmol), or Cx43 (25 pmol), dNTPs (0.125 mM each, Promega), dithiothrietol (DTT; 10 mM), 1x buffer (Invitrogen). 1 mM $MgCl_2$, and 2.5 U DNA Taq Polymerase (Invitrogen). PCR amplification of Cx30, Cx31.1, Cx32, Cx36, Cx37, Cx45, Cx46, Cx47, Nestin, and GAPDH was performed in reactions containing forward and reverse primers Cx30 (200ng/ul), Cx31.1 (200ng/ul), Cx32 (200 ng/ul), Cx36 (200ng/ul), Cx37 (200 ng/ul), Cx45 (200 ng/ul), Cx46 (200 ng/ul), Cx47 (25 pmol), Nestin (25 pmol), or GAPDH (10 pmole), dNTPs (0.125 mM each, Promega), 1x PCR buffer (Clontech), and Amplitaq Taq Polymerase (1 U, Clontech). PCR amplification of Cx26 and Cx43 was performed under the following conditions: 3 minutes at 94°C, 30 cycles of 30 seconds at 94°C, 90 seconds at 55°C, 2 minutes at 72°C. PCR amplification of Cx30 and Cx31.1 consisted of the following conditions: 3 minutes at 94°C, 30 cycles of a two step protocol consisting of 30 seconds at 94°C, 2 minutes at 65°C. PCR amplification of Cx32 and GAPDH consisted of the following conditions: 3 minutes at 94°C, 30 cycles of 30 seconds at 94°C, 1 minute at 60°C, 2 minutes at 72°C.

PCR amplification of Cx36 consisted of the following conditions: 3 minutes at 94°C, 30 cycles of 30 seconds at 94°C, 90 seconds at 69°C, 2 minutes at 72°C. PCR amplification of Cx37, Cx45 and Cx46 consisted of the following conditions: 3 minutes at 94°C, 30 cycles of 30 seconds at 94°C, 1 minute at 60°C, 2 minutes at 72°C. PCR amplification of Cx47 consisted of the following conditions: 3 minutes at 94°C, 35 cycles of seconds at 94°C, 2 minutes at 65°C, 2 minutes at 72°C. PCR amplification of Nestin consisted of the following conditions: 3 minutes at 94°C, 30 cycles of 30 seconds at 94°C, 1:30 minutes at 60°C, 2 minutes at 72°C. For all PCR reactions an additional extension at 72°C for 7 minutes was performed and the samples were kept at 4°C thereafter. All PCR reactions were performed in a Perkin-Elmer 2400 thermal cycler. PCR products were electrophoresed through a 1.5 % agrose gel, stained with ethidium bromide and photographed on a MultiImage™ Light Cabinet (Alpha Innotech Corporation) gel documentation system.

Statistical Analysis

Data were analyzed using two-way factorial analysis of variance (ANOVA) tests (multiple comparisons) or unpaired Student's t-tests (two group comparisons) as applicable. Following detection of a statistically signifcant F value, post hoc Tukey tests were performed to detect which comparison differed from control . Unpaired student t-tests were used to detect differences between two indendent groups. P values of <0.05 were considered statistically significant (as shown as *); P values of <0.01 were considered highly statistically significant (shown as **).

Table 2. Primer pairs used to amplify Cx and GAPDH mRNA from KO and WT brain areas.

Primer Name	Strand	Primer Sequence (5'-3')	Amplicon length
Cx32FB	forward	5'CGCCTCTCACCTGAATACAA'3	223 bps
Cx32FB	reverse	5'TGTTCACCAGCATAGGAGAA'3	
Cx32 (1065)	forward	5'GTGGCGTGAATCGGCACTCTAC'3	593 bps
Cx32 (1066)	reverse	5'CTCCGCCACGTTGAGGATAATG'3	
Cx32DP	forward	5'CTGCTCTACCCGGGCTATGC'3	386 bps
Cx32DP	reverse	5'CAGGCTGAGCATCGGTCGCTCTT'3	
Cx26FB	forward	5'GGATGTGGCAGTCAGTATCA'3	368 bps
Cx26FB	reverse	5'TCTTGGCAGGAAGAAGTGTC'3	
Cx30 (1074)	forward	5'GCCAGGGTGCAAGAACGTCTGC'3	535 bps
Cx30 (1073)	reverse	5'GGCATGGTTGGGTGGTTTCTC'3	
Cx31.1 (1084)	forward	5'AGCGGGGTGGACTCTGGTGG'3	734 bps
Cx31.1 (1083)	reverse	5'TTGCTCATCGGTGCCTTCGTG'3	
Cx36 (1088)	forward	5'AGCGGAGGGAGCAAACGAGAAG'3	533 bps
Cx36 (1087)	reverse	5'CTGCCGAAATTGGGAACACTGAC'3	
Cx37 (1062)	forward	5'AGAGCGGTTGCGGCAGAAAGAGG'3	551 bps
Cx37 (1061)	reverse	5'TGGATGAGAGCCCGTTGTAGGTG'3	
Cx43	forward	5'CCTGCCGCAATTACAACAAG'3	201 bps
Cx43	reverse	5'AAGGTCGCTGATCCACGATA'3	
Cx45 (1092)	forward	5'GAGGTGGGCTTTCTAATAGGGCAG'3	528 bps
Cx45 (1091)	reverse	5'ATGGGGGTTGTTTTGGTGATGG'3	
Cx46 (1054)	forward	5'TCTACGCCCACCCTCATCTATCTG'3	782 bps
Cx46 (1053)	reverse	5'GGCTTGCTGGCTGGAGTCTGC'3	
Cx47	forward	5'CGGTGGTGAGTCCATCTATT'3	692 bps
Cx47	reverse	5'CGTACATGACCAGCAAGAAG'3	
Gapdh	forward	5'TGGTGCTGAGTATGTCGTGGAGT'3	292 bps
Gapdh	reverse	5'AGTCTTCTGAGTGGCAGTGATGG'3	

III. RESULT S

3.1 Anatomical abnormalities detected in the midbrain of KO mice.

In our first series of analyses, we compared serial coronal sections (4 μm) of 3 month old KO mice to age-matched C57Bl/6 mice. Morphological abnormalities in the midbrain of KO mice (n=3) were detected as compared to C57BL/6 (n=3) animals. Pilot studies using sections between bregma –1.6 to bregma –2.4 indicated that the pyramidal cell layer was approximately 1.5 to 2-fold thicker in all CA cell fields and grossly hyperchromatic compared to C57BL/6 mice, apparently as a result of the dense packing of pyramidal cell bodies (compare Figure 6 A and E for overall hippocampal morphology; Figure 6 B and F for CA1 thickness and density; Figure 6 C and G for CA3 thickness and density). Qualitatively, it appeared that the number of pyramidal neurons was increased in the KO mouse. Perhaps even more striking was the disruption of midbrain cytoarchitecture in KO mice. A disorganization of the medial layer of CA1 was evident in KO animals possibly contributing to an inappropriate expansion of posterior subicular neurons (arrowhead, Figure 6A). These cells are not present in sections between bregma –1.6 to bregma –2.4 in control C57/B mice (compare arrowhead in Figure 6 A and 6 E). Furthermore, ventricular disruption was evident in KO midbrain with a striking compression of the dorsal third ventricle and profound alteration in habenular cytoarchitecture (compare Figure 6 D and 6 H). This compression appeared qualitatively to be the result of an increase in the number of thalamic neurons in medial midbrain (data not shown). We hypothesized that loss of free passage through the dorsal third ventricle led to an expansion of the ventricular passage ventral to the hippocampus proper (compare arrows in Figure 6 A and E).

We were aware that these preliminary studies were confounded by the genetic background of the KO mouse, an undefined mix of 129sv and C57BL/6. The adult 129 mouse exhibits some fundamental anatomical and behavioural differences relative to the C57Bl/6 animal. Notably, these differences include alterations in corpus callosum thickness, ventricle morphology, and hippocampal cytoarchitecture (Livy & Wahlsten, 1997; Walsten, 1982). The behavioural corollary of these and other morphological differences is impairment of 129 mice on working and learning memory tasks, a lower seizure threshold, and enhanced susceptibility to ischemic and anoxic neuropathological insult compared to C57BL/6 animals (Royle et al, 1999; Contet et al, 2001; Fujii et al, 1997; Tankersley et al, 1994). Salient to this thesis, Kempermann et al (1997) revealed that the C57BL/6 mice differed significantly from other strains, with a ~ 1.5-fold higher proliferative activity of resident neural stem cells in the hippocampus. Thus, we could not definitively state that the cytoarchitectural alterations observed in our pilot study results from the loss of Cx32 during cerebral development. Changes in cerebral morphology could simply represent pre-existing strain differences. To accurately assess cerebral changes in the KO mouse, we backbred our KO animals into a C57Bl/6 lineage and raised appropriate WT controls from pairing of Cx32 heterozygous pups. Genetically matched littermates were used at the F3 generation to perform subsequent studies.

To confirm the identity of our backbred KO and WT littermates, genotyping was performed on the progeny using PCR primers that detect a 1300 bp amplicon of the KO allele and a 750 bp amplicon of the WT allele (Figure 7 A). These results were confirmed by RT-PCR using RNA template and protein extracted from whole brain (i.e not

dissected into anatomical regions) of KO and WT mice (Figure 7 B, left panel). The absence of genomic DNA contamination and reagent contamination was demonstrated by performing appropriate parallel control reactions (i.e. RT reactions carried out in the absence of enzyme to detect genomic DNA contamination in the RNA template and PCR carried out in the absence of template to detect reagent contamination (Figure 7 B, right panel)).

With these appropriate strain controls, we repeated our histological analyses of Nissl-stained serial midbrain coronal sections (4 μm). KO and WT animals were 3 months of age at the time of analysis. In this second analysis, we failed to detect the striking gross anatomical differences noted our pilot study. These observations underline the importance of analyzing WT littermates or establishing genetically matched colonies when evaluating CNS alterations in KO mice.

In our third analysis, we focused our attention on a single anatomical structure. The hippocampal formation is one of the most 'plastic' structures in the adult CNS and is associated with memory and learning (West et al, 1994). RT-PCR and Western analysis were performed on dissected hippocampi (dorsal and ventral) pooled from n=3 mice per group to confirm expression of Cx32 transcript (Figure 7 C) and protein (Figure 7 D). Cx32 mRNA and protein was detected in WT mice but, as expected, was absent in KO littermates. Control reactions included PCR carried out in the absence of template to detect reagent contamination (Figure 7 C, no template). GAPDH was amplified from the same RT product used to detect Cx32 to demonstrate template integrity of both KO and WT products (Figure 7 C). Control immunoblots were performed in the absence of primary antibody to detect nonspecific bands recognized by the secondary antibody and

tertiary reagent (Figure 7 D, no primary control). A specific Cx32 band with the expected mobility of 27 kDa was detected in the hippocampal formation of WT, but not KO mice.

Morphological analysis of Nissl-stained midbrain sections containing dorsal hippocampus demonstrated an obvious enrichment of intensely stained cells in the DG and pyramidal layers of the hippocampal formation. This enrichment was seen in 10 out of 12 KO mice analyzed. Figure 8 demonstrates numerous hyperchromatic cells in the polymorphonuclear layer and infra- and suprapyramidal blades of the DG in KO animals (Figure 8 A). Infiltration of these cells into the CA3c and CA1 fields of the hippocampal formation was noted in anterior hippocampal sections (see Figure10 F). Figure 8 C depicts a magnified view, of pyramidal cells in the CA3c field of the hippocampus and granule cells in the DG from 3 different KO and WT animals. Note that WT animals exhibit hyperchromatic cells with comparable morphology to the enriched population detected in KO animals, albeit at lower frequency (compare Figure 8 C KO and WT). In previous studies, cells with a similar staining phenotype in WT mice have been shown to be capable of self-renewal and differentiation following injury and kainic acid-induced seizures; a phenotype indicative of neural stem cells and partially committed neural precursors (Gray & Sundstrom, 1998). Thus, the location and staining pattern of the enriched population in the KO mouse is consistent with that of neural stem cells and/or neural precursors known to be present in the subgranular zone and hilus of the hippocampus in all mouse strains, although at extremely low levels (Kuhn et al, 1996; Eriksson et al,1998; Kempermann et al, 1997).

Figure 6. The midbrain of the 129/C57Bl KO mouse is cytoarchitecturally different from a WT C57Bl mouse. Coronal sections of the dorsal hippocampal formation (between bregma -2.10 to -2.30) of 3 month old mixed breed KO (A-D) and C57Bl WT (E-H) mouse. Note that the overall layering in the hippocampal formation (A,E), specifically in the CA1 (B,F) and CA3c (C,G) pyramidal layer, is thicker in the KO and the cells are more densely stained relative to a WT C57Bl mouse (compare arrows in A and E). (D,H) depict ventricular abnormalities and habenular displacement in the KO relative to a WT C57Bl mouse.

B,F
C,G
A,E
D,H
A
E
B
F
C
G
D
H

Figure 7. Genotype and expression analysis of the KO mouse backbred into a C57Bl background. **(A)** Genotyping of KO and WT littermates using PCR primers that detect a 1300 bp amplicon of the KO allele and a 750 bp amplicon of the WT allele. **(B)** The left panel depicts RT-PCR for Cx32 using KO and WT whole brain RNA template. Primers detect a 593 bp amplicon of WT Cx32. The right panel depicts WT control RT-PCR reactions demonstrating the absence of genomic DNA contamination (-RT) or reagent contamination (no template) in WT reactions. **(C)** The left panel depicts RT-PCR for Cx32 using RNA extracted from KO and WT hippocampal formation (n=3 animals/sample). The right panel depicts RT-PCR for GAPDH amplified from the same RT product used to detect Cx32 to demonstrate integrity of both KO and WT RNA template. **(D)** The left panel depicts an immunoblot of hippocampal protein (n=3 animals/sample) confirming that there is no Cx32 protein in the KO, but that protein is present in WT mice. The right panel depicts a control immunoblot processed in the absence of primary antibody to detect nonspecific bands recognized by the secondary antibody and tertiary reagent.

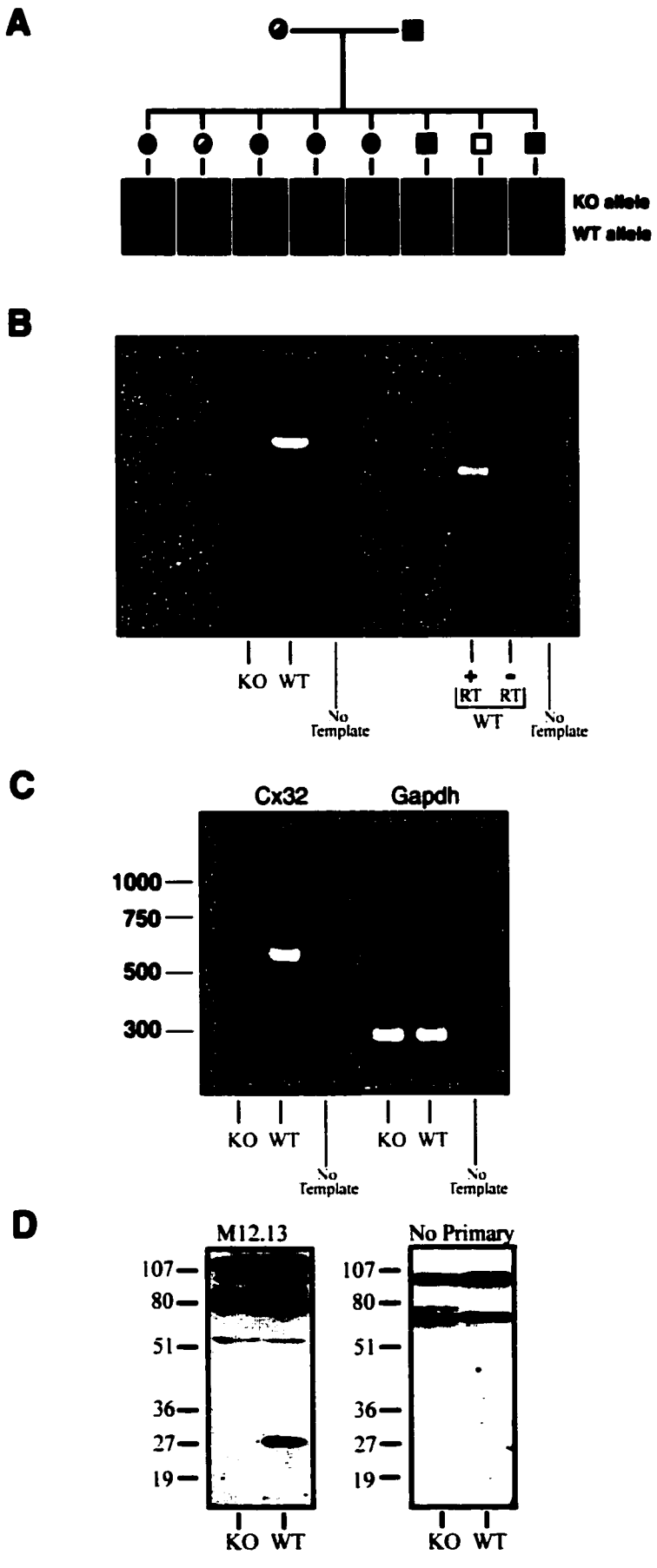
A
KO allele
WT allele
B
KO
WT
No Template
+ RT
- RT
WT
No Template
C
Cx32
Gapdh
1000
750
500
300
KO
WT
No Template
KO
WT
No Template
D
M12.13
No Primary
107
80
51
36
27
19
KO
WT
KO
WT

Figure 8. Nissl (cresyl violet)-stained sections of hippocampus from KO and WT mice. (**A**) An enrichment of hyperchromatic cells (arrow) is noted in the superior and inferior limbs of the DG in KO mice. The enriched cell population can be distinguished from other cells on the basis of hyperchromaticity and morphology. (**B**) WT littermate at the same level of hippocampus. (**C**) Higher magnification of hyperchromatic cells in three KO and WT animals. Note that rare hyperchromatic cells can be detected in WT sections with a substantial increase in the number of intensely stained cells noted in the CA3c pyramidal cell layer and granule cell layer of the DG of KO sections.
(A,B, Scale bars, 200 μm, C Scale bars 30 μm)

A

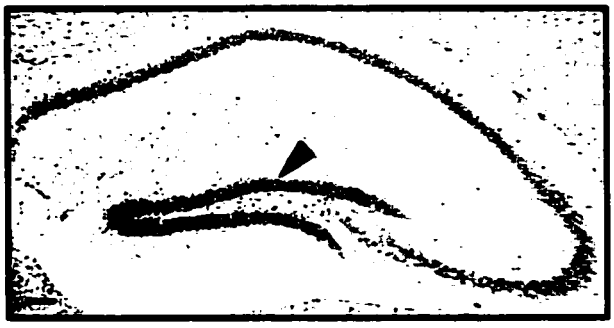

KO

B

WT

C

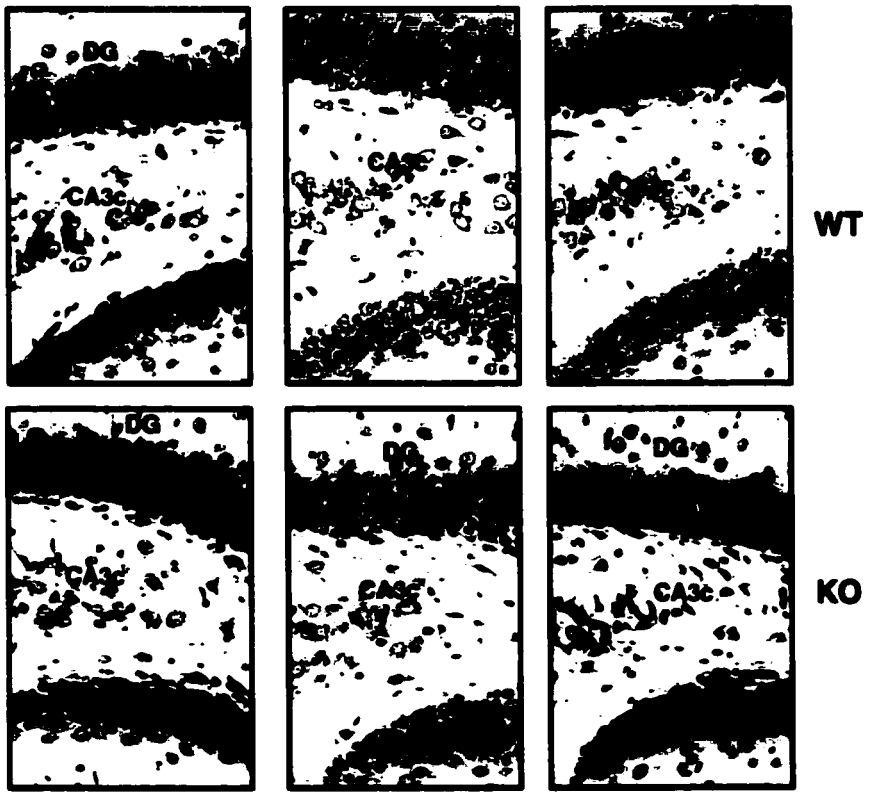

3.2 Quantitation of the hyperchromatic cell population in hippocampal formation of KO and WT mice

To quantify the hyperchromatic population detected in KO and WT hippocampal formation, serial 4 μm sections were cut through the midbrain of n=5 KO and n=5 WT 3 month old mice. Figure 9A depicts the location of the hippocampus in the adult mouse brain. Sections were Nissl-stained with cresyl-violet and assigned to one of six anatomically distinguishable levels (indicated in Figure 9 B and 10 E) according to the Franklin and Paxinos (1997) coordinates. Coronal section were cuts starting from anterior to posterior midbrain, as depicted in Figure 9 B. The enriched cell population was distinguished from other cells in the pyramidal cell fields and the DG based on hyperchromaticity using Image-Pro software by 4 independent evaluators. The hippocampal formation in each section was digitally imaged at 200x magnification and reconstructed as a digital photo-montage. Representative sections are depicted in Figure 10 F. Cell profiles exhibiting hyperchromatic Nissl-stained bodies and oblong or oval shape often with discernable darkly stained neuritic extensions were identified using Image-Pro software. Cells located in the pyramidal cell fields and the DG (Figure 10 E) were selected (Figure 10F, hyperchromatic cells are indicated in red). Values obtained by each investigator were averaged to yield a single data point per area of interest (DG or pyramidal cell fields) per section. Quantitative results are presented in Figure 10 A and C, respectively. Data are expressed as the mean number of hyperchromatic cell profiles observed per 100 μm^2 in the DG and pyramidal cell fields of KO and WT animals at each of the six anatomical sections through the hippocampal formation. Figure 10 B and D demonstrate that the area of DG and pyramidal cell fields of KO and WT are equal indicating that all sections were obtained at the appropriate level and that there were no

gross morphological abnormalities in hippocampal size between KO and WT. Note the 3-fold increase in hyperchromatic cell profiles in the DG of KO relative to WT animals (Figure 10 A). While all KO animals accumulate these hyperchromatic cells in the DG and CA3c cell fields, penetrance into the CA3a-b cell fields, CA2, and the dorsal aspect of CA1 is only observed at anterior levels (Figure 10 C). There was no obvious difference in the thickness of neuronal layers in the KO DG or pyramidal cell layers relative to WT. This observation suggests that there are not more neurons in the hippocampal formation of KO mice, but rather that a subpopulation of these hyperchromatic cells have not differentiated into morphologically 'normal' adult neurons. This hyperchromatic population is restricted primarily to the DG, a region known to exhibit neurons with proliferative capacity in WT animals following hippocampal damage.

Figure 9. Location of the hippocampal formation and anatomical levels chosen for further analysis in the murine brain. **(A)** Location of the hippocampal formation in mouse brain. **(B)** Serial coronal sections (4 μm) were cut from anterior to posterior through the midbrain of n=5 KO and n=5 WT 3 month old mice. Six anatomical levels were chosen for further analysis (a to f).

A

B

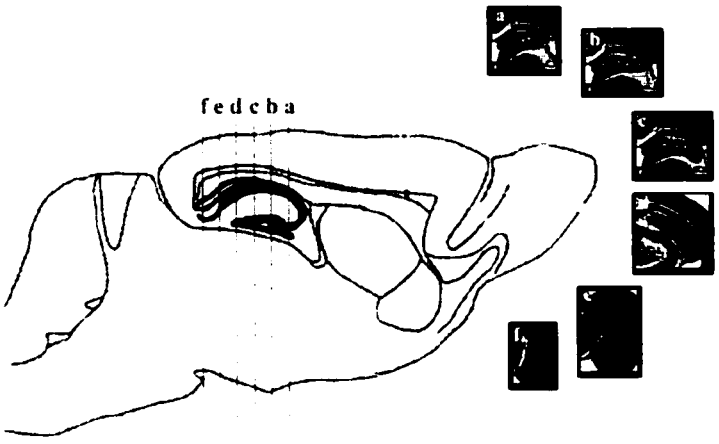

Figure 10. Quantitation of the hyperchromatic cells in KO and WT mouse hippocampal formations. Morphologically distinct cell profiles in both the DG and pyramidal cell layers were counted at six distinct anatomical levels. DG: Dentate gyrus; CA1, CA2, CA3: Pyramidal cell fields. **(A,C)** Quantitation of the hyperchromatic subpopulation in DG and CA1 pyramidal cell fields of WT and KO animals at each of six levels. Data are expressed as the mean number of morphologically distinct, hyperchromatic cell profiles observed per 100 μm^2as described in Materials and Methods. **(B,D)** Area of DG and pyramidal cell fields. **(E)** Schematic of the hippocampus at level 1: bregma –1.26 to –1.66, level 2: bregma -1.68 to –2.08, level 3: bregma – 2.10 to –2.50, level 4: bregma -2.52 to –2.92, level 5: bregma -2.94 to –3.32 and level 6: bregma 3.36 to –3.76 (adapted from Franklin & Paxinos, 1997). The red shading represents AOI analyzed to determine the number of hyperchromatic cells in both the DG and in the polymorphonuclear layer of DG. The pink shading represents the AOI analyzed to determine the number of hyperchromatic cells in the pyramidal cell field in CA1, CA2, and CA3. **(F)** Detection of hyperchromatic cells (red) using ImagePro software in six representative KO and WT hippocampal sections. (Scale bars, 100 μm) Data represents Mean ± SEM. [ANOVA, Tukeys test, $p<0.05$]

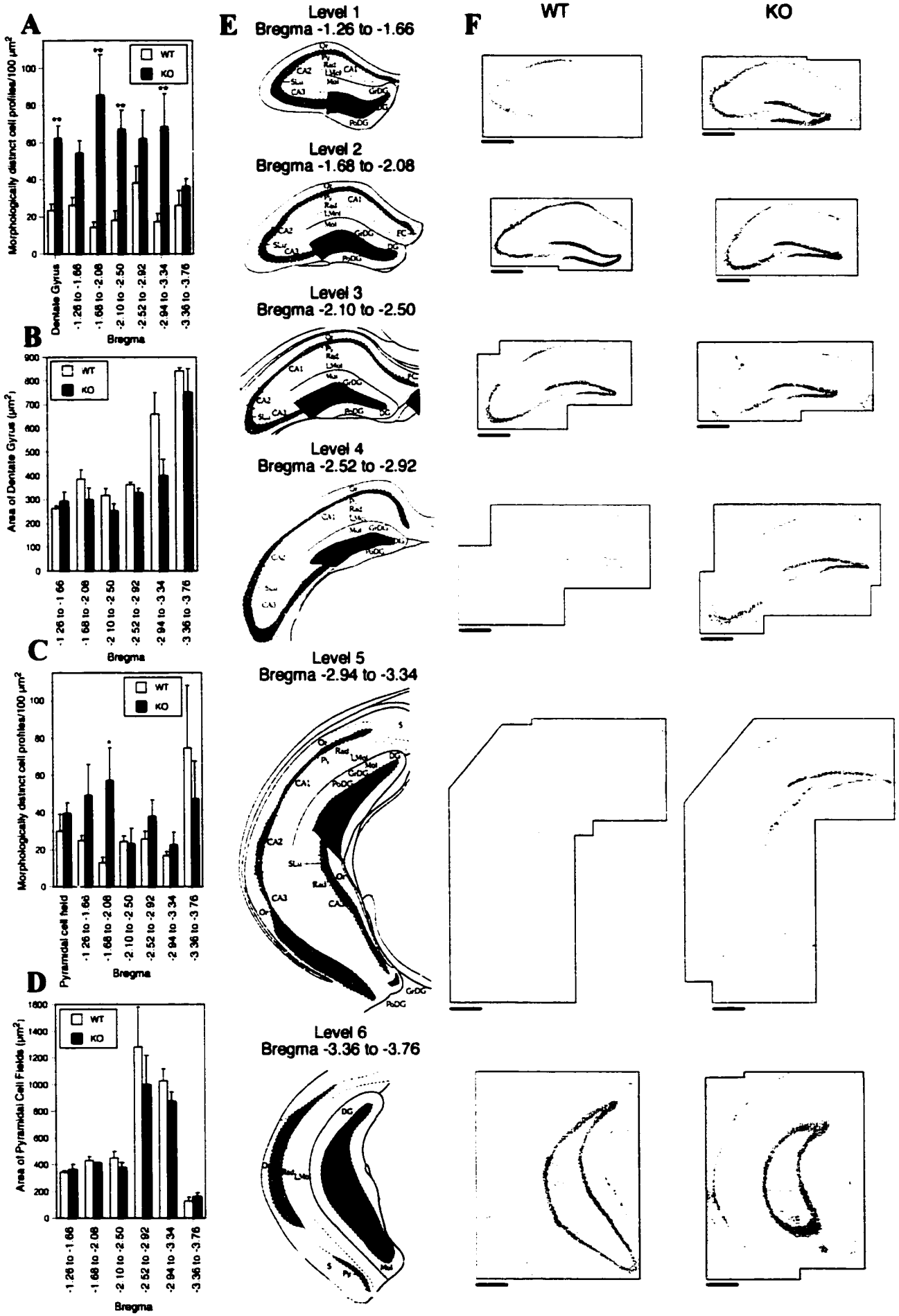
A
Morphologically distinct cell profiles/100 µm²
WT
KO
Dentate Gyrus
-1.26 to -1.66
-1.68 to -2.08
-2.10 to -2.50
-2.52 to -2.92
-2.94 to -3.34
-3.36 to -3.76
Bregma
B
Area of Dentate Gyrus (µm²)
C
Morphologically distinct cell profiles/100 µm²
Pyramidal cell field
D
Area of Pyramidal Cell Fields (µm²)
E
Level 1
Bregma -1.26 to -1.66
Level 2
Bregma -1.68 to -2.08
Level 3
Bregma -2.10 to -2.50
Level 4
Bregma -2.52 to -2.92
Level 5
Bregma -2.94 to -3.34
Level 6
Bregma -3.36 to -3.76
F
WT
KO

3.3 Characterization of lineage markers in the KO and WT hippocampal formation by immunohistochemistry and Western analysis

Serial midbrain coronal sections (4 μm) through the KO and WT mice hippocampal formation were analyzed *in situ* with antibodies that recognize various cell lineages (i.e. astrocytes, oligodendrocytes, and neurons at various stages of differentiation). To confirm these immunohistochemical results, protein was extracted from microdissections of the hippocampal formation for Westerns. In some cases, the dorsal DG and the CA3c pyramidal cell field located within the limbs of the DG were separated by microdissection and analyzed separately. The following antibodies were used: nestin (marker of neural progenitors, Osada et al, 1995; Messam et al, 2000), proliferating cell nuclear antigen (PCNA; marker of actively dividing cells, Jin et al, 2001; Gobetto et al, 1995), A2B5 (marker for bipolar oligodendrocyte precursor cells, Schnitzer & Schachner, 1982; Eisenbarth et al, 1979), 04 (marker for dividing pre-oligodendrocytes, Sasaki et al, 2000), growth associated protein 43 (GAP43; marker for proliferating neuroblasts, oligodendrocyte pre-progenitors and progenitors, McIntosh & Parkinson, 1990; Mani et al, 2001), microtubule-associated protein 1 (MAP1; marker for differentiated neurons and glia, Bernhardt et al, 1985), class III beta-tubulin isotype (TuJ1; marker for neural progenitors committed to a neuronal lineage, Lee et al, 1990), neuronal nuclear protein (NeuN; marker for terminally differentiated adult neurons, Mullen et al, 1992; Wolf et al, 1996), neurofilament 160 (NF160; marker for terminally differentiated adult neurons (Angeletti et al, 1985; Lee, 1985), glial fibrillary acidic protein (GFAP; marker of astrocytes, Repressa et al, 1993; Niquet et al, 1994), and galactocerebroside (GalC; marker of differentiated oligodendrocytes, Rostami et al,

1984). The specificity of the immunohistochemical reactions were confirmed by incubating adjacent sections with secondary and tertiary reagents in the absence of primary antibodies. No immunoreactivity was detected in these controls (data not shown).

Nestin. Nestin is an intermediate filament (class IV) expressed in precursor cells of several cell types and is associated with germinal centers in the developmental progression of the mammalian brain (Gage et al, 1998; Osada et al, 1995). Nestin is transiently expressed during neurogenesis, restricted initially to neuroepithelial cells and radial glia and later to neural progenitor cells (Hockfield & McKay, 1985; Frederiksen and McKay, 1988; Lendahl et al, 1990; Doetsch et al, 1997). In rat brain, nestin expression appears at the time of neuronal migration from E11 and diminishes by P6 in the spinal cord and by P21 in the cerebellum (Messam et al, 2000). If nestin immunoreactivity is enhanced in KO animals, then it is likely that the enriched population is composed of neural stem or progenitor cells. Figure 11 A,C show the hyperchromatic cells in cresyl violet-stained sections of the dorsal KO and WT hippocampal formation between bregma -1.94 to -2.30. Figure 11B,D are adjacent sections within 8 μm stained with anti-nestin. Arrows depict some representative nestin-positive cells (Figure 11 B,D). Note that the number of nestin-positive cells is enriched in the KO mouse relative to the WT. It is important to state that we cannot definitely conclude that the hyperchromatic population is double-labelled with anti-nestin. The intensity of anti-nestin staining was extremely faint and required cobalt-enhancement of the DAB substrate to be detected. Given this technical constraint, we were unable to reliably detect immunolabelling in sections counter-stained with cresyl violet (data not

shown). Our ability to detect some nestin-positive cells in the WT brain, albeit lower frequency than KO, is consistent with demonstrations that cells with comparable morphology are capable of regeneration in the damaged WT DG (Gray & Sundstrom, 1998). The reliability of our observations was confirmed by densitometric analysis of the DG from n=7 sections and n=8 sections from n=4 KO and WT mice between bregma -1.94 to bregma -2.30. Data are presented as the mean percent area exhibiting staining ± standard error of measurement (SEM) of the KO and WT (Figure 11 E). A statistically significant increase in nestin-positive imunoreactivity was observed in the KO as compared to the WT. Figure 12 depicts a magnified view (60X) of the nestin-positive cells found in the DG of the hippocampus of KO and WT mice.

Enrichment in nestin immunoreactivity in KO animals was confirmed by Western analysis. Lysates were extracted and pooled from the hippocampi of three mice per group (Figure 11 F,G). Nestin is a 440 kDa intermediate filament that is cleaved post-translationally into a 200-160 kDa species and degraded into multiple smaller fragments. Western analysis of lysates containing the complete hippocampal formation failed to detect full-length protein (Figure 11 F) but did detect degradative products of nestin (~46 kDa) in both KO and WT samples (Figure 11 G). An increase in the amount of degraded protein was noted in KO hippocampi (Figure 11 G). Nestin-positive progenitors are known to be restricted to the DG in WT mice, so we sought to improve sensitivity by microdissecting the DG from dorsal hippocampal formation of WT (n=2) and KO animals (n=1) and using a biotin/avidin tertiary enhancement immunoblotting technique. Using these protein lysates and tertiary signal amplification, we were able to detect fully processed nestin in both KO and WT DG (Figure 11 H). A marked increase in nestin

levels was noted in the KO DG (Figure 11 H).

PCNA. PCNA is a DNA polymerase delta accessory protein expressed by actively dividing cells during the S phase of the cell cycle (Gobetto et al, 1995). Figure13 A,C are cresyl-violet stained sections of the dorsal hippocampus of KO and animals. Figure 13 B,D are adjacent sections within 8 μm stained with anti-PCNA. No indication of enhanced cell proliferation was observed. These data suggest that the hyperchromatic cells are not actively dividing. Densitometry is depicted in Figure13 E. Data are presented as the mean percent area exhibiting staining ± SEM of n=5 sections and n=2 sections from n=3 KO and n=1 WT mice. No reliable difference was observed between KO and WT mice. Western analysis confirmed that equal amounts of PCNA protein are present in the KO and WT hippocampal formation (Figure 13 C). Lysates were pooled from n=3 mice/group.

A2B5 and O4. Anti-A2B5 monoclonal antibody is a cell surface ganglioside that selectively labels intracellular compartments and cell membranes of proliferating oligodendrocyte precursor cells (Niquet et al, 1994). The expression of A2B5 immunoreactivity is lost during glial maturation (Repressa et al, 1993). However, this antibody is not exclusively restricted to oligodendrocytes, it is also expressed by a small percentage of neurons and astrocytes (Zhang et al, 2000; Schnitzer & Schachner, 1982). Figure 14 A,C depict representative cresyl-violet stained sections of the dorsal hippocampus of KO and WT animals. Figure 14 B,D are adjacent sections (within 8 μm) immunoreactive with anti-A2B5. In the present study, immunohistochemical analysis failed to detect A2B5-postive cells in the WT or KO (Figure 14 B,D). Western analysis

was not performed as anti-A2B5 reacts with a glycolipid antigen that cannot be separated by SDS-PAGE.

To confirm, that marked changes in oligodendrocyte lineage markers were not detected in KO hippocampal formation relative to WT, Western analysis was performed with anti-O4. Anti-O4 is a monoclonal antibody that reacts with galactocerebroside sulfatide found on the surface of differentiated oligodendrocytes and with an unidentified antigen, POA, expressed on the surface of intermediate oligodendrocyte progenitors (Cammer & Zhang, 1999; Hardy & Friedrich, 1996; Armstrong et al, 1992). Western analysis failed to detect O4-positive protein in the KO or WT hippocampus (Figure 14 E). As a positive control, we were able to identify a faint band in the whole brain lysates of the WT mice with an apparent molecular weight of 72 kDa (Figure 14 E) consistent with previous reports (Sasaki et al, 2000). Faint immunohistochemical staining was detected in the white matter (corpus callosum, fimbria, and stratum alveus (data not shown).

GAP43. Anti-GAP43 reacts with a growth-associated phosphoprotein expressed by mature neurons undergoing neurite extension. GAP43 protein is also present in axons and axonal growth cones of cells in the O-2A lineage (bipotential precursors and oligodendrocyte, type-2 astrocytes; Repressa et al, 1993). As in previous figures, Figure 15 depicts cresyl-violet stained sections (A,C) and adjacent (within 8 μm) immunoreacted sections (B,D) from KO and WT animals. Faint staining was detected in processes along the subgranular zone at the border between the granular zone and hilus, and in the CA3c pyramidal cell field of the KO mouse (Figure15 B). The WT animal demonstrated a much more extensive network of immunopositive projections throughout

the DG. Densitometry was not performed. Western blotting confirmed that levels of the 46 kDa GAP43 protein were reduced in the KO relative to WT (Figure 15 E).

MAP1. Anti-MAP1 labels MAP1 protein present in neuronal axons and dendrites. Figure 16 A,C depicts cresyl-violet stained sections; Figure 16 B,D depicts adjacent (within 8 μm) immunoreacted sections. There was a moderate but statistically significant reduction in MAP1 immunoreactivity in the DG of KO mice relative to WT. Densitometry of n=5 sections and n=8 sections from n=3 KO and n=4 WT mice is depicted in Figure 16 E.

TUJ1. Anti-TUJ1is a neuron-specific marker for committed neurons. Anti-TUJ1 predominantly stains pyramidal neurons, interneurons, and the dendrites of granule cells in the hippocampus (Repressa et al, 1993). Figure 17 depicts cresyl-violet (A,C) and adjacent immunoreacted (B,D) sections. A dramatic reduction in staining was noted in the KO relative to the WT in the DG and CA3c region (compare Figure 17 B and D) but not in other CA fields (data not shown). This difference was confirmed by densitometric analysis of n=4 sections and n=4 sections from n=2 KO and n=2 WT mice (Figure 17 E) and was detected by Western analysis of lysates extracted from the entire hippocampal formation (Figure 17 F).

NeuN. Anti-NeuN (or monoclonal antibody A60) detects a neuron-specific nuclear protein and is used to identify terminally differentiated neurons. The NeuN protein binds to DNA with unknown function (Mullen et al, 1992; Wolf et al, 1996). Anti-NeuN labels nuclei and, to a lesser extent, perikarya and proximal neuronal processes of almost all neuronal cell types found in the CNS of adult mice. NeuN becomes immunologically detectable in neurons when they have become post-mitotic

(Mullen et al, 1992; Wolf et al, 1996). Figure 18 depicts digitized photomontages of the dorsal hippocampal formation of KO (Figure 18 A) and WT (Figure 18 C) mice. An overall reduction in the intensity of immunoreactivity was detected in the KO relative to the WT. Insets (Figure 18 B,D) depict higher power magnification of the areas outlined in Figure 18A and C. Note that some neurons in the KO are intensely stained with small nuclei while entire loci are NeuN-negative (Figure 18 B). Homogenous staining of all cells is detected in the WT (Figure 18 D).

These observations were confirmed by densitometry (Figure 18 E) and by Western analysis (Figure 18 F). NeuN is detected as multiple bands on immunoblots with 2-3 isoforms ranging between 46-48 kDa range and another band detected at~66 kDa (Mullen et al, 1992). A decrease in the 48 and ~66 kDa isoforms was detected by Western analysis.

NF160. Anti-NF160 labels intermediate cytoskeletal filaments of differentiated neurons (Angeletti et al, 1985). Figure 19(A,C) depicts cresyl-violet stained sections; Figure 19 (B,D) represents adjacent (within 8 μm) sections reacted with anti-NF160 and digitized at the same magnification as in (A,C). Note the reduction in NF160 immunoreactivity. This reduction was confined to the hilar region of the DG. As depicted in Figure 19 (E,F), there was no difference in the intensity of stain in the CA3b/lateral CA3c pyramidal cell field. The decreased immunoreactivity was confined to the medial CA3c depicted in Figure 19 B,D and located in the insets in Figure 19 E,F. Densitometry confirmed that percent area of DG exhibiting staining was only slightly reduced in KO and WT (Figure 19 G). A moderate reduction in overall protein levels was also detected by Western analysis (Figure 19 H).

GFAP. Anti-GFAP is a polyclonal antibody used to identify astrocytes. Figure 20A-D depicts cresyl violet and GFAP-immunoreactivity in representative KO and WT animals. Note that the Nissl and immunoreacted sections are approximately 8-12 μm apart. No overall difference in GFAP- immunoreactivity was detected (Figure 20 E). No change in protein levels of the 50 kDa GFAP protein (Repressa et al, 1993) in the hippocampal formation between KO and WT was detected by Western analysis (Figure 20 F). However, a difference in the localization pattern in KO and WT animals was consistently detected. Compare intense immunoreactivity in the polymorphonuclear layer of the DG notably in cells corresponding to the hyperchromatic cell population in the subgranular zone in the KO (Figure 20 B) relative to the WT (Figure 20 D). In the WT, GFAP-positive cells were detected to a greater extent in the granule cell layer of the DG and to a lesser extent in the subgranular zone compared to KO.

GalC. Anti-GalC- identifies committed and post-mitotic oligodendrocytes. GalC is a major glycolipid constituent of myelin and cell membranes of myelin-forming cells (Rostami et al, 1984). In some animals, faint, but elevated GalC labeling was detected in the subgranular zone, hilus, and CA3c area in the KO (Figure 21 C) relative to the WT (Figure 21 D). This increase was not consistently observed in n=5 sections and n=4 sections from n=3 KO and n=2 WT mice as indicated by densitometric analysis (Figure 21 E). We were able to detect GalC by Western analysis. No difference in overall levels was observed (Figure 21 C). (As a technical aside, note that, while we were able to retain sufficient glycolipid epitope during extraction and SDS-PAGE analysis to detect GalC, we were unable to perform immunobloting using anti-A2B5).

Figure 11. Nestin protein levels are increased in the DG of KO animals. (A,C) Nissl-stained sections of KO and WT dorsal hippocampus, respectively. Note the enriched population of hyperchromatic cells in the polymorphonuclear layer and along the superior and inferior limbs of the DG of KO animals. **(C, D)** Adjacent sections to A and C immunoreacted with anti-nestin. **(C)** The arrows point to select cells that appear to be nestin-positive. **(D)** Nestin immunoreactive cells (arrows) are detected in WT. Note that there are more nestin-positive cells in the KO DG relative to the WT. **(E)** Densitometry measuring the extent of nestin immunoreactivity in the KO and WT DG. Data are expressed as the percent area of the DG AOI exhibiting positive immunoreactivity (Mean ± SEM). Asterisks indicate a statistically significant increase in nestin-positive cells in the KO as compared to the WT [t-test, $p<0.05$] Western analysis of lysates extracted from the entire hippocampal formation (dorsal and ventral) failed to detect the full length nestin protein (200 kDa) in KO or WT samples **(F)** but did detect an increase in nestin degradative products (~46 kDa) in KO samples relative to WT. **(H)** Western analysis of lysates prepared from microsections of DG in the dorsal hippocampal formation detected a marked increase in nestin protein in KO relative to WT. (Scale bars, 100 μm)

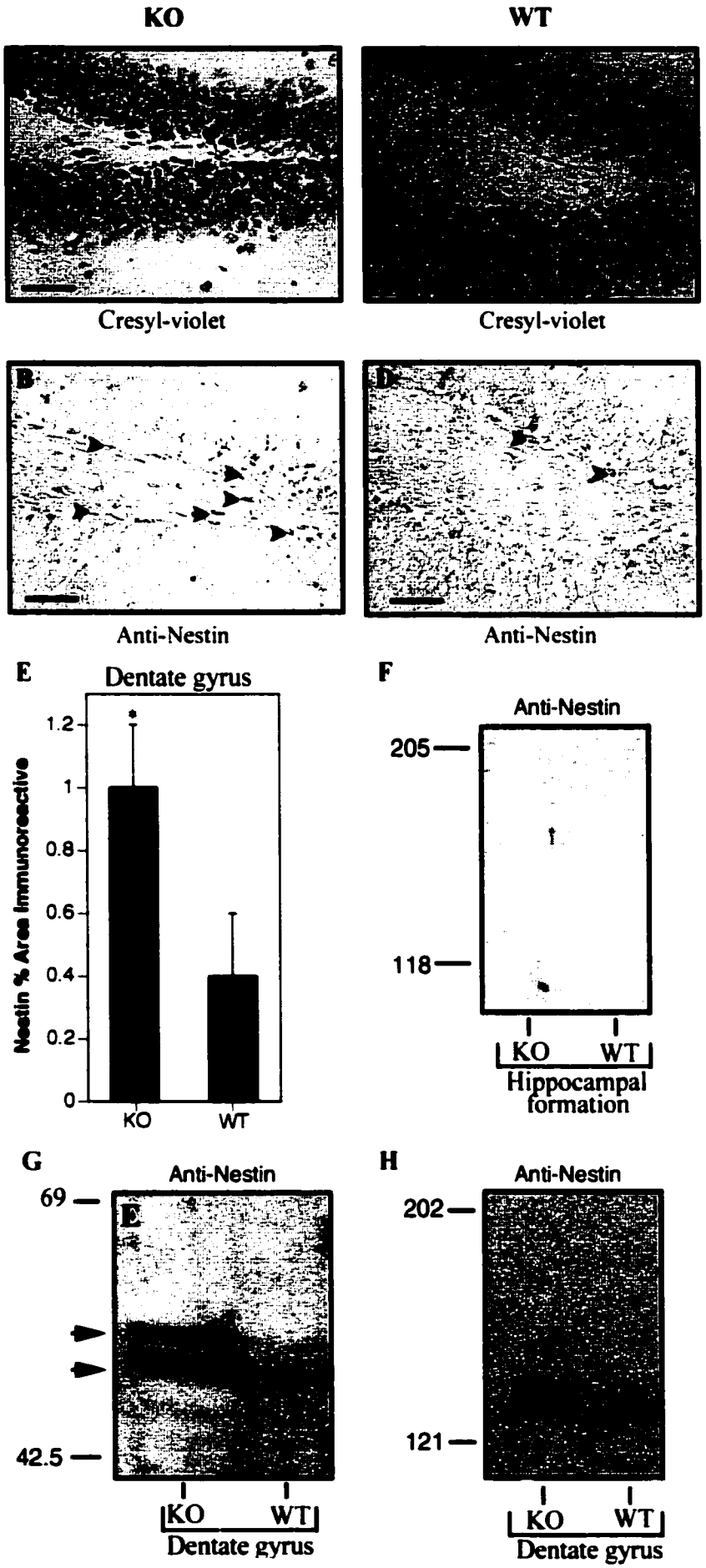
KO
WT
Cresyl-violet
Cresyl-violet
B
D
Anti-Nestin
Anti-Nestin
E
Dentate gyrus
Nestin % Area Immunoreactive
1.2
1
0.8
0.6
0.4
0.2
0
KO
WT
F
Anti-Nestin
205
118
KO
WT
Hippocampal formation
G
Anti-Nestin
69
42.5
KO
WT
Dentate gyrus
H
Anti-Nestin
202
121
KO
WT
Dentate gyrus

Figure 12. Nestin-positive cells in the DG of KO and WT mice. There are more nestin-positive cells in the DG of the KO relative to WT mice, as indicated by arrows. (scale bars, 20μm)

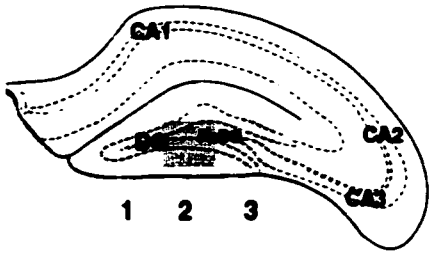

KO Dentate Gyrus

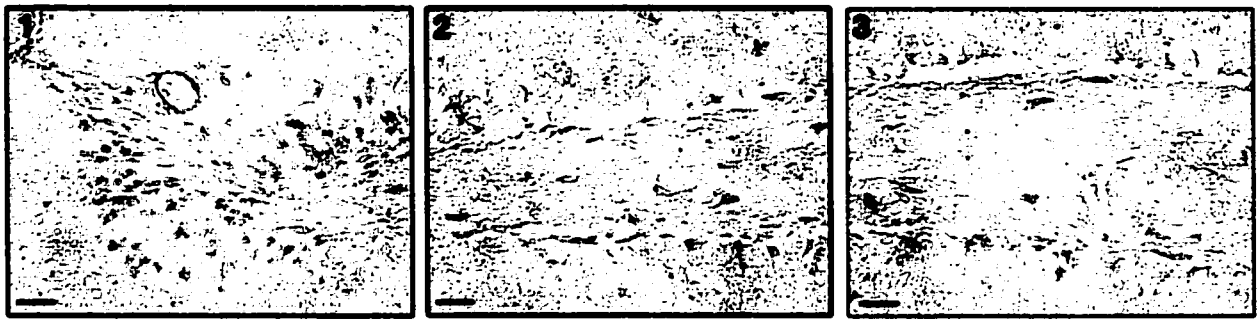

WT Dentate Gyrus

Figure 13. PCNA protein levels are comparable in KO and WT hippocamapal formation. **(A,C)** Nissl-stained sections of dorsal hippocampal formation of the KO and WT. **(B,D)** Adjacent sections to A and C immunoreacted with anti-PCNA. **(E)** Quantitative densitometry measuring the percent area of KO and WT DG exhibiting PCNA-immunoreactivity. Data represent Mean ± SEM. **(F)** Western analysis confirms that there are equivalent levels of PCNA protein present in the KO and WT hippocampal formation. (Scale bars, 100 μm)

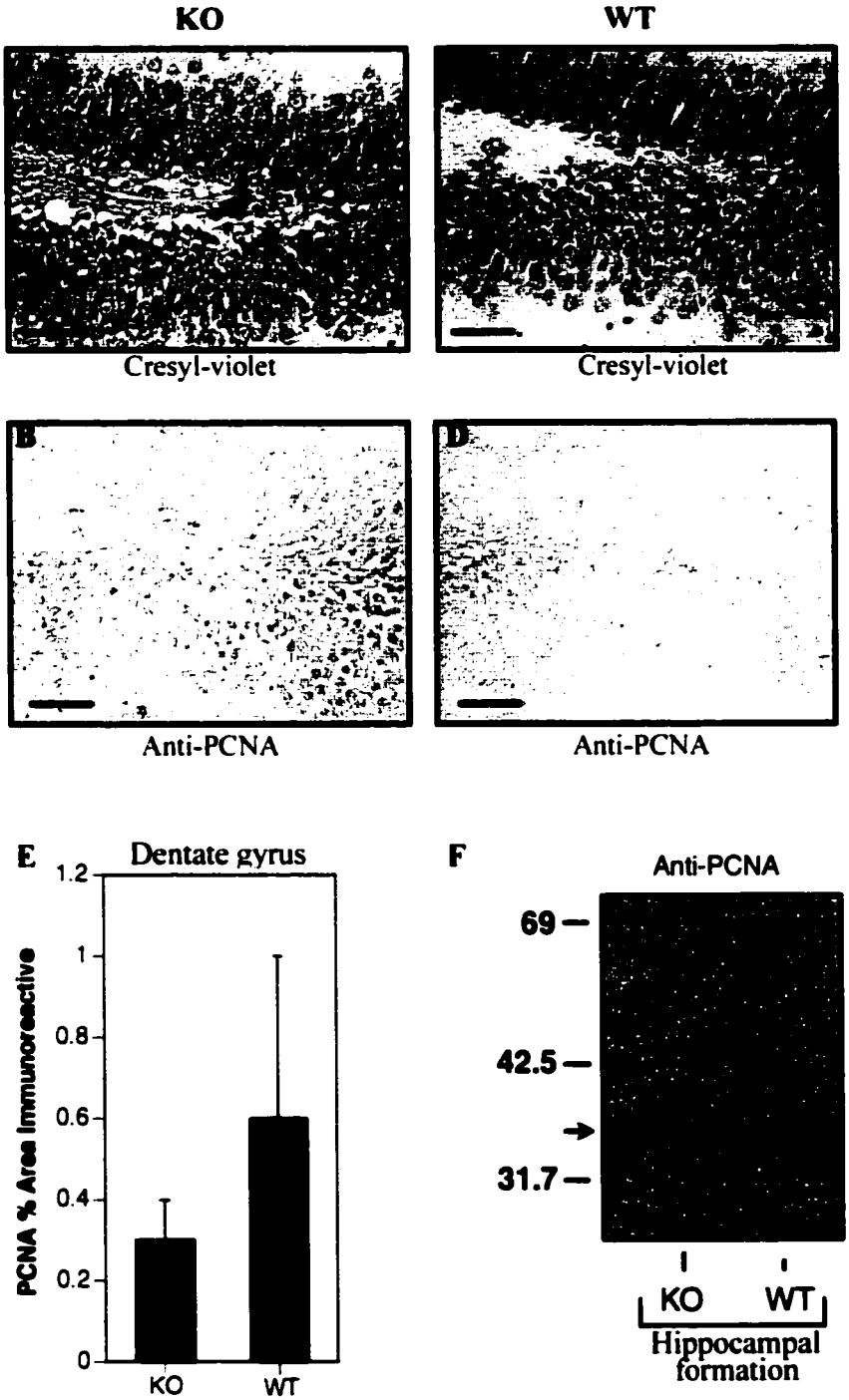
KO
WT
Cresyl-violet
Cresyl-violet
B
D
Anti-PCNA
Anti-PCNA
E
Dentate gyrus
PCNA % Area Immunoreactive
1.2
1
0.8
0.6
0.4
0.2
0
KO
WT
F
Anti-PCNA
69
42.5
31.7
KO
WT
Hippocampal formation

Figure 14. Expression of anti-A2B5 and anti-O4 oligodendrocyte lineage markers are not detected in KO or WT hippocampal formation. **(A,C)** Nissl-stained sections of dorsal hippocampal formation of the KO and WT. **(B,D)** Adjacent sections to A and C immunoreacted with anti-A2B5. No A2B5-positive cells were detected in the KO or WT DG. **(B)** Western analysis failed to detect O4 protein in the KO and WT DG. WT whole brain lysates with immunoblotted as a positive control for O4 protein (72 kDa). (Scale bars, 100 μm)

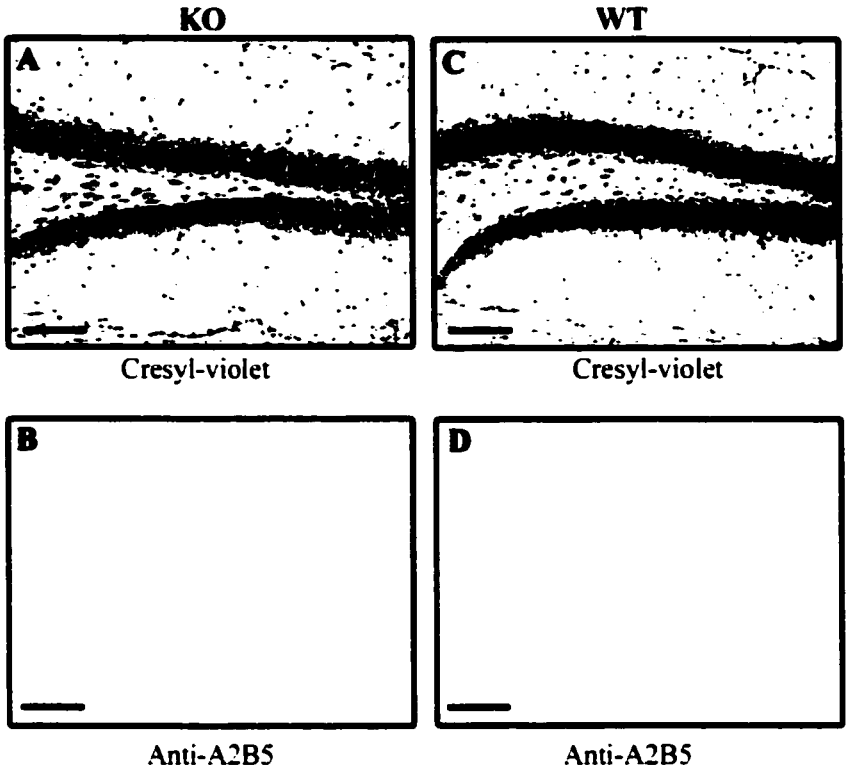
KO
WT
A
C
Cresyl-violet
Cresyl-violet
B
D
Anti-A2B5
Anti-A2B5

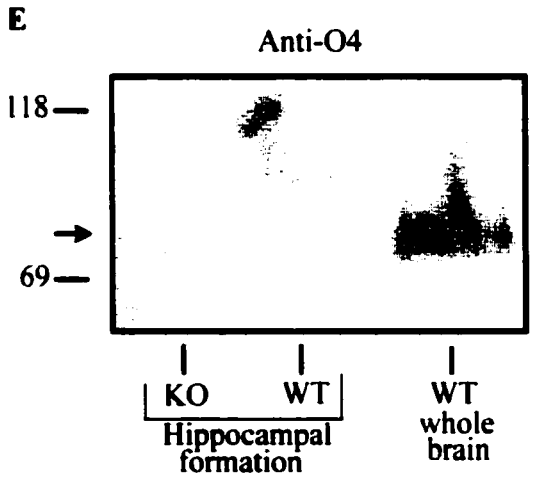
E
Anti-O4
118
69
KO
WT
Hippocampal formation
WT whole brain

Figure 15. GAP43 protein levels are reduced in the DG and hippocampus of KO animals (A,C) Nissl-stained sections of dorsal hippocampal formation of the KO and WT. **(B,D)** Adjacent sections to A and C immunoreacted with anti-GAP43. (anti-GAP43. Note the faint staining detected in processes along the subgranular zone at the border between the granular zone and hilus, and in the CA3c pyramidal cell fields of the KO mouse **(B)** The WT demonstrates a more extensive network of GAP43-staining projections throughout the DG (**D**). **(E)** Western analysis demonstrates that the levels of GAP43 protein (46 kDa) were reduced in the KO relative to WT hippocampal formation. (Scale bars, 100 μm)

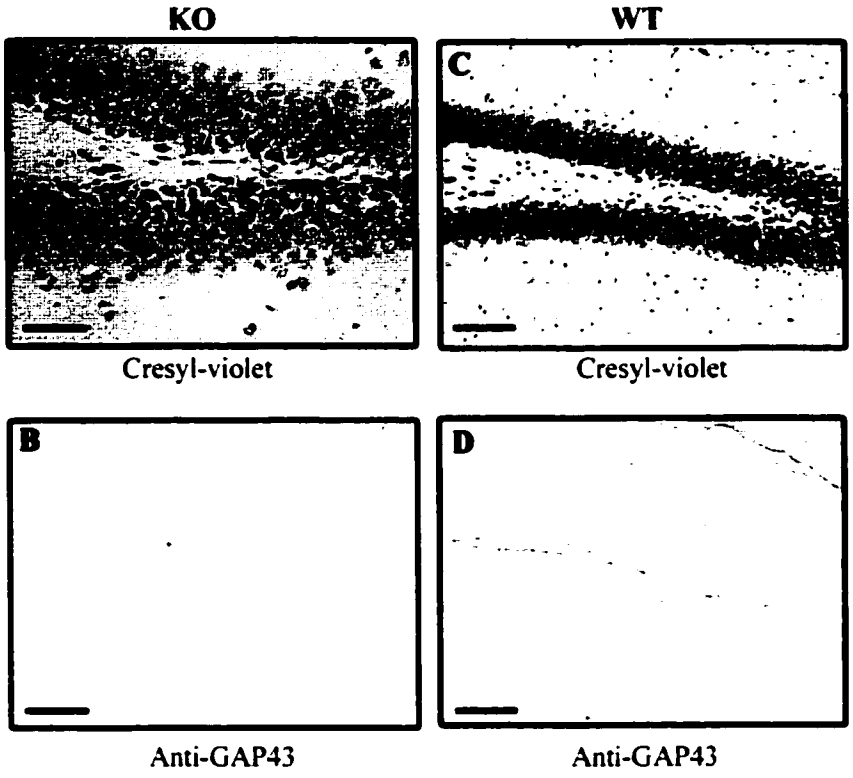
KO
WT
C
Cresyl-violet
Cresyl-violet
B
D
Anti-GAP43
Anti-GAP43

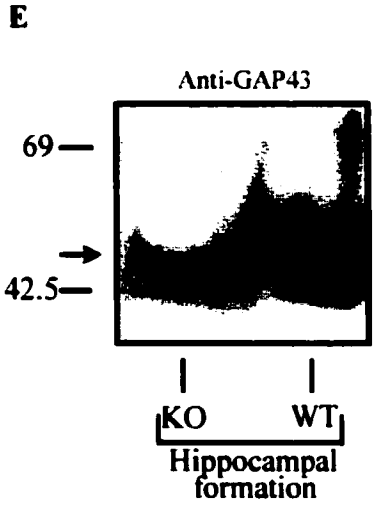
E
Anti-GAP43
69
42.5
KO
WT
Hippocampal formation

Figure 16. MAP1 protein levels are moderately reduced in the hippocampal formation of KO animals. **(A,C)** Nissl-stained sections of dorsal hippocampal formation of the KO and WT. **(B,D)** Adjacent sections to A and C immunoreacted with anti-MAP1There is a moderate but statistically significant reduction in MAP1-staining in the DG KO relative to WT. **(E)** Densitometry on the percent area of the KO and WT DG exhibiting MAP1-immunoreactivity. The asterisks indicate that there is a statistically significant increase in MAP1-positive staining in the KO as compared to the WT. Data represent Mean ± SEM [t-test, $p<0.01$] (scale bars, 100 μm)

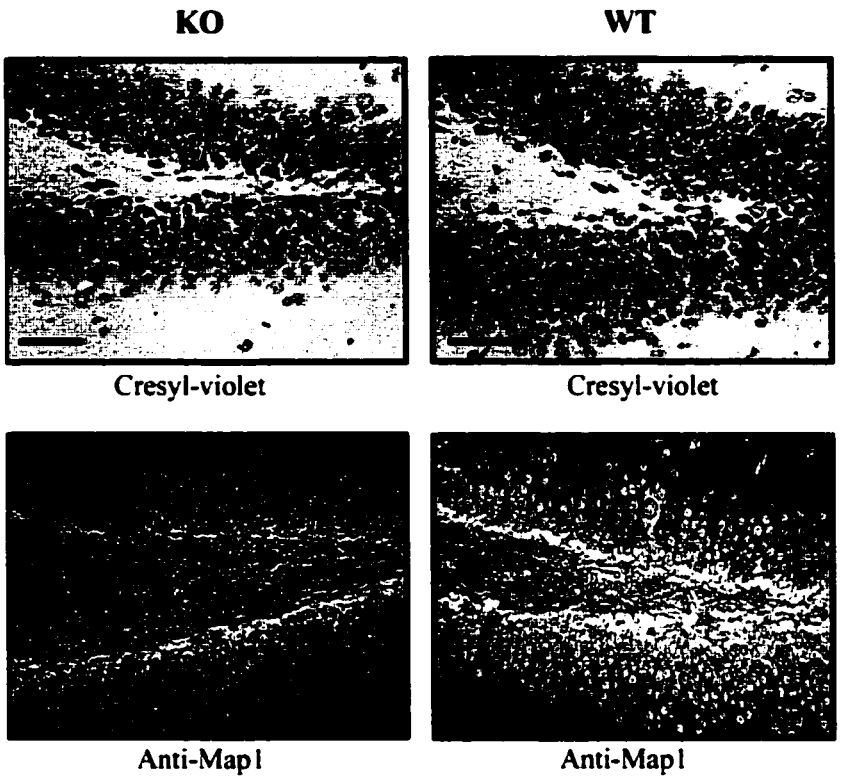
KO
WT
Cresyl-violet
Cresyl-violet
Anti-Map1
Anti-Map1

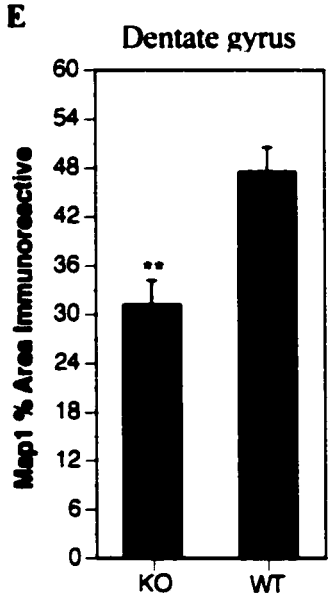
E
Dentate gyrus
Map1 % Area Immunoreactive
60
54
48
42
36
30
24
18
12
6
0
**
KO
WT

Figure 17. TUJ1 immunoreactive protein is dramatically reduced in the KO DG (A,C) Nissl-stained sections of dorsal hippocampal formation of the KO and WT. **(B,D)** Adjacent sections to A and C immunoreacted with anti-TUJ1A dramatic reduction in staining was noted in the KO relative to the WT in the DG and CA3c region. **(E)** Densitometry on the percent area of the KO and WT DG exhibiting TUJ1-immunoreactivity. The asterisks indicate that there is a statistically significant increase in TUJ1-positive cells in the KO as compared to the WT. Data represent Mean ± SEM [t-test, $p<0.01$] **(F)** Western analysis of lysates extracted from the entire hippocampal formation detected less anti-TUJ1 immunoreactive protein in the KO relative to WT. (Scale bars, 100 μm)

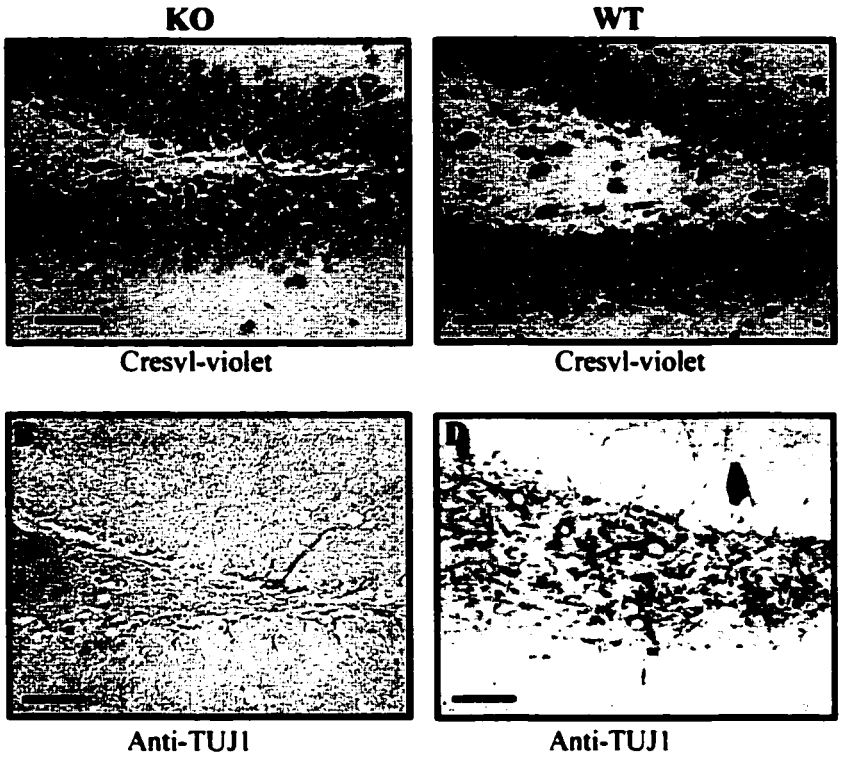
KO
WT
Cresyl-violet
Cresyl-violet
Anti-TUJ1
Anti-TUJ1

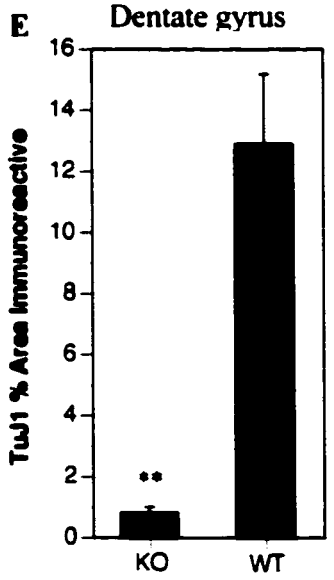
E
Dentate gyrus
TuJ1 % Area Immunoreactive
16
14
12
10
8
6
4
2
0
**
KO
WT

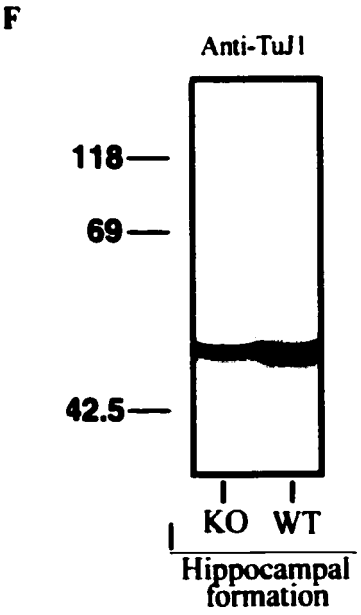
F
Anti-TuJ1
118
69
42.5
KO
WT
Hippocampal formation

Figure 18. NeuN immunoreactivity is reduced in KO hippocampal neurons. **(A,C)** There is lighter NeuN-staining in the KO DG relative to the WT. Homogenous staining of all cells is detected in WT. In KO, select neurons are stained more intensely than WT while other cells are weakly stained. **(B,D)** Insets depict higher power magnification of the areas outlined in A, C. **(E)** Densitometry on the percent area of the KO and WT DG exhibiting NeuN-immunoreactivity. The asterisks indicate that there is a statistically significant increase in NeuN-positive cells in the KO as compared to the WT. Data represent Mean ± SEM [t-test, $p<0.05$] **(F)** Western analysis demonstrates that there is less NeuN protein (48 and ~66 kDa) in the KO relative to WT hippocampal formation. (Scale bars, 100 μm)

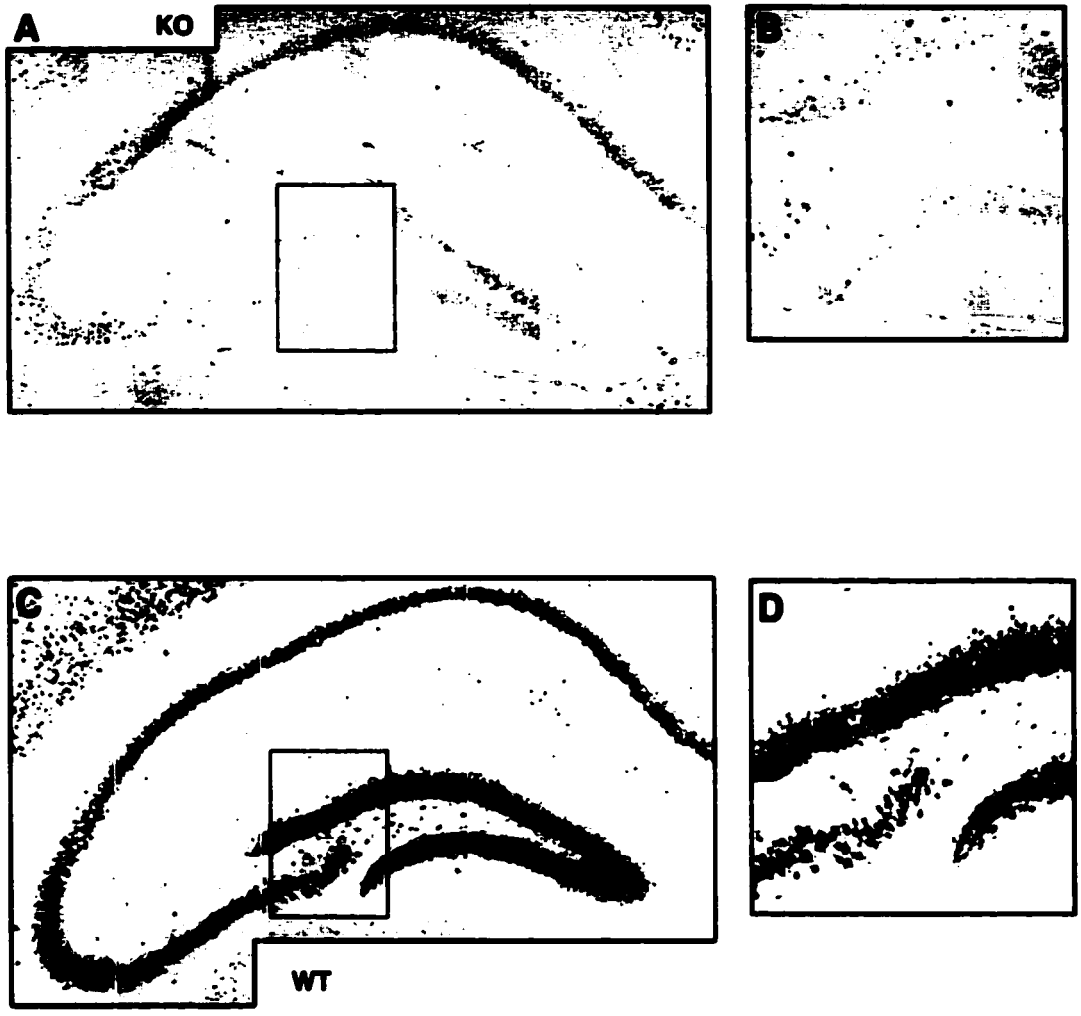
A
KO
B
C
WT
D
E
Dentate gyrus
NeuN % Area Immunoreactive
36
32
28
24
20
16
12
8
4
0
*
KO
WT
F
Anti-NeuN
118
69
42.5
KO
WT
Hippocampal formation

Figure 19. NF160 proteins levels are reduced in the hilar region of the DG. **(A,C)** Nissl-stained sections of dorsal hippocampal formation of the KO and WT. **(B,D)** Adjacent sections to A and C immunoreacted with anti-NF160. (Scale bars, 100 μm). **(E,F)** The reduction in NF160-immunoreactiviyt was confined to the hilar region of the DG(Scale bars, 200 μm) **(G)** Densitometry on the percent area of the KO and WT DG exhibiting NF160-immunoreactivity. Densitometry confirmed that the overall staining in the DG was comparable. Data represent Mean ± . **(H)** Western analysis detected an overall reduction in NF160 protein in the hippocampal formation of the KO relative to WT.

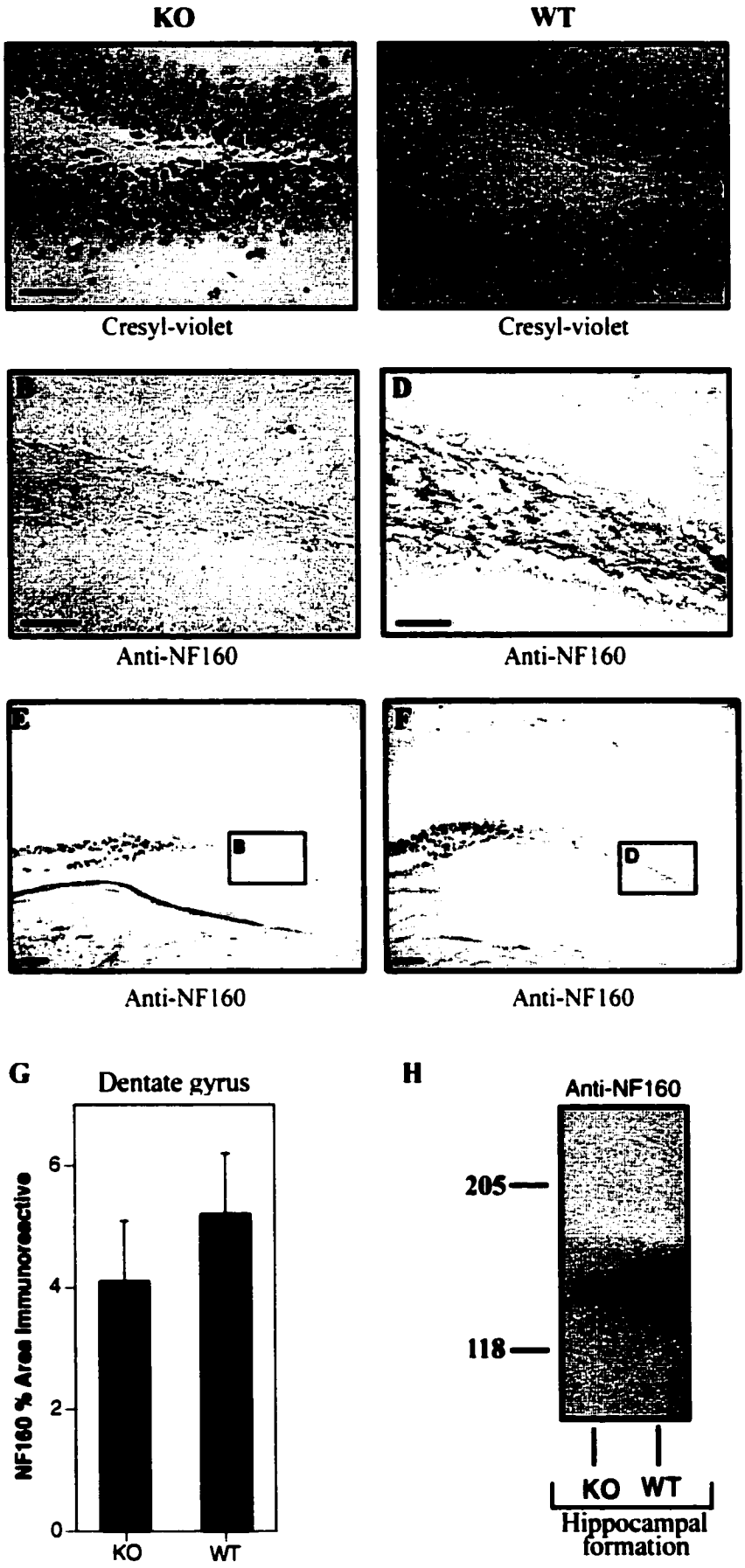
KO
WT
Cresyl-violet
Cresyl-violet
Anti-NF160
Anti-NF160
Anti-NF160
Anti-NF160
G
Dentate gyrus
NF160 % Area Immunoreactive
6
4
2
0
KO
WT
H
Anti-NF160
205
118
KO
WT
Hippocampal formation

Figure 20. GFAP protein levels are comparable in KO and WT hippocampal formation , but there is a change in protein localization in the DG of KO mice. **(A,C)** Nissl-stained sections of dorsal hippocampal formation of the KO and WT. **(B,D)** Adjacent sections to A and C immunoreacted with anti-GFAP. A marked difference in the localization of GFAP in KO and WT animals was consistently detected in the DG. **(E)** Densitometry on the percent area of the KO and WT DG exhibiting GFAP-immunoreactivity. These data confirm that there is an equal amount of GFAP-immunoreactivity in the KO and WT. Data represent Mean ± SEM **(F)** Western analysis detected a slight increase in GFAP protein (50 kDa) in the KO relative to WT hippocampal formation. (scale bars, 100 μm)

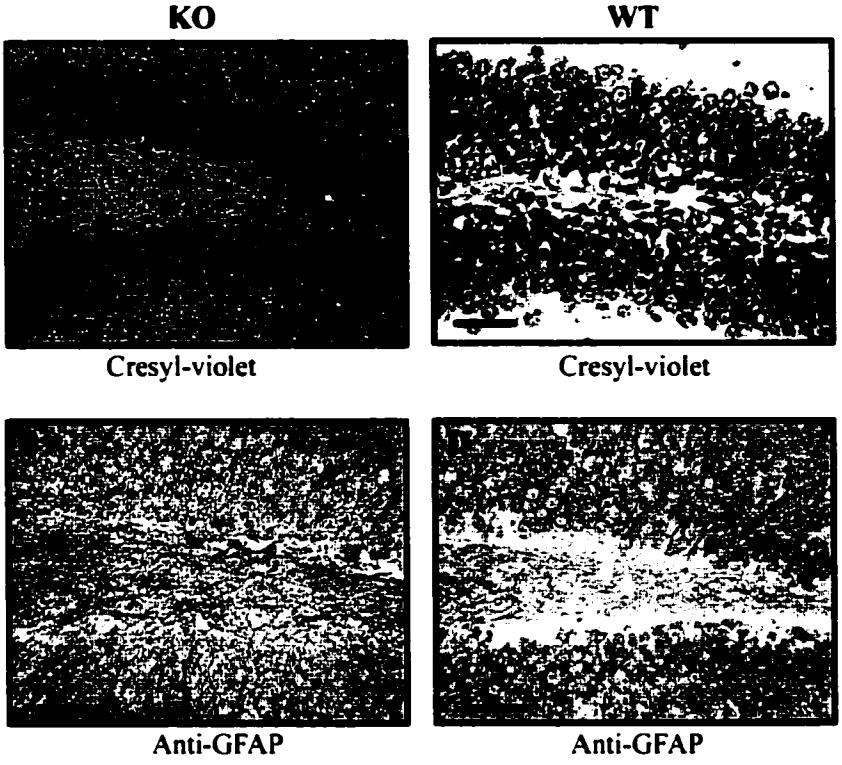
KO
WT
Cresyl-violet
Cresyl-violet
Anti-GFAP
Anti-GFAP

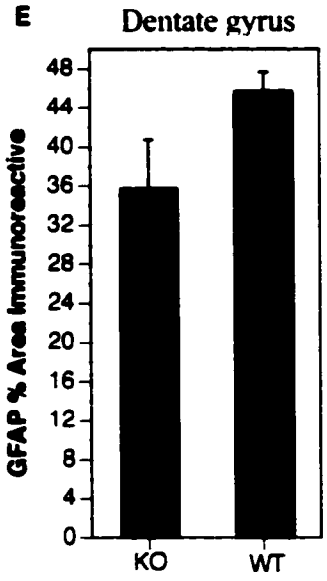
E
Dentate gyrus
GFAP % Area Immunoreactive
48
44
40
36
32
28
24
20
16
12
8
4
0
KO
WT

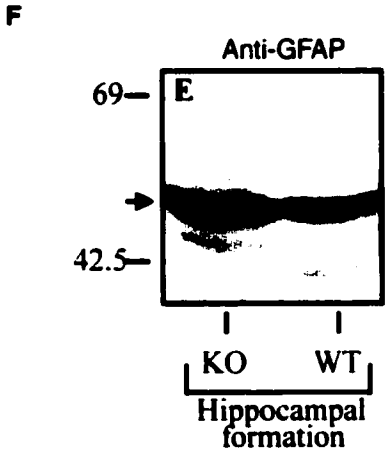
F
Anti-GFAP
69
42.5
E
KO
WT
Hippocampal formation

Figure 21. GalC protein levels are comparable in KO and WT hippocampal formation . (A,C) Nissl-stained sections of dorsal hippocampal formation of the KO and WT. **(B,D)** Adjacent sections to A and C immunoreacted with anti-GalC anti-GalC. Few GalC-immunoreactive cells could be detected in KO or WT DG . **(E)** Densitometry on the percent area of the KO and WT DG exhibiting GalC-immunoreactivity. Data represent Mean ± SEM. **(F)** Western analysis detected equal amounts of GalC protein in the KO and WT hippocampal formation. (Scale bars, 100 μm)

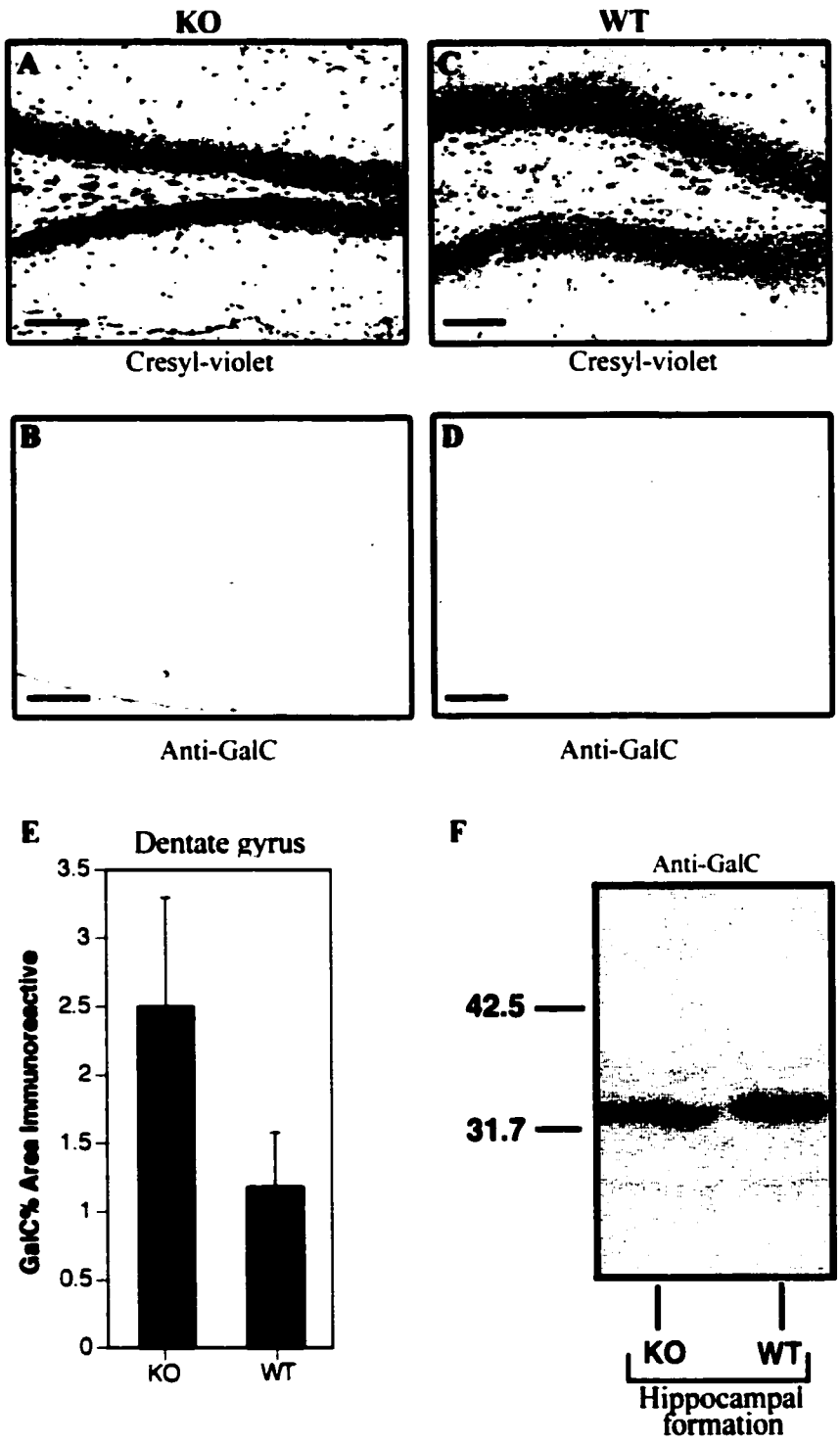
KO
WT
A
C
Cresyl-violet
Cresyl-violet
B
D
Anti-GalC
Anti-GalC
E
Dentate gyrus
GalC% Area Immunoreactive
3.5
3
2.5
2
1.5
1
0.5
0
KO
WT
F
Anti-GalC
42.5
31.7
KO
WT
Hippocampal formation

3.4 *In vitro* characterization of primary hippocampal cultures from KO and WT mice

Neural stem cells are defined by their capacity for self-renewal and their ability to differentiate into functional neurons or glia. To confirm the proliferative potential of the hyperchromatic cells found in the KO hippocampal formation, we cultured enzymatically dissociated cells under conditions known to promote neural stem cell division but not survival of primary neurons or glia. Clonogenic assays were performed to determine whether single cells from KO or WT hippocampi cultured under these conditions could proliferate and form colonies (< 7 cells) (Williams et al, 1997). The hippocampi from KO and WT mice were enzymatically disassociated and single cells plated in media containing basic-fibroblast growth factor (bFGF) for 7 days. Cultures were then double-labelled with anti-nestin and anti-NeuN, anti-nestin and anti-enolase, or anti-nestin and anti-GFAP. Figure 22 demonstrates a greater number of KO colonies compared to WT cultured under these conditions. The majority of the KO colonies were anti-nestin positive. The nestin-positive colonies were composed of large phase-dark oblong cells with a small percentage of small phase-bright round cells. Few adult neuronal colonies (enolase- or NeuN immunoreactivity) were detected. Rare WT colonies expressed the neuron-specific markers NeuN- and enolase. Nestin-positive progenitor colonies were not detected in WT cultures. No GFAP-positive astrocytes were identified in KO or WT cultures (data not shown). These data indicate that a larger percentage of single cells dissociated from KO hippocampi are capable of self-renewal than from WT hippocampi.

If KO colonies are, in fact, composed of neural stem cells, then they should be able to differentiate into neurons or glia. After 7 days of treatment with bFGF to promote proliferation, we determined whether KO and WT colonies could be differentiated into

neurons by exposure to BDNF. Figure 23 demonstrates that there were a greater number of KO colonies compared to WT consistent with data presented in Figure 22. The majority of the KO colonies were NeuN- and Enolase-positive neurons following 7 days of bFGF exposure and a subsequent 5 days of BDNF treatment. The differentiated NeuN- and enolase-positive cells were phase-bright, extended processes and expressed mature neuronal markers. The rare WT colonies were NeuN- and enolase-positive neurons. These data indicate that the KO hippocampal formation contains undifferentiated neural precursors that, in response to bFGF, proliferate and generate colonies of cells that can differentiate into neurons.

Figure 22. Hippocampal KO cells cultured in the presence of bFGF express neural stem cell markers. A greater number of colonies were detected in KO cultures relative to WT after 7 days of culture. The majority of KO colonies were nestin-positive. Few adult neuronal colonies (enolase- **(Left Panel)** or NeuN-immunoreactive **(Right Panel)** were detected. No GFAP-positive astrocytes were detected (data not shown)

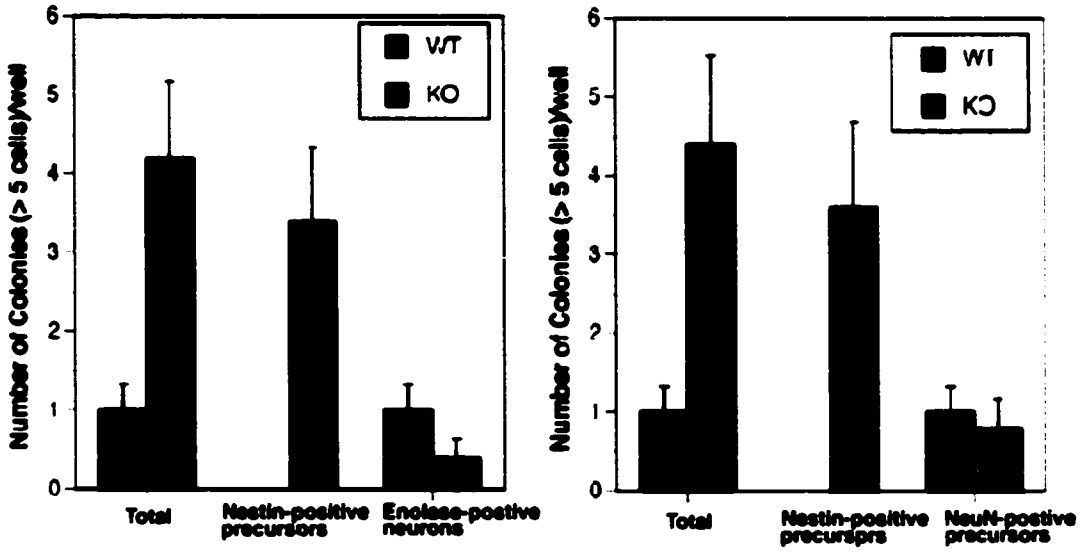
Number of Colonies (> 5 cells)/well
6
5
4
3
2
1
0
WT
KO
Total
Nestin-positive precursors
Enolase-postive neurons
Number of Colonies (> 5 cells)/well
WT
KO
Total
Nestin-positive precursprs
NeuN-postive precursors

Figure 23. bFGF-treated KO colonies can be terminally differentiated to neurons by exposure to brain derived neurotrophic factor (BDNF). There were a greater number of KO colonies compared to WT, consistent with the data presented in Figure 22. The majority of the bFGF treated colonies became enolase- and NeuN-positive following 5 days of BDNF treatment indicative of neuronal differentiation. A minority of precursor colonies (nestin-immunoreactive) failed to differentiate.

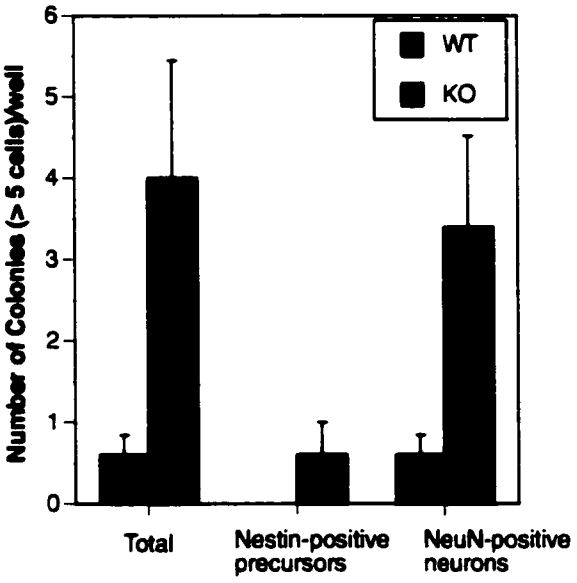

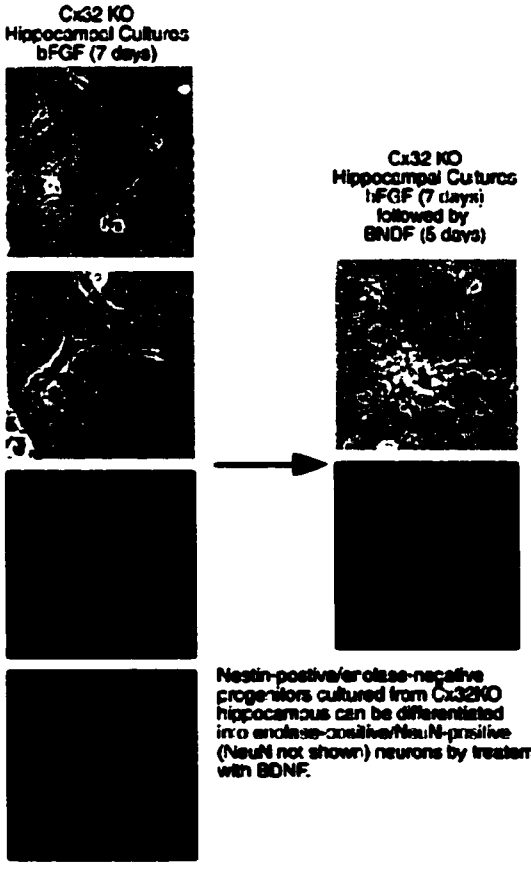

Nestin-positive/enolase-negative progenitors cultured from Cx32KO hippocampus can be differentiated into enolase-positive/NeuN-positive (NeuN not shown) neurons by treatment with BDNF.

3.5 Expression of connexin-family members in the KO and WT brain

Why does the KO hippocampus exhibit an enriched population of putative neural stem cells relative to the WT animal? We cannot definitively state that the appearance of these cells in the DG is caused by loss of Cx32 expression during cerebral development. Retention of this population in adult mouse brain may be the result of gene compensation (i.e. *de novo* expression of another Cx or gene product in the KO brain). Compensatory gene expression could arise as a result from loss of Cx32 or as a result of genetic heterozygozity in KO mouse despite use of KO and WT littermates. Thus, Cx32 may play a direct or indirect role in the enrichment of these cells. It has been well documented that the expression of Cxs in the brain is diverse, with specific cell types expressing different family members (Dermietzel et al, 1989; Nadarajah et al, 1997). This cell-specific distribution may have functional implications controlling progression through different developmental stages (for review refer to Guthrie & Gilula, 1989).

To examine the hypothesis that the enriched cell population in the DG is due to Cx compensation, we used RT-PCR analysis to establish expression of 10 different Cxs in the 3 month adult KO and WT mouse. Eleven brain regions were examined: hippocampal formation, subventricular zone, striatum, thalamus, hypothalamus, occipital lobe, entorhinal cortex, frontal cortex, parietal/temporal cortex, cerebellum, and brainstem. In hippocampal dissections, special care was taken to minimize contamination by the adjacent corpus callosum. RT-PCR was performed on RNA template from the eleven KO and WT mice brain regions using Cx primers pairs recognizing Cx26, Cx30, Cx31.1, Cx32, C36, Cx37, Cx43, Cx45, Cx46 and Cx47. The Cx32 amplicon detected by Cx32 primers is depicted in Figure 24. Cycle and primer concentrations were optimized such that gene amplification fell within approximate linear range for semi-quantitative analysis (data not shown). Cx expression in KO brain regions was

compared to WT in at least two separate experiments (n=2-5 brains per sample/experiment). Gels were qualitatively assessed as to whether expression was increased, decreased, or comparable. These data provide a preliminary screen of Cx changes in the KO brain relative to WT.

In the present study, the data indicate that a loss of Cx32 results in increased mRNA expression of Cx26, Cx30, Cx36, Cx37, and Cx47 in the hippocampus of KO mice relative to WT (Figure 25 A). Recent studies have demonstrated by *in situ* hybridization that Cx36 and Cx47 are expressed at high levels in the DG of WT animals (Rash et al, 2000; Rozental et al, 2000; Teubner et al, 2001; Belluardo et al, 1999). Cx26 is expressed in cortical progenitor cells of the neocortex (Bittsman & LoTurco, 1999). Cx30 has been localized in astrocytes (Nagy et al, 1999; Kunzelmann et al, 1999), Cx37 is known to be expressed by endothelial cells in brain (Traub et al, 1998; Willecke et al, 1991). Table 3 (Figure 25 B) summarizes the changes in connexin gene expression in the hippocampus in the KO and WT animal. Based on these studies, it will be interesting to further examine the localization of these upregulated Cxs in the KO by *in situ* hybridization

Table 4 summarizes the changes in connexin gene expression in all of the eleven brain areas studied in KO and WT animals. As in the hippocampal formation, Cx30, Cx36 and Cx37 are consistently upregulated in the subventricular zone, entorhinal cortex, and parietal/temporal cortex of KO mice relative to WT (depicted in Figure 26). The pattern of Cx upregulation in the hippocampal formation and subventricular zone is of great interest, because these are two areas that express the largest population of neural stem cells in WT mice (Gage et al, 1998). We have shown that there is an enrichment of these cells in KO hippocampus, but have yet to examine the subventricular zone. Other areas exhibiting similar changes in connexin expression

are the entorhinal cortex and parietal/temporal cortex. To our surprise, there was no detectable upregulation of Cx45, which, like Cx32, is strongly expressed by oligodendrocytes (Nicholson et al, 1999), and, as such, is an obvious candidate to compensate for the loss of Cx32.

Figure 24. Location of primers used to detect Cx32 transcript. Genomic organization of Cx32 gene and the KO construct depicting Exons 1 and 2 and the location of the Cx32 primers in the Cx32 open reading frame. These primers detect Cx32 amplicon in the WT not present in KO.

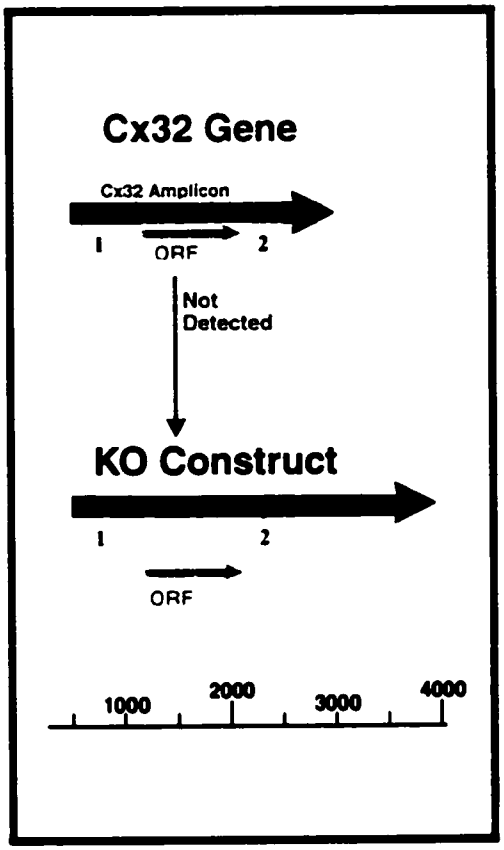
Cx32 Gene
Cx32 Amplicon
1
ORF
2
Not
Detected
KO Construct
1
2
ORF
1000
2000
3000
4000

Figure 25. Cx mRNA expression in the hippocampal formation of KO and WT mice determined by RT-PCR. **(A)** 5 ug of DNAse-treated RNA pooled from n=3 animals per sample was random primed with reverse transcriptase and PCR amplification was performed using Cx primers (Table 2). GAPDH amplification was performed to demonstrate template integrity. For experimental details see Materials and Methods. Note the increase in Cx26, Cx30, Cx36, Cx37 and Cx47 amplicon in Cx32 KO mice relative to WT. GAPDH amplicon are equivalent providing qualitative confirmation that equivalent amounts of mRNA template were reverse-transcribed and PCR-amplified in KO and WT. **(B)** Comparison of Cx gene expression in the KO and WT hippocampal formation. Expression levels were qualitatively assessed by visual comparison of ethidium-bromide-stained amplicons following RT-PCR and gel electrophoresis **(A)**: +++ (brightest);++ (bright); + (band present); +/- (slightly detectable band); and – (no band present). GAPDH amplification was performed to demonstrate template integrity.

A

Hippocampus

B

Connexins	KO	WT
Cx26	+	+/-
Cx30	+++	+/-
Cx31.1	-	-
Cx36	+	-
Cx32	-	+
Cx37	+	+/-
Cx43	+++	+++
Cx45	+	+
Cx46	-	-

Figure 26. Cx mRNA expression in subventricular zone, entorhinal cortex, parietal/temporal cortex and hypothalamus of KO and WT mice determined by RT-PCR. 5 ug of DNAse-treated RNA pooled from n=3 animals per sample was random primed with reverse transcriptase and PCR amplification was performed using Cx primers (Table 2). GAPDH amplification was performed to demonstrate template integrity. For experimental details see Materials and Methods..

Subventricular zone

Entorhinal Area

Parietal/Temporal Cortex

Hypothalamus

Figure 27. Cx mRNA expression in thalamus, frontal cortex, striatum and brainstem of KO and WT mice determined by RT-PCR. 5 ug of DNAse-treated RNA pooled from n=3 animals per sample was random primed with reverse transcriptase and PCR amplification was performed using Cx primers (Table 2). GAPDH amplification was performed to demonstrate template integrity. For experimental details see Materials and Methods..

Thalamus

Frontal Cortex

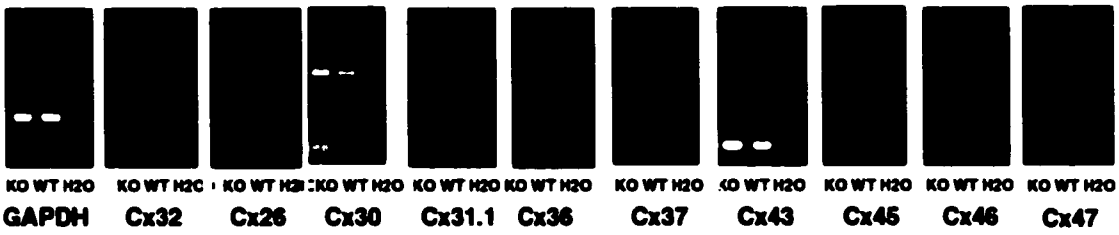

Striatum

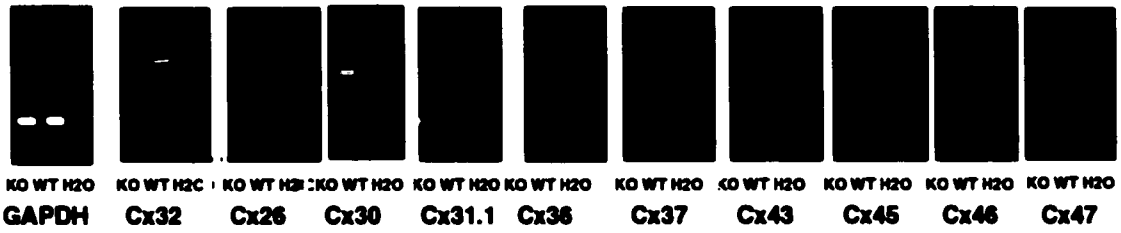

Brainstem

Figure 28. Cx mRNA expression in cerebellum and occipital cortex of KO and WT mice determined by RT-PCR. 5 ug of DNAse-treated RNA pooled from n=3 animals per sample was random primed with reverse transcriptase and PCR amplification was performed using Cx primers (Table 2). GAPDH amplification was performed to demonstrate template integrity. For experimental details see Materials and Methods.

Cerebellum

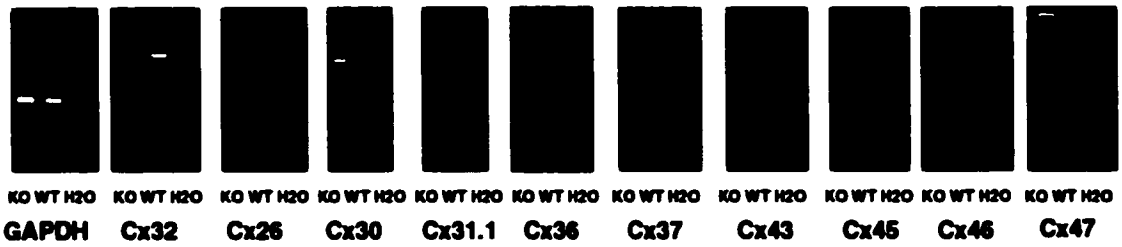

Occipital

Table 4. Comparison of Cx gene expression in KO and WT brain regions. Expression levels were qualitatively assessed by visual comparison of ethidium-bromide-stained amplicons following RT-PCR and gel electrophoresis electrophoresis (see Figure 26,27,28): +++ (brightest);++ (bright); + (band present); +/- (slightly detectable band); and – (no band present). GAPDH amplification was performed to demonstrate template integrity.

	Connexin Primers														
	Cx26		Cx30			Cx32			Cx37			Cx45			Cx47
Various Brain Areas	KO	WT		KO	WT		KO	WT		KO	WT		KO	WT	
Hippocampus	+	+/-		-	-		+	+/-		++	++		-	-	
Subventricular Zone	+/-	-		-	-		+	-		++	++		-	-	
Entorhinal Cortex	-	-		-	-		++	-		++	++		-	-	
Parietal/ Temporal Cortex	-	-		-	-		-	-		++	++		-	-	
Hypothalamus	-	-		-	-		-	-		-	++		-	-	
Thalamus	-	-		-	-		+/-	+/-		++	++		-	-	
Frontal cortex	-	-		-	-		+	+		++	++		-	-	
Striatum	-	+/-		-	-		+	-		++	++		-	-	
Brainstem	-	-		-	-		+/-	++		+	+		-	-	
Cerebellum	-	+		-	-		+	-		++	++		-	-	
Occipital cortex	-	-		-	-		+/-	-		+	+		-	-	

*+ and – measures the intensity of the bands

IV. DISCUSSION

Communication through gap junction channels is the primary means of cell-cell communication during neurogenesis (for a review see Rozental et al, 2000). This observation leads to the hypothesis that altering expression of the structural units of gap junctions will affect cerebral development. It is not known how the growth and differentiation of CNS cells are modulated by gap junctions. Thus, Cx KO mice represent one means of examining the role of Cx-mediated communication on neuronal differentiation and cerebral development. As reviewed in Chapter 1, Introduction, there are over 15 types of Cx protein family members that can form heteromeric or homomeric channels. In the present study, we characterized cerebral abnormalities in adult KO mice. These abnormalities were interpreted to be the result of cerebral development in the absence of Cx32 protein. Cx32 was chosen because: (1) it is implicated in oligodendrocyte development and differentiation (Scherer et al, 1995; Kunzelmann et al, 1997), (2) expression in developing CNS is maximal during the later stages of cortical maturation (Naderajah et al, 1997), (3) expression increases in an *in vitro* model of neuronal differentiation as suggested by my honours thesis research (See Figure 4, Chapter 1, Introduction), (4) it is one of the predominant Cxs expressed during development (Naderajah et al, 1997; Dermietzel et al, 1989), and (5) recent studies have identified CNS defects in CMTX patients (Bahr et al, 1999). To reiterate our purpose, we hypothesized that the loss of Cx32 expression would influence CNS development resulting in identifiable cerebral abnormalities in adult animals. To test this hypothesis, we performed histological analysis of midbrain regions from adult mice lacking Cx32. To minimize the possible effects of genetic background, we compared these KO mice to

their WT littermates, 3 months of age as pilot studies detected dramatic structural differences in mixed strain KO animals versus C57Bl WTs. Since Cx32 is predominately expressed in oligodendrocytes in developing and adult brain, we expected oligodendrocytes to be less developed in the KO mouse relative to WT (i.e. alterations in corpus callosum). Surprisingly, we did not observe any oligodendrocyte abnormalities in the midbrain of KO mice. We did detect subtle abnormalities in neuronal organization in the hippocampal formation, specifically an enrichment of hyperchromatic cells observed along the infra- and suprapyramidal blades (also known as the subgranular zone) and the polymorphonuclear layer of the DG in KO animals. A similar staining profile is observed in neural progenitors know to be expressed in the DG at extremely low levels in WT mice (Gray & Sundstrom, 1998).

In quantifying the enriched population we found an approximate 3-fold increase in hyperchromatic cell profiles throughout the DG of KO animals with cells infiltrating CA3c field of the hippocampal formation at anterior levels. No difference in thickness in the cell density of KO granule or pyramidal cell layers relative to WT was detected, suggesting not that there are more neurons in the hippocampal formation of KO mice but rather that a subpopulation of these cells have not differentiated into morphologically 'normal' adult neurons. These data indicate that a unique population of cells, with morphological characteristics exhibited by neural progenitors, are enriched in the uninjured KO mouse. This population is restricted primarily to the DG, a region known to exhibit neurons with proliferative capacity in WT animals following hippocampal damage (for a review see Gage, 2000).

It has been demonstrated by many that the progenitors from the adult hippocampus have stem cell-like properties, such as proliferative self-renewal and the capacity to generate multiple CNS lineages (Gage et al, 1998). To establish whether the enriched KO cells exhibited a similar phenotype, we cultured adult KO and WT hippocampal cells under conditions know to promote neural progenitor growth and performed clonogenic assays to establish the proliferative potential of these cells. We hypothesized that if the KO mouse expressed more putative neural progenitors then we should be able to detect more proliferating colonies expressing immunogenic markers *in vitro* than in WT cultures. In support of this hypothesis, we found that the yield of nestin-positive colonies in serum-free bFGF stimulated cultures of KO animals was significantly greater than that of WT animals. Gage et al (1995) has demonstrated that rat cells isolated from the rat hippocampus in the presence of bFGF express region-specific migration and neuronal differentiation after transplantation to the adult rat brain. To confirm that the KO nestin-positive colonies had the capacity to differentiate into neurons, we removed bFGF and treated colonies with BDNF *in vitro*. KO colonies differentiated in NeuN- and enolase-positive neurons, but failed to express GFAP indicative of astrocytic differentiation under these conditions. A subcloning experiment (i.e. neurosphere assay) will be performed to demonstrate if the KO progenitor cells have capacity for continual self-renewal and further investigation will be done on to determine their multi-potentiality.

Does the hyperchromatic cell population in the DG and hippocampus express lineage markers of neural stem cells *in* vivo? We were unable to perform double-labelling studies on the paraffin-embedded tissue stained with cresyl-violet and

immunoreacted for CNS lineage markers and, as such, are basing our conclusions on staining of adjacent sections. Our data suggest that a large proportion of the hyperchromatic cells (or, at the very least, cell neighbours in the same region) appear to express nestin, an intermediate filament found in stem or progenitor cells. Furthermore, there are more nestin-positive cells in the KO relative to the WT. These data were confirmed by the densitometric analysis, with a statistically significant increase in nestin-positive immunoreactivity and confirmed by Western analysis, with a marked increase in the KO DG. The hippocampal formation, specifically the DG, has an increased capacity for structural plasticity (Muller et al, 1996). This plasticity is probably due to the fact that a high proportion of granule cells in the subgranular zone of the DG display signs of ongoing proliferation and differentiation, albeit at an extremely low level (Altman & Bayer, 1990). In our studies, the nestin-positive cells in the KO DG do not appear to be actively dividing. Western analysis confirms that equal amounts of PCNA protein are present in the KO and WT hippocampal formation, but mitotic division is probably confined to the glial cells in the molecular layer. At this time we are unable to determine if the hyperchromatic cells in the DG are proliferating. In adulthood, the majority of neural stem cells remain quiescent, whereas others divide rapidly (Altman & Bayer, 1990; Gobetto et al, 1995) and it may be the KO progenitor population is quiescent until activated by cerebral injury. Proliferative capacity and lineage of this population in the subgranular zone will be addressed in uninjured and injured KO and WT brain in future studies using BrdU labeling.

We were surprised to observe that A2B5 and O4 are not expressed in the subgranular zone of the KO DG, suggesting that the enriched hyperchromatic population

are not destined to become oligodendrocytes and astrocytes. Faint GAP43 staining, a marker of axonal extension (neurites) and oligodenrocyte progenitors was detected in the KO DG, but at significantly lower levels than in WT. In mammalian CNS, failure to express GAP43 affects regulation of the cell cycle in proliferating precursors at the time that neurogenesis is being initiated; daughter cells fail to differentiate and undergo apoptosis (Mani et al, 2001). We have yet to determine whether the apoptotic index is altered in the adult KO DG relative to WT.

The significantly lower expression levels of neuronal lineage markers TUJ1 and NeuN in the KO DG relative to the WT was also unexpected. It is important to note that the TUJ1 reduction was confined only to the region of the DG in which the hyperchromatic cells were detected. The NeuN reduction was more widespread, with patches or groups of cells found within neuronal cell layers of the hippocampus lacking protein. We speculate that these reductions are indicative of a 'younger' more plastic phenotype. This speculation is tentative. It may be that the majority of hyperchromatic cells (putative neural progenitors) in the KO brain subpopulation have not yet begun to differentiate. It is interesting that a small number of cells express TUJI along the subgranular zone, and the external limbs of the DG, but that this was not the case for NeuN. Messam et al (2000) has similarly showed small numbers of TUJ1-positive human fetal brain cells double-label with nestin within the first few weeks in culture. When placed in context with our *in vivo* immunhistochemical and Western data and our *in vitro* data, this suggests that a subset of KO progenitor cells preferentially differentiate into neurons. Certainly, the KO brain is composed of a significant numbers of neurons. There are no striking neuropathologies. Animals appear unaffected in general behaviour

although we will be pursuing more precise behavioural measurements of learning and memory. Both MAP1 and NF160 are expressed in KO hippocampal neurons. These mature lineages markers demonstrated a moderate reduction in staining in the KO DG relative to WT, but the proteins appear to be functioning in that cytoarchitecture is maintained and, as indicated, no gross neuropathology is detected. Furthermore, we know that KO progenitor cells are capable of differentiation to a neuronal phenotype when treated with BDNF, as demonstrated by our *in vitro* studies. We have yet to determine if these cells can fully differentiate into all three lineages (i.e. oligodendrocytes, neurons and/or astrocytes). Combined analysis of all neuronal lineage markers tested (GAP43, TUJ1, NeuN, MAP1, NF160) suggests that the KO DG appears to be in a more juvenile state relative to WT.

It is unlikely that the hyperchromatic population is composed of mature astrocytes and oligodendrocytes, as determined by the rare expression of GFAP and GalC. For the most part, no difference in overall levels were observed between KO and WT. GFAP immunoreactivity can, however, be used to identify at least two additional populations of cells, ependymal cells (Johansson et al, 1999), adult stem cells (Alvarez-Buylla & Loise, 1995; Doetsch et al, 1999; Messam et al, 2000) and radial glial (Kalman & Ajtai, 2001; Clarke et al, 1994). We did observe an interesting qualititative difference in GFAP localization by immunohistochemistry, with more cells in the DG hilus immunopositive in the KO relative to WT. This difference was not statistically significant in densitometric analysis and was not detected by Western immunoblotting. It may be that rare progenitors in this region co-express nestin and GFAP although further empirical data are required to validate this hypothesis

To summarize our histochemical, immunocytochemical, and Western blot analysis, it would appear that a hyperchromatic subpopulation of cells, expressing of a variety of early neuronal and glial lineage markers, is enriched in the KO DG relative to WT littermates. These data lead us to conclude that the KO mouse may be an *in vivo* model of neural progenitor enrichment. That is to say, more neural progenitors are retained in the adult KO animal than can be detected in a WT animal.

How is this enrichment achieved? Altering Cx32 expression may have a direct or indirect role on cerebral development. For example, expression of another Cx may be increased in the KO brain to compensate for the loss of Cx32. Intercellular signals that pass through Cx32 or other Cx-mediated gap junction channels may be vital for stem cell viability, proliferation, and differentiation. To screen for compensentatory Cx expression in KO and WT hippocampus, we examined mRNA levels of other Cx family members by RT-PCR. We demonstrate that a loss of Cx32 results in increased mRNA expression of Cx26, Cx30, Cx36, Cx37, and Cx47 in the adult hippocampal formation of KO mice relative to WT. Out of the other ten brain regions analyzed, the subventricular zone, parietal/temporal cortex, and entorhinal cortex demonstrated similar patterns of Cx expression. To our surprise, there was no upregulation in Cx45 mRNA expression, which is another Cx known to be expressed in oligodendrocytes. This suggests that Cxs expressed at high levels in similar cell types may not be functionally redundant. It will be interesting to examine areas exhibiting the same trends in Cx compensation as the hippocampal formation for an enriched population of progenitor cells.

CONCLUSION

The empirical data provide substantive evidence that the enriched population of hyperchromatic cells present in the KO hippocampus are neural stem or progenitor cells. Clearly, loss of Cx32 expression influences CNS development. This conclusion is based on the following observations: 1) KO mice express approximately 3-fold more hyperchromatic cell profiles in the hippocampal formation than WT. The morphology of these cells is consistent with a neuronal precursor phenotype. 2) KO but not WT hippocampal cultures express the neural stem cell marker nestin when treated with bFGF and are capable of colony formation indicative of self-renewal. FGF-treated KO cells, expressing neural progenitor markers, can be terminally differentiated to NeuN- and enolase-positive neurons by BDNF. 3) There is an increase in neural progenitor lineage markers in the KO hippocampal formation, and specifically the DG, relative to WT and a decrease in terminally differentiated neuronal markers. These data are summarized in Figure 29. We do not know how the loss of Cx32 mediates this enrichment. Altering Cx expression during development may inhibit deletion of DG neural precursors during development or, alternatively, inhibit terminal differentiation of granule cells in the DG. Both hypotheses remain speculative. Furthermore, it may not be the loss of Cx32 per se, but compensensatory increases in other gene products responsible for the putative progenitor enrichment. We demonstrate that Cx26, Cx30, Cx36, Cx37, and Cx47 are consistently upregulated in KO hippocampal formation and subventricular zone relative to WT. These areas are known to: (a) express Cx32 and (b) exhibit endogenous neural stem cells in WT animals. Cx30, Cx37, Cx36, and Cx47 are also upregulated in

entorhinal cortex and parietal/temporal cortex. It will be interesting to examine these other areas for other enriched progenitor populations.

Significance of this research

With increasing age the hippocampus is susceptible to degeneration. It appears that we have an *in vivo* genetic model in which the adult neural stem cell populations are enriched thereby providing a larger pool of cells for study. This model could prove to be a significant advance in the study of neural stem cells if validated. The KO mouse would allow researchers to more effectively characterize adult neural stem cells and more effectively identify molecular mechanisms controlling stem cell fate over the course of development. This raises the possibility that the human neurons depleted by disease or injury could be replenished *in situ*.

Figure 29. Neuronal progenitor enrichment in the adult KO mouse hippocampal formation. In the present study, we have identified an enriched (3-fold increase) hyperchromatic cell population in the KO DG. This population was demonstrated to be restricted primarily to the DG, a region known to exhibit neurons with proliferative capacity in WT animals following hippocampal damage. Increased expression of nestin-positive cells in the KO DG relative to WT was detected, as determined by immunohistochemical analysis. Western analysis confirms that there is more nestin protein in the DG of KO animals. No indication of enhanced cell proliferation was observed, as no PCNA-positive cells were detected in either KO or WT. We failed to detect A2B5 or O4 expression in the KO or WT, both lineage markers first identified in cells destined to be oligodendrocytes. We did detect faint GAP43-staining along the subgranular zone at the border between the granular zone and hilus, and in the CA3c pyramidal cell field of the KO mouse. Reduced staining and protein levels were detected in the KO animal for neuronal lineage markers: NeuN, TuJ1, MAP1, NF160 and GalC. No overall difference in GFAP-immunoreactivity, although there is a difference in GFAP-localization, specifically along the subgranular zone of KO animals. Thus, the enriched hyperchromatic population in the KO DG appears to be a heterogeneous population, composed of uncommitted neural progenitors and cells expressing juvenile glial and neuronal lineage markers. These data suggest that the KO hippocampal formation is in a more juvenile state relative to WT and, as a result, may be more plastic. Empirical testing is required to confirm this hypothesis. In the model figure, positive lineage markers identified in the subgranular zone of the DG are colour-coded red; Negative or faint staining of lineage markers identified in this same region are colour coded blue. Green shading indicates that the enriched hyperchromatic cells found in the KO DG are likely to be CNS pre-progenitors, neuronal progenitors or glial progenitors. Given the location of the hyperchromatic cells and based on the immunohistochemical analysis, we hypothesize that this subpopulation are neuronal stem/progenitor cells. Cx32 may have a direct or indirect role (i.e. *de novo* expression of another Cx in the KO brain) in the enrichment of the hyperchromatic cells found in the KO DG. The KO animal demonstrated altered Cx expression patterns, notably the upregulation of related family members Cx26, Cx30, Cx36, Cx37, and Cx47. Thus, loss of Cx32 and/or the increase in the other Cxs may inhibit differentiation of neuronal precursor cells of the KO DG. It is tempting to speculate that Cx-mediated communication plays a role in neural stem cell differentiation and/or is involved in apoptotic deletion of excess/undifferentiated neural stem cell.

Differentiation of Adult Neural Stem Cells

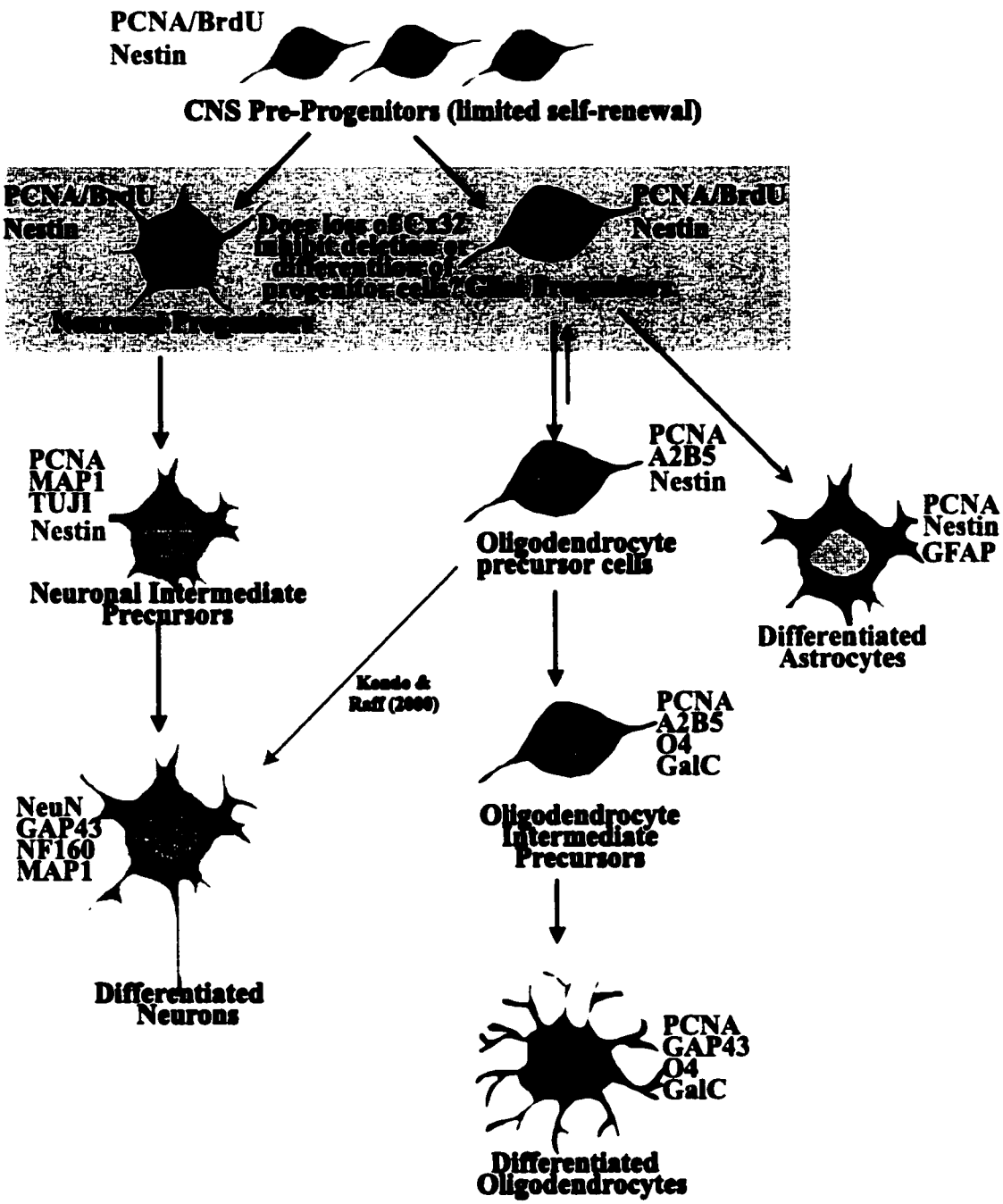

REFERENCES

Abrams, CK, Oh, S, Ri, Y & Bargiello, T. (2000). Mutations in Connexin32: the Molecular and Biophysical Bases for the X-linked form of Charcot-Marie-Tooth Disease. *Brain Research Reviews,* **32**: 203-214.

Ahmad, S, Diez, JA, George, CH & Evans, HW. (1999). Synthesis and Assembly of Connexins *In Vitro* into Homomeric and Heteromeric Functional Gap Junction Hemichannels. *Biochemical Journal*, **339**: 247-253.

Ainsworth, PJ, Bolton, CF, Murphy, BC, Stuart, JA & Hahn, AF. (1998). Genotype/Phenotype Correlation in Affected Individuals of a Family with a deletion of the Entire Coding Sequence of the Connexin32 Gene. *Human Genetics*, **103**: 242-244.

Alvarez-Bullya, A & Loise, C. (1995). Neuronal Stem Cells in the Brain of Adult Vertebrates. *Stem Cells,* **13**: 263-272.

Alvarez-Buylla, A & Temple, A. (1999). Stem Cells in the Developing and Adult Nervous System. *Current Opinion Neurobiology*, **9**:135-141. Review

Altman, J & Bayer, SA. (1990). Migration and Distribution of Two Populations of Hippocampal Granule Cell Precursors During the Perinatal and Postnatal Periods. *The Journal of Comparative Neurology*, **301**: 365-381.

Angeletti, RH, Trojanowski, JQ, Carden, M, Schlaepher, WW & Lee, VM. (1985). Domain Structure of Neurofilament Subunits as Revealed by Monoclonal Antibodies. *Journal of Cellular Biochemistry*, **27**:181-187.

Armstrong, RC, Dorn, HH, Kufta, CV, Friedman, E & Dubois-Daicq, ME. (1992). Pre-Oligodendrocytes from Adult Human CNS. *The Journal of Neuroscience*, **12**:1538-1547.

Bahr, M, Timmeran, V, Nelis, M, Broeckoven, C & Dichgans, J. (1999). Central Visual, Acoustic, and Motor Pathway Involvement in a Charcot-Marie-Tooth Family with an Asn205Ser Mutation in the Connexin32 Gene. *The Journal of Neurology and Neurosurgury Psychiatry,* **66**: 202-206.

Barnea A & Nottebohm F. (1989). Seasonal recruitment of hippocampal neurons in adult free-ranging black-capped chickadees. *Protocols of National Academic Science USA*, **91**:714-718

Barrio, LC, Castro, C & Gomez-Hernandez, JM. (1999). Altered Assembly of Gap Junctions Caused by COOH-Terminal Connexin32 Mutants of CMTX. *Annals New York Academy of Science*, **883**:526-529.

Bayer SA, Yackel JW, Puri PS. (1982). Neurons in the Rat Dentate Gyrus Granular Layer Substantially Increase During Juvenile and Adult Life. *Science*, **216**:890-2.

Belliveau, DJ & Naus, CCG. (1995). Cellular Localization of Gap Junction mRNAs in Developing Rat Brain. *Developmental Neuroscience*, **17**: 81-96.

Belliveau DJ, Kidder GM, Naus CC. (1991). Expression of gap junction genes during postnatal neural development. *Developmental Genetics*, **12**:308-317

Belluardo, N, Trovato-Salinaro, A, Mudo, G, Hurd, YL & Condorelli, DF. (1999). Structure, Chromosomal Location, and Brain Expression of Human Cx36 Gene. *Journal of Neuroscience Research*, **57**: 740-752.

Bennett, MVL, Barrio, LC, Bargiello, TA, Spray DC, Hertzberg, E & Saez, JC. (1991). Gap Junctions: New Tools, New Answers, New Questions. *Neuron*, **6**: 305-320.

Bennett, SA, Arnold, JM, Chen, J, Stenger, J, Paul, DL & Roberts, DC. (1999). Long-Term Changes in Connexin32 Gap Junction Protein and mRNA Expression Following Cocaine Self-Administration in Rats. *European Journal of Neuroscience*, **11**: 3329-3338.

Bennett, MV & Goodenough, DA. (1978). Gap Junctions, Electrotonic Coupling, and Intercellular Communication. *Neuroscience Research Program Bulletin*, **16**: 1-486.

Bergoffen J, Scherer SS, Wang S, Oronzi-Scott M, Bone L, Paul DL, Chen K, Sensch MW, Chance P, Fischbeck, K. (1993). Connexin mutations in X-linked Charcot-disease Tooth diseases. *Science*, **262**: 2039-2042.

Bernhardt, R, Huber, G & Matus, A. (1985). Differences in the Developmental Patterns of Three Microtubule-Associated Proteins in the Rat Cerebellum. *Journal of Neuroscience*, **5**: 977-991.

Bruzzone, R, White, TW, Paul, DL. (1996). Connections with Connexins: the Molecular Basis of Direct Intercellular Signalling. *European Journal of Biochemistry*, **238**: 1-27.

Bruzzone, R & Ressot, C. (1997). Connexins, Gap Junctions and Cell-Cell Signalling in the Nervous System. *European Journal of Neuroscience*, **9**:1-6.

Cameron, RS & Rakic, P. (1991). Glial Cell Lineage in the Cerebral Cortex: A Review and Synthesis. *Glia*, **4**: 124-137.

Cammer, W & Zhang, H. (1999). Atypical Glial Cells in Demyelinated and Hypomyelinated Mouse Brains. *Brain Research*, **837**:188-192.

Castro, C, Gomez-Hernandez, J, Silander, K & Barrio, L. (1999). Altered Formation of Hemichannel and Gap Junction Channels Caused by C-Terminal Connexin-32 Mutations. *The Journal of Neuroscience*, **19**:3752-3760.

Chiasson, BJ, Tropepe, V, Morshead, CM & Van der Kooy, D. (1999). Adult Mammalian Forebrain Ependymal and Subependymal Cells Demonstrate Proliferative Potential, but only Subependymal Cells have Neural Stem Cell Characteristics. *The Journal of Neuroscience*, **19**: 4462-4471.

Circirata, F, Parenti, R, Spinella, F, Giglio, S, Tuorto, F, Zuffardi, O & Gulisano, M. (2000). Genomic Organization and Chromosomal Localization of the Mouse Connexin36 Gene. *Gene*, **251**: 123-130.

Clarke, SR, Shetty, AK, Bradley, JL & Turner, DA. (1994). Reactive Astrocytes Express the Embryonic Intermediate Neurofilament Nestin. *Neuroreport*, **5**: 1885-1888.

Contet, C, Rawlins, JN & Deacon, RM. (2001). A Comparison of 129S2/SvHsd and C57BL/6JolaHsd Mice on a Test Battery Assessing Sensorimotor, Affective and Cognitive Behaviours: Implications for the Study of Genetically Modified Mice. *Behavioural Brain Research*, **28**: 33-46.

Craig CG, D'Sa R, Morshead CM, Roach A & Van Der Kooy, D. (1999). Migrational Analysis of the Constitutively Proliferating Subependyma Population in Adult Mouse Forebrain. *Neuroscience*, **93**: 1197-1206.

Davies TC, Barr KJ, Holstead J, Zhu D & Kidder, GM. (1996). Multiple Members of the Connexin Gene Family Participate in Preimplantation Development of the Mouse. *Developmental Genetics*, **18**:234-243.

Dermietzel, R, Farooq, M, Kessler, JA, Altaus, H, Hertzberg EL & Spray, DC. (1997). Oligodendrocytes Express Gap Junction Proteins Connexin32 and Connexin45. *Glia*, **20**:101-114.

Dermietzel, R, Hwang, TK & Spray, DS. (1990). Review Article: The Gap Junction Family: Structure, Function and Chemistry. *Anatomy and Embryology*, **182**: 517-528.

Dermietzel, R & Spray, DC. (1993). Gap Junctions in the Brain: Where, What Type, How Many and Why? *Trends in Neuroscience*, **16**: 186-191.

Dermietzel, R, Traub, O, Hwang, TK, Beyer, E, Bennett, MVL. & Spray,DC. (1989). Differential Expression of Three Gap Junction Proteins in Developing and Mature Brain Tissues. *Protocols of National Academic Science USA*, **86**: 10148-10152.

Doetsch, F, Caille, I, Lim, DA, Garcia-Verdugo, JM, and Alvarez-Buylla, A. (1999). Subventricular zone astrocytes are neural stem cells in the adult mammalian brain. *Cell*, **97**: 703716.

Doetsch, F, Garcia-Verdugo, JM & Avlarex-Buylla, A. (1997). Cellular Composition and Three-Dimensional Organization of the Subventricular Germinal Zone in the Adult Mammalian Brain. *The Journal of Neuroscience*, **17**: 5046-5061.

Eisenbarth, GS, Walsh, FS & Nirenberg, M. (1979). Monoclonal Antibody to a Plasma Membrane Antigen of Neurons. *Protocols of National Academic Science USA*, **76**:4913-4917.

Eriksson PS, Perfilieva E, Bjork-Eriksson T, Alborn AM, Nordborg C, Peterson DA, Gage FH. (1998). Neurogenesis in the Adult Human Hippocampus. *Nature Medicine*, **4**:1313-7.

Franklin, KBJ & Paxinos, GT. (1997). The Mouse Brain: in Stereotaxis Coordinates. First Edition. Academic Press, 304 pages.

Frederiksen, K, and McKay, RD. (1988). Proliferation and Differentiation of Rat Neuroepithelial Precursor Cells *In Vivo*. *The Journal of Neuroscience*, **8**: 1144-1151.

Fricker, RA, Carpenter, MK, Winkler, C, Greco, C, Gates, MA & Bjorklund, A. (1999). Site-Specific Migration and Neuronal Differentiation of Human Neural Progenitor Cells after Transplantation in the Adult Rat Brain. *The Journal of Neuroscience*, **19**: 5990-6005.

Fujii, M, Hideaki, H, Meng, W, Vonsattel, JP & Huang, Z. (1997). Strain-Related Differences in Susceptibility to Transient Forebrain Ischemia in SV-129 and C57Black/6 Mice. *Stroke*, **28**: 1805-1811.

Gage,F. (2000). Mammalian Neural Stem Cells. *Science*, **287**:1433-1438.

Gage, FH, Kempermann, G, Palmer, TD, Peterson, DA & Ray, J. (1998). Multipotent Progenitor Cells in the Adult Dentate Gyrus. *Journal of Neurobiology*, **36**:249-266. Review.

Gage FH, Coates PW, Palner TD, Kuhn HG, Fisher LJ, Suhunen JO, Peterson DA, Suhr ST & Ray, J. (1995). Survival and differentiation of adult neuronal progenitor cells transplanted to the adult brain. *Protocols of National Academic Science USA*, **92**:11879-11883.

Garcia, CA. (1999). A Clinical Review of Charcot-Marie-Tooth. *Annals New York Academy Science*, **14**:883:69-76. Review.

Goodman CX, Spitzer NC. (1979). Embryonic development of identified neurons: differentiation from neuroblast to neuron. *Nature*, **280**:208-214.

Gould E, Beylin A, Tanapat P, Reeves A, Shors TJ. (1999). Learning enhances adult neurogenesis in the hippocampal formation. *Nature Neuroscience*, **2**:260-265.

Gould, E & Cameron, HA. (1996). Regulation of Neuronal Birth, Migration and Death in the Rat Dentate Gyrus. *Developmental Neuroscience*, **18**: 22-35.

Gobetto, A, Aimar, P, Bonfanti, L, Ghidella, S, Lossi, L & Merighi, A. (1995). Cell Proliferation in the Post-Natal and Adult Mammalian Central Nervous System. *Italian Journal of Anatomy Embryology*, **100**: 167-175.

Gramsch, B, Gabriel, HD, Wiemann, M, Grummer, R, Winterhager, E, Bingmann, D & Schirrmacher, K. (2001). *Experimental Cell Research*, **264**: 397-407.

Gray, WP & Sundstrom, LE. (1998). Kainic Acid Increases the Proliferation of Granule Cell Progenitors in the Dentate Gyrus of the Adult Rat. *Brain Research*, **790**: 52-59.

Guthrie, SC & Gilula, NB. (1989). Gap junctional communication and development. *Trends in Neuroscience*, **12**:12-6.

Hockfield, S, and McKay, RD. (1985). Identification of major cell classes in the developing mammalian nervous system. *The Journal of Neuroscience*, **5**: 3310-3328.

Hardy, RJ & Friedrich, VL. (1996). Oligodendrocyte Progenitors are Generated Throughout the Embryonic Mouse Brain, but Differentiate in Restricted Foci. *Development*, **122**: 2059-2069.

Husler, DF, Eckert, FR, Irmer, U, Krisciukaitis, A, Mindermann, A, Pleiss, J, Rehkopf, DB, Sharovskaya, J & Traub, O. (1998). Intercellular Communication via Gap Junction Channels. *Bioelectrochemistry and Bioenergetics*, **45**: 55-65.

Jin K, Minami M, Lan JQ, Mao XO, Batteur S, Simon RP, Greenberg DA. (2001). Neurogenesis in dentate subgranular zone and rostral subventricular zone after focal cerebral ischemia in the rat. *Protocols of National Academic Science USA*, **98**:4710-5

Johansson, CB, Momma, S, Clarke, DL, Risling, M, Lendahl, U, Frisen, J. (1999). Identification of a Neural Stem Cell in the Adult Mammalian Central Nervous System. Cell, 96: 25-34.

Kalman, M & Ajitai, BM. (2001). A Comparison of Intermediate Filament Markers for Presumptive Astroglia in the Developing Rat Neocortex: Immunostaining Against Nestin Reveals more Detail, than GFAP or Vimentin. *International Journal of Developing Neuroscience*, **19**: 101-8.

Kempermann, G, Kuhn, HG & Gage, FH. (1997). Genetic Influence on Neurogenesis in the Dentate Gyrus of Adult Mice. *Protocols of National Academic Science USA*, **94**: 10409-10414.

Kempermann, G, Kuhn, HG & Gage, FH. (1998). Experience-Induced Neurogenesis in the Senescent Dentate Gyrus. *The Journal of Neuroscience*, 18: 3206-3212.

Kirn, JR & Nottebohm, F. (1993).Direct Evidence for Loss and Replacement of Projection Neurons in Adult Canary Brain. *The Journal of Neuroscience*, **13**:1654-1663.

Kirschenbaum, B, Doetsch, F, Lois, C & Alvarez-Buylla, A. (1999). Adult Subventricular Zone Neuronal Precursors Continue to Proliferate and Migrate in the Absence of the Olfactory Bulb. *The Journal of Neuroscience*, **19**: 2171-2180.

Kondo, T & Raff, M. (2000). Oligodendrocyte Precursor Cells Reprogrammed to Become Multipotential CNS Stem Cells. *Science*, **289**: 1754-1757.

Kuhn, G, Dickinson-Anson, H & Gage, FH. (1996). Neurogenesis in the Dentate Gyrus of the Adult Rat: Age-Related Decrease of Neuronal Progenitor Proliferation. *The Journal of Neuroscience*, **16**: 2027-2033.

Kukekov, VG, Laywell, ED, Suslov, O, Davies, K, Scheffler, B, Thomas, SLB, O'Brian, TF, Kusakabe, M & Steindler, DA. (1999). Multipotent Stem/Progenitor Cells with Similar Properties Arise from Two Neurogenic Regions of Adult Human Brain. *Experimental Neurology*, **156**: 333-344.

Kunzelmann, P, Schroder, W, Traub, O, Steinhauser, C, Dermietzel, R & Willecke, K. (1999). Late Onset and Increasing Expression of the Gap Junction Protein Connexin30 in Adult Murine Brain and Long-Term Cultured Astrocytes. *Glia*, **25**: 111-119.

Kunzelmann P, Blumcke I, Traub O, Dermietzel R, Willecke K. (1997). Coexpression of Connexin45 and -32 in Oligodendrocytes of Rat Brain. *Journal of Neurocytology*, **26**:17-22.

Lacanda, F, Warlow, PM, Sheikh, S, Furlan, F, Steinberg, TH & Civitelli, R. (2000). Connexin43 Deficiency Causes Delayed Ossification, Craniofacial Abnormalities, and Osteoblast Dysfunction. *The Journal of Cell Biology*, **151**:931-944.

Laird, DW. (1996). The Life Cycle of a Connexin: Gap Junction Formation, Removal, and Degradation. *Journal of Bioenergetics and Biomembranes*, **28**: 311-317.

Lee, VM. (1985). Neurofilament Protein Abnormalities in |C12 Cells: Comparison with Neurofilament Proteins of Normal Cultured Rat Sympathetic Neurons. *The Journal of Neuroscience*, **11**:3039-3046.

Lee, VM, Rebhun, LI & Frankfurter, A. (1990). Posttranslational Modification of Class III β-Tubulin. *Proceedings of National Academic Science USA*, **87**:7195-7199.

Lendahl, U, Zimmerman, LB, and McKay, RD. (1990). CNS stem cells express a new class of intermediate filament protein. *Cell*, **60**: 585595.

Livy, DJ & Wahlsten, D. (1997). Retarded Formation of the Hippocampal Commissure in Embryos from Mouse Strains Lacking a Corpus Callosum. *Hippocampus*, **7**: 2-14.

Lo, CW. (1999). Genes, Gene Knockouts, and Mutations in the Analysis of Gap Junctions. *Developmental Genetics*, **24**:1-4.

Lois C & Alvarez-Buylla, A . (1994). Long-distance neuronal migration in the adult mammalian brain. *Science*, **264**: 1145-1148.

Loewenstein, WR. (1981). Junctional Communication: The Cell-to-Cell Membrane Channel. *Physiological Reviews*, **61**: 829-913.

Luskin MB, Zigova T, Soteres BJ & Steward, RR. (1997). Neuronal Progenitor Cells Derived from the Anterior Subventricular Zone of the Neonatal Rat Forebrain Continue to Proliferate in Vitro and Express a Neuronal Phenotype. *Molecular and Cellular Neuroscience*, **8**: 351-366.

Mani, S, Shen, Y, Schaefer, J & Meiri, KF. (2001). Failure to Express GAP43 during Neurogenesis Affects Cell Cycle Regulation and Differentiation of Neural Precursors and Stimulates Apoptosis of Neurons. *Molecular and Cellular Neuroscience*, **17**: 54-66.

Martini, R & Carenini, S. (1998). Formation and Maintenance of Myelin Sheath in the Peripheral Nerve: Roles of Cell Adhesion Molecules and the Gap Junction Protein Connexin32. *Microscopy Research and Techniques*, **41**: 403-415.

McIntosh, H & Parkinson, D. (1990). GAP-43 in Adult Visual Cortex. *Brain Research.* **518**:324-328.

Messam, CA, Hou, J & Major, EO. (2000). Coexpression of Nestin in Neural and Glial Cells in the Developing Human CNS Defined by a Human-Specific Anti-Nestin Antibody. *Experimental Neurology*, **161**:585-596.

Moennikes O, Buchmann A, Ott T, Willecke K & Schwarz, M. (1999). The Effect of Connexin32 Null Mutation on Hepatocarcinogenesis in Different Mouse Strains. *Carcinogenesis*, **20**:1379-1382.

Morrison, SJ, Shah, NM & Anderson, DJ. (1997). Regulatory Mechanisms in Stem Cell Biology. *Cell*, **88**:287-98

Mullen, RJ, Buck, CR & Smith, AM. (1992). NeuN, A Neuronal Specific Nuclear Protein in Vertebrates. *Development*, **116**:201-211.

Naderajah, B, Jones, AM, Evans, WH & Parnavelas, JG. (1997). Differential Expression of Connexins During Neocortical Development and Neuronal Circuit Formation. *The Journal of Neuroscience*, **17**: 3096-3111.

Naderajah, B & Parnavelas, JG. (1999). Gap Junction-Mediated Communication in the Developing and Adult Cerebral Cortex. *Novartis Foundations Symposium*, **219**: 157-170.

Nagy, JI, Patel, D, Ochalski, PAY & Stelmack, GL. (1999). Connexin30 in Rodent, Cat, and Human Brain: Selective Expression in Gray Matter Astrocytes, Co-Localization with Connexin43 at Gap Junctions and Late Developmental Appearance. *Neuroscience*, **88**: 446-468.

Nelles, E, Butzler, C, Jung, D, Temme, A, Gabriel, H, Dahl, U, Traub, O, Stumpel, F, Jungermann, K, Zielasek, J, Toyka, K, Dermietzel, R & Willecke, K. (1996). Defective Propagation of Signals Generated by Sympathetic Nerve Stimulation in the Liver of Connexin32-Deficient Mice. *Proceedings of National Academic Science USA*, **93**: 9565-9570.

Neuberg, DHH, Carenini, S, Schachner, M, Martini, R & Suter, U. (1998). Accelerated Demyelination of Peripheral Nerves in Mice Deficient in Connexin32 and Protein Zero. *Journal of Neuroscience Research*, **53**: 542-550.

Niessen, H, Harz, H, Bedner, P, Kramer, K & Willecke, K. (2000). Selective Permeability of Different Connexin Channels to the Second Messenger Inositol 1,4,5-Triphosphate. *Journal of Cell Science*, **113**: 1365-1372.

Nicholson, S, Ressot, C, Gomes, D, Andrea, P, Perea, J, Duval, N & Bruzzone, R. (1999). Connexin32 in Peripheral Nervous System. *Annals New York Academy of Sciences*, **14**:168-183.

Niquet, J, Ben-Ari, Y & Repressa, A. (1994). Glial Reaction after Seizure Induced Hippocampal Lesion: Immunohistochemical Characterization of Proliferating Glial Cells. *Journal of Neurocytology*, **23**: 641-656.

Osada, T, Ichikawa, M & Costanzo, RM. (1995). Is Nestin a Marker for Chemosensory Precursor Cells. *Brain Research*, **683**:254-257.

Paul, DL. (1986). Molecular Cloning of cDNA for Rat Liver Gap Junction Protein. *The Journal of Cell Biology*, **103**: 123-133.

Parent JM, Yu TW, Leibowitz RT, Geschwind DH, Sloviter RS & Lowenstein DH. (1997). Dentate Granule Cell Neurogenesis is Increased by Seizures and Contribute to Aberrant Network Reorganization in the Adult Rat Hippocampus. *Journal of Neuroscience*, **17**:3727-3738.

Peibner, W, Kocher, M, Treuer, H & Gillardon, F. (1999). Ionizing Radiation-Induced Apoptosis of Proliferating Stem Cells in the Dentate Gyrus of the Adult Rat Hippocampus. *Molecular Brain Research*, **71**:61-68.

Pfahnl, A, Zhou, X, Werner, R & Dahl, G. (1997). A Chimeric Connexin Forming Gap Junction Hemichannels. *European Journal of Physiology*, **433**: 773-779.

Princen, F, Robe, P, Gros, D, Jarry-Guichard, T, Glelen, J, Merville, MP & Boors, V. (2001). Rat Gap Junctions Connexin30 Inhibits Proliferation of Glioma Cell Lines. *Carcinogenesis*, **22**: 507-513.

Purves, D, Augustine, GJ, Fitzpatrick, D, Katz, LC, LaMantia, AS & McNamara, JO. (1997). Neuroscience: 1st Edition. Sinauer Associates, Inc, Sunderlands, Massachusetts. Pgs 337-393.

Quist, AP, Rhee, SK, Lin, H & Lal, R. (2000). Physiological Role of Gap-Junctional Hemichannels: Extracellular Calcium-Dependent Isomotic Volume Regulation. *The Journal of Cell Biology*, **148**: 1063-1074.

Rash, JE, Staines, WA, Yasumura, T, Patel, D, Furman, CS, Stelmack, GL & Nagy, JI. (2000). Immunogold Evidence that Neuronal Gap Junctions in Adult Rat Brain and Spinal Cord Contain Connexin-36 but not Connexin-32 or Connexin-43. *Protocols of National Academic Science USA*, **97**: 7573-7578.

Represa, A, Niquet, J, Charriaut, Marlangue, C & Ben-Ari, Y. (1993). Reactive Astrocytes in the Kainic Acid-Damaged Hippocampus have the Phenotypic Features of Type-2 Astrocytes. *Journal of Neurocytology* , **22**:299-310.

Ressot C, Gomes D, Dautigny A, Pham-Dinh D & Bruzzone, R. (1998). Connexin32 Mutatiosn Associated with X-linked Charcot-Marie-Tooth Disease Show Two Distinct Behaviours: Loss of Function and Altered Gating Properties. *The Journal of Neuroscience*, **18**:4063-4075.

Rostami, A, Eccleston, PA, Silberberg, DH, Hirayama, M, Lisak, RP, Pleasure, DE & Phillips, SM. (1984). Generation and Biological Properties of a Monoclonal Antibody to Galactocerebroside. *Brain Research*, **298**:203-208.

Rozental R, Mehler MF, Morales M, Andrade-Rozental AF, Jessler JA & Spray DC. (1993). Differentiation of hippocampal progenitor cells in vitro: temporal expression of intercellular coupling and voltage- and ligand-gated responses. *Developmental Biology*, **167**:350-362.

Rozental, R, Morales, M, Mehler, MF, Urban, M, Kremer, M, Dermietzel, R, Kessler, JA & Spray, DC. (1998). Changes in the Properties of Gap Junctions during Neuronal Differentiation of Hippocampal Progenitor Cells. *The Journal of Neuroscience*, **18**: 1753-1762.

Rozental, R, Srinivas, M, Gokhan, S, Urban, M, Dermietzel, R, Kessler, JA, Spray, DC & Mehler, MF. (2000). Temporal Expression of Neuronal Connexins During Hippocampal Ontogeny. *Brain Research Reviews*, **32**: 57-71.

Roy NS, Wang S, Jiang L, Kang J, Benraiss A, Harrison-Restelli C, Fraser RA, Couldwell WT, Kawaguchi A & Okano, H. (2000). *In vitro* neurogenesis by progenitor cells isolated from the adult human hippocampus. *Nature Medicine*, **6**:271-277.

Royle, SJ, Collins, FC, Rupniak, HT, Barnes, JC & Anderson, R. (1999). Behavioural Analysis and Susceptibility to CNS Injury of Four Inbred Strains of Mice. *Brain Research*, **816**: 337-349.

Sahenk Z & Chen, L. (1998). Abnormalities in the Axonal Cytoskeleton Induced by a Connexin32 Mutation in Nerve Xenografts. *Journal of Neuroscience Research*, **51**: 174-184.

Sahenk Z & Mendell, JR. (1999). Alterations in Nodes of Ranvier and Schmidt-Lanterman Incisures in Charcot-Marie-Tooth Neuropathies. *Annals New York Academy Science*, **883**:508-12.

Sasaki, R, Matsumoto, A, Itoh, K, Kawabe, T, Ota, Y, Yamada, K, Maruta, T, Soejima, T & Sugimura, K. (2000). Target Cells of Apoptosis in the Adult Murine Dentate Gyrus and O4 Immunoreactivity after Ionizing Radiation. *Neuroscience Letters*, **279**: 57-60.

Scherer SS, Deschenes SM, Xu, Y, Grinspan, JB, Fischbeck, KH & Paul, DL. (1995). Connexin32 is a Myelin-Related Protein in the PNS and CNS. *Journal of Neuroscience*, **15**: 8281-8294.

Scherer SS, Xu YT, Nelles E, Fischbeck K, Willecke K & Bone, LJ. (1998). Connexin32-Null Mice Develop Demyelinating Peripheral Neuropathy. *Glia*, **24**:8-20.

Schnitzer, J & Schachner, M. (1982). Cell type Specificity of a Neural Cell Surface Antigen Recognized by the Monoclonal Antibody A2B5. *Cell Tissue Research* **224**:625-636.

Spray, DC. (1998). Gap Junction Proteins: Where They Live and How They Die. *Circulatory Research*, **83**: 679-681.

Spray, DC & Dermeitzel, R. (1995). X-Linked Dominant Charcot-Marie-Tooth Disease and other Potential Gap Junction Diseases of the Nervous System. *Trends in Neuroscience*, **18**: 256-262.

Srinivas, M, Rozental, R, Kojima, T, Dermietzel, R, Mehler, M, Condorelli, DF, Kessler, JA & Spray, DC. (1999). Functional Properties of Channels Formed by the Neuronal Junction Protein Connexin36. *The Journal of Neuroscience*, **19**:9848-9855.

Tankersley, CG, Fitzgerald, RS, & Kleeberger, SR. (1994). Differential Control of Ventilation Among Inbred Strains of Mice. *American Journal of Physiology*, **267**: R1371-R1377.

Teubner, B, Odermatt, B, Guldenagel, M, Sohl, G, Degan, J, Bukauskas, FF, Dronengold, J, Verselis, VS, Jung, YT, Kozak, CA, Schilling, K & Willecke, K. (2001). Functional Expression of the New Gap Junction Gene Connexin47 Transcribed in Mouse Brain and Spinal Cord Neurons. *The Journal of Neuroscience*, **21**: 117-1126.

Traub, O, Hertlein, B, Kasper, M, Eckert, R, Krisciukaitis, A & Willecke, K. (1998). Characterization of the Gap Junction Protein Connexin37 in Murine Endothelium, Respiratory Epithelium, and After Transfection in Human Hela Cells. *European Journal of Cellular Biology*, **77**: 313-322.

Vaney, DI & Weiler, R. (2000). Gap Junctions in the Eye: Evidence for Heteromeric, Heterotypic and Mixed-Homotypic Interactions. *Brain Research Reviews*, **32**: 115-120.

VanSlyke, JK & Musil, LS. (2000). Analysis of Connexin Intracellular Transport and Assembly. *Methods*, **20**: 156-164.

Walsten, D. (1982). Deficiency of Corpus Callosum Varies with Strain and Supplier of the Mice. *Brain Research*, **13**: 329-347.

Walicke P, Cowan WM, Ueno N, Baird A & Guillemin R. (1986). Fibroblast Growth Factor Promotes Survival of Dissociated Hippocampal Neurons and Enhances Neurite Extension. *Protocols of National Academic Science USA*, **83**:3012-3016.

Watt, FM & Hogan, BLM. (2000). Out of Eden: Stem Cells and Their Niches. *Science*, **287**: 1427-1430.

Weissman, IL. (2000). Translating Stem and Progenitor Cell Biology to the Clinic: Barriers and Opportunities. *Science*, **287**: 1442-1445.

West, MJ, Coleman, PD, Flood, DG & Troncoso, JC. (1994). Differences in the Pattern of Hippocampal Neuronal Loss in Normal Aging and Alzheimer's Disease. *The Lancet*, **344**: 769-772.

White, TW & Bruzzone, R. (1996). Multiple Connexin Proteins in Single Intercellular Channels: Connexin Compatibility and Functional Consequences. *Journal of Bioenergetics and Biomembranes*, **28**: 339-349.

White, TW, Deans, MR, Kelsell, DP & Paul, DL. Connexin Mutations in Deafness. (1998). *Nature*, **394**: 630.

White TW & Paul, DL. (1999). Genetic Diseases and Gene Knockouts Reveal Diverse Connexin Functions. *Annual Reviews Physiology*, **61**: 283-310.

Willecke, K. & Haubrick, S. (1996). Connexin Expression Systems: To What Extent do they Reflect the Situation in the Animal? *Journal of Bioenergetics and Biomembranes*, **28**: 319-326.

Willecke, K, Heynkes, R, Dahl, E, Stutenkemper, R, Hennemann, H, Jungbluth, S, Suchyna, T & Nicholson, BJ. (1991). Mouse Connexin37: Cloning and Functional Expression of a Gap Junction Gene Highly Expressed in Lung. *Journal of Cell Biology*, **114**: 1049-1057.
Willecke, K, Temme, A, Teubner, B & Thomas, OTT. (1999). Characterization of Targeted Connexin32-Deficient Mice: A Model for the Human Charcot-Marie-Tooth (X-Type) Inherited Disease. *Annals of New York Academy of Science*, **14**:303-309.

Williams, BP, Park, JK, Alberta, JA, Muheback, SG, Hwang, GY, Roberts, TM & Hwang, GY. (1997). *Neuron*, **18**: 553-562.

Wolf, HK, Buslei, R, Schmidt-Kastner, PK, Pietsch, T, Wiestler, OD & Blumcke, I. (1996). NeuN: A Useful Neuronal Marker for Diagnostic Hispathology. *The Journal of Histochmeistry and Cytochemistry*, **44**: 1167-1171.

Yoshimura, T, Satake, M, Ohnishi, A, Tsutsumi, Y & Fujikura, Y. (1998). Mutations of Connexin32 in Charcot-Marie-Tooth Disease Type X Interfere with Cell-to-Cell Communication but not Cell Proliferation and Myelin-Specific Gene Expression. *Journal of Neuroscience Research*, **51**:154-161.

Zhang, S, Ge, B & Duncan, ID. (2000). Tracing Human Oligodendroglial Development *In Vitro*. *Journal of Neuroscience*, **59**: 421-429.

Zhao, S, Fort, A & Spray, DC. (1999). Characteristics of Gap Junction Channels in Schwann Cells from Wild-Type and Connexin-Null Mice. *Annals New York Academy of Science*, **883**: 533-537.

SANDY BEYKO
Curriculum vitae

BIOGRAPHICAL SKETCH:

Current position
• Biochemistry M.Sc program
Faculty of Medicine, Ottawa University, Ottawa, ON, Canada

Research Focus:
• B.Sc Thesis Topic: The role of Connexin32 in cell signalling during neuronal development and differentiation.

•M.Sc Thesis Topic: Anatomical abnormalities in the central nervous system of Cx32 knockout mice. Implications for Cx32-mediated neuronal development.

Citizenship:
• Canadian

Language:
• English (spoken and written)

Contact Address:
• Faculty of Medicine, Department of Biochemistry, Microbiology and Immunology.
University of Ottawa, 451 Smyth Rd, Ottawa, ON, K1H 8M5, Canada
Tel: (613) 520-5800, ext.8246; fax: (613) 562-5440; email: sbeyko@hotmail.com

EDUCATION:

• B.Sc. Honours (Neuroscience, Carleton University, Ottawa, ON), April 1999.
• M.Sc (Biochemistry, University of Ottawa, Ottawa, ON) - October 2001

COMPETIVE HONOURS & AWARDS

• 2000	Roche Graduate Student Award, CSBMC (National), $250.00
• 1999	Travel Funds from the Eva Princz Memorial Fund (University), $750.00
• 1999	Undergraduate Travel Fellowships for the Biochemistry and Molecular Biology 1999 Meeting, Charles C. Hancock (International), $280.00 US
• 1999	Deans' Honour list (University)

RESEARCH SCHOLARSHIPS & FUNDING

•1999 -2001 Soft-Funded Research Bursary
Project: Cerebral Abnormalities in Cx32 Deficient Mice
Role: Graduate Student
Amt: $14,000 (1st year); $15,000 (2nd year)

• 1999 National Cancer Institute/Canadian Cancer Society
Project: Cancer Control Strategy
Role: Graduate Student
Amt: $1264.00

RESEARCH EXPERIENCE:

Research Assistant (1999)
• Faculty of Medicine, Department of Biochemistry, Microbiology and Immunology
University of Ottawa, Ottawa, ON, Canada
Laboratory of Dr. Steffany A.L. Bennett
Co-author and researcher on a National Cancer Institute-funded report to identify cancer control strategies in OECD countries.

Research Technician (1998 - 1999)
• Institute of Biochemistry, Carleton University, Ottawa, ON, Canada
Laboratory of Dr. Steffany A.L. Bennett

TECHNICAL SKILLS:

• Western and Northern Analysis
• Tissue Culture
• Immunohistochemistry and histological staining
• Stereology/Microtome sectioning and paraffin embedding
• Light and Fluorescence Microscopy
• *In situ* Hybridization

PUBLICATIONS:

Referred Papers
1999
Beyko, S, Paul DL, Bennett, SAL. (1999). Increased Connexin32 Protein Expression During Differentiation of Neuronal Precursors. *Faseb Journal* **13**: A1575-A1575, Suppl. S April 23.

Published Reports
1999
Bennett, JA, Brewer, C, **Beyko, S**, Bennett SAL. Cancer Control Strategies in OECD countries, (Ottawa Health Canada). Accepted for publication in December 1999.

Web-based Publications
Bennett, JA, Brewer, C, **Beyko, S**, Bennett SAL. Cancer Control Strategies in OECD countries, Environmental Scan. URL:http://www.uottawa.ca/~sbennet/ccsIndex.html

Published Abstracts
1998
Beyko S, Kraychik M, Bennett SAL. (1998). Analysis of the gap junction protein Cx32 during

neuronal differentiation: western and immunohistochemical analysis. Ottawa Life Sciences National Conference Proceedings, pg 34 (Ottawa, Canada, oral and poster presentation)

Beyko S and Bennett SAL. (1998). Study of connexin32 protein expression during neuronal development and differentiation. Submitted (San Francisco 1999 Joint Hemisphere Meeting USA, Canadian Society of Biochemistry, Molecular and Cellular Biology)

Beyko, S, Chen, J, Kleine, L, Franks, D, and Bennett SAL. (2000). Cerebral Abnormalities in Cx32 Deficient Mice. Canadian Federation of Biological Societies, pg 110 (Ottawa, Canada, poster presentation)

Beyko, S, Chen, J, and Bennett SAL. (2000). Cerebral Abnormalities in Cx32 Deficient Mice. Society for Neuroscience 30th Annual Meeting, pg 311 (New Orleans, USA, poster presentation)

Beyko, S, Chen, J, Sellitto, C, Franks, DJ, Paul, DL, and Bennett, SAL. (2001). Neuronal Progenitor Enrichment in the Adult Cx32 Knockout Mouse. Ottawa Life Sciences National Conference Proceedings (Ottawa, Canada, poster presentation)